International Doctorate School in Information and Communication Technologies

DIT - University of Trento

LAB-ON-CELL AND CANTILEVER-BASED SENSORS FOR GENE ANALYSIS

Lara Odorizzi

Advisor:

Dr. Leandro Lorenzelli

Fondazione Bruno Kessler (Trento)

Abstract

Nowadays, both gene mutations detection and function investigation are expected to assume a key role in diseases understanding and in many other biotechnological fields. In fact, gene mutations are often cause of genetic diseases and gene function analysis itself can help to have a broader vision on cells health status. Traditionally, gene mutations detection is carried out at pre-translational/sequence level (transcriptomic approach). On the other hand, the function of innumerable sequenced genes can be investigated by delivering them into cells through transfection methods and observing their expression result at post-translational level (proteomic approach). In this context, Micro-ElectroMechanical Systems (MEMSs) offer the intrinsic advantages of miniaturization: low sample and reagent consumption, reduction of costs, shorter analysis time and higher sensitivity. Their applications range from the whole cell assays to molecular biology investigations. On this subject, the thesis deals with two different tools for gene analysis: a Lab-on-Cell and cantilever-based sensors for in-vitro cell transfection and label-free Single Nucleotide Polymorphisms (SNPs) detection, respectively. Regarding the first topic, an enhanced platform for single-site electroporation and controlled transfectants delivery has been presented. The device consists of a gold MicroElectrode Array (MEA) with multiple cell compartments, integrated microfluidics based on independent channels and nanostructured titanium dioxide (ns-TiO_2) functionalized electrodes. Different activities have been reported, from the study of the microfabrication substrates bioaffinity and device development to the electroporation results. The functional characterization of the system has been carried out by electroporating HeLa cells with a small fluorescent dye and then, in order to validate the approach for gene delivery, with plasmid for the enhanced expression of the Green Fluorescent Protein (pEGFP-N1). The second research activity has been focused on a detection module aimed at the integration in a Lab-on-Chip (LOC) for the early screening of autoimmune diseases. The proposed approach consists of piezoresistive SOI-MEMS cantilever arrays operating in static mode. Their gold surface (aimed at the binding of specific thiolated DNA probes) has been deeply analyzed by means of Atomic Force Microscopy (AFM) and X-ray Photoelectron Spectroscopy (XPS) revealing an evident gold non-uniformity and low content together with oxygen and carbon contaminations. Different technological and cleaning solutions have been chosen in order to optimize the system. However, other improvements will be required. Moreover, the feasibility of the spotting technique has been demonstrated by verifying microcantilever mechanical resistance and good surface coverage without cross-contaminations. Finally, as future perspective, possible biological protocols and procedures have been also proposed and discussed starting from literature.

Keywords

Lab-on-Cell; Cell Electroporation; Functionalization; Microcantilever Array; DNA Hybridization.

Contents

Chapter 1

1 Introduction

1.1 The Context: Gene Analysis in the "-*Omic*" Era

The *"-Omic"* era and in particular the related genome sequencing have strongly increased the scientific interest towards gene analysis. A deeper understanding of gene function by means of efficient cell transfection and a rapid identification of DNA mutations are in fact more and more required in most of the biotechnological fields, from the study of eukaryotic gene regulation and expression in general to Single Nucleotide Polymorphisms (SNPs) detection for diagnosis purposes.

Nowadays, different chemical and physical transfection techniques are used to deliver nucleic acids (or other molecules of interest) into cells. Among the physical methods, bulk electroporation lacks the spatio-temporal control over the process: it does not allow to select single or specific groups of cells (desirable requirement especially in highly heterogeneous tissues) and to monitor the transfection result in real-time. Moreover, a good biocompatibility and the possibility to perform multiple tests on the same chip represent necessary requirements, especially in perspective of high-throughput screening.

On the other hand, gene analysis at sequence level needs portability, automation, reduction of sample and reagent volumes, and the possibility, starting from a crude sample (whole blood or saliva), to provide a genetic profile without labelling procedures.

In order to comply these demands and especially the request of high-throughput *in-vitro* screening with spatio-temporal control over the process and fast label-free gene analysis, alternative microscale approaches are increasingly required. In this context, Micro-ElectroMechanical Systems (MEMSs) are emerging as alternative miniaturized and portable instrumentation for biomedical applications providing high sensitivity with low reagents consumption.

1.2 Thesis Content and Innovative Aspects

On this subject, the thesis deals with two different tools for gene analysis: a Lab-on-Cell and cantilever-based sensors for *in-vitro* cell transfection and SNPs detection, respectively:

(1) Lab-on-cell: integrated platform for the electroporation of cells grown in adhesion.

This research activity has been described from the choice of the microfabrication materials suitable for the cell line culture to the real electroporation results, representing the most substantial experimental part. This activity mainly presents the improvements of an electroporation system for cells grown in adhesion [Vassanelli 2008] comprising multiple cell compartments, underlying microfluidics, and patterning of the electrode active areas with nanostructured titanium dioxide (ns-TiO_2). Multiple cell compartments and underlying microfluidics make possible the delivery of different transfectants solutions into specific areas of the same cell population, while the surface functionalization improves cell adhesion, specifically where the voltage is applied to adherent cells. Thus, the demand of high-throughput systems for *in-vitro* cell assays with good biaffinity properties has been satisfied from a technological point of view and experimentally demonstrated by the obtained successful gene tranfection. Both biological and physical factors have been taken into account for the optimization of the experiments. Further technological and experimental improvements have been discussed in conclusions.

(2) Cantilever-based sensors: detection module aimed at the integration in a Lab-on-Chip (LOC) system for early diagnosis and screening of autoimmune disorders based on typing of Human Leukocyte Antigens (HLAs).

Nowadays, microcantilever-based sensors feasibility for DNA detection has been demonstrated. However, they are not consolidated for diagnosis purpose. Moreover, less attention is given to the surface analysis and functionalization procedure. As for the previous topic, surface holds a key role. The upper layer of the microcantilevers has been deeply analyzed. Technical changes and cleaning procedures have been chosen in order to optimize it and also the sample deposition procedure has been assessed. However, since this research activity regards preliminary studies devoted to the system optimization for the subsequent

and a real usage of the array for SNPs detection, biological protocols and procedures have been proposed and discussed in conclusions.

1.3 Structure of the Thesis

This thesis begins with the description of the state of the art related to gene analysis in ***Chapter 2. "State of the Art"***. In particular, this Chapter is divided into two sections in order to deepen different approaches for gene study: *Cell Transfection* (*Section 2.1*) and *Gene Sequence Analysis for Diagnostics* (*Section 2.2*). Starting from traditional techniques employed to deliver genes into mammalian cells (viral-mediated processes, chemical, mechanical and physical approaches) (*Paragraph 2.1.1*), the attention is focused on electroporation. Some theory about pore formation and resealing is introduced in *Paragraph 2.1.1.1*. Then, in *Paragraph 2.1.1.2* bulk electroporation is compared with single-cell electroporation. In this context, the emerging role of probes and microsystems is highlighted by presenting an overview of the main advances achieved in this field, with particular attention towards microdevices for both suspended and adherent cell electroporation (*Paragraph 2.1.1.3*). The significant role of materials bioaffinity and the related phenotypic behaviour consequent to cell-substrate interaction are discussed in *Paragraph 2.1.2*. Finally, *Section 2.1* closes with the main current requirements in perspective of real high-throughput cell *in-vitro* screenings and the thesis contribution in this direction (*Paragraph 2.1.3*). On the other hand, *Section 2.2* regards, as anticipated, gene study at sequence level. It introduces LOCs emphasizing the need of label-free DNA detection. *Paragraph 2.2.1* is devoted to label-free systems, in particular microcantilever-based sensors. Their two different working modes (static and dynamic) are here described, together with possible read-out systems whose suitability for in liquid DNA detection is discussed. As in the previous Section, also this one ends with moving beyond the state of the art for real application of microcantilevers in diagnostics. The importance of surface and functionalization procedure study, discussed in this thesis, is here anticipated (*Paragraph 2.2.2*).

Chapter 3. "Lab-on-Cell for Gene Transfection" is devoted to the first research activity concerning an integrated platform for adherent cell electroporation. The choice of different candidate substrates for its microfabrication is described in *Paragraph 3.1.1*. The Pulsed

Microplasma Cluster Source (PMCS) technique employed for their functionalization with ns-TiO_2 is explained in *Paragraph 3.1.2* as well as the deposited film characterization and related features. Then, a deep investigation of the substrates surface chemical composition (*Paragraph 3.1.3*) precedes the real bioaffinity experiments carried out to define both cell viability and morphology on the materials (*Paragraph 3.1.4*). The schematic representation explaining the working principle and structure of the proposed system is shown in *Paragraph 3.2* which is followed by the real development steps of the device: electroporation module (*Paragraph 3.3*) divided into the MicroElectrode Array (MEA) microfabrication (*Paragraph 3.3.1*) and procedure for electrodes functionalization with ns-TiO_2 (*Paragraph 3.3.2*); microfluidics development and final packaging (*Paragraph 3.4*) with the relative microfluidic structure testing (*Paragraph 3.4.1*). *Section 3.5* reports the experimental method for cell electroporation. It includes the description of the electroporation set-up (*Paragraph 3.5.1*) and the choice of biological and physical factors suitable for the electroporation protocols (*Paragraph 3.5.2*). The real functional characterization of the devices represented by the biological tests is discussed in *Section 3.6* showing the electroporation results with a preliminary value of electroporation efficiency calculated after gene transfection (*Paragraph 3.6.1*). Finally, this Chapter ends with the conclusions summarizing all the activities performed and the obtained results (*Paragraph 3.7*).

Chapter 4. "Cantilever-based Sensors for Gene Analysis" is devoted the second research topic focused on a DNA detection module to be integrated, in future, into a LOC system. After an introduction about the general subject, the design of the microcantilevers is shortly described (*Paragraph 4.1*), whereas in *Paragraph 4.2* the main microfabrication steps for the structures realization are summarized. Most part of this research activity is aimed at the characterization of the Au immobilization layer of the microcantilevers, as described in *Section 4.3*: after the first AFM and XPS analysis demonstrating non-uniformity and low content of Au, technical changes and a cleaning procedure are proposed as improvements (*Paragraph 4.3.1* and *4.3.2*). Besides the surface analysis, Chapter 4 reports the study of the functionalization procedure (*Section 4.4*). More precisely, after an introduction on functionalization procedures, this section is divided into *Paragraph 4.4.1* and *Paragraph 4.4.2* which describe the deposition of phosphate buffer and fluorescein on the microfabricated cantilever arrays, respectively. Also this Chapter reports, at the end, the conclusions summarizing the research steps and the achieved results (*Paragraph 4.5*).

In ***Chapter 5 "Conclusions"*** main activities and results are reported and discussed. In particular, similarly to *Chapter 2*, this final part of the thesis is divided into two sections. The first one (*Section 5.1*) reports the results concerning the Lab-on-Cell platform; the second one those regarding the cantilever-based array sensors (*Section 5.2*). More precisely, the first part is focused on the electroporation protocol optimization (*Paragraph 5.1.1*) and on the improvements of the platform itself (*Paragraph 5.1.2*). The possibility to entrap the cells and to have internal reference electrodes is also discussed in *Paragraph 5.1.3*. New applications of the Lab-on-Cell are suggested in *Paragraph 5.1.4*. On the other hand, in the *Section 5.2* the problem of having a low content of Au and C contamination is discussed in order to find out possible solutions (*Paragraph 5.2.1*). Finally, starting from literature, the steps for the real usage of the proposed detection module in diagnostics are listed giving suggestions regarding biological protocols and procedures (*Paragraph 5.2.2*), from the sensitive layer generation to the DNA target hybridization and response evaluation. Future applications are cited in *Paragraph 5.2.3*.

Acknowledgments, ***Bibliography*** and ***Annexes*** sections complete this thesis.

Chapter 2

2 State of the Art

As introduced in *Chapter 1. Introduction*, thanks to the completion of the whole human genome sequencing, functional genomics and proteomics tools have recently gained significant attention. In fact, the interest towards gene analysis is increasing at different levels and especially aimed at study (1) function by delivering genes into cells and observing their relative expression; (2) sequence in order to detect DNA mutations for diagnosis purposes. The following sections *(2.1. Cell Transfection* and *2.2. Gene Sequence Analysis for Diagnostics)* summarize the main state of the art advances in both the analysis fields.

2.1 Cell Transfection

At present, it is well known that the plasma membrane represents the cell dynamic and flexible structural component mainly acting as selective barrier against molecules crossing [Alberts 2000]. It has been broadly studied in order to develop an efficient transfection method. The word *transfection* refers to exogenous DNA molecules transfer into receiving cells. Once transfected, DNA is generally maintained in the cell cytoplasm for two-three days. During this period, foreign genes undergo many regulative pathways which control the chromosomal material expression of the host cell. Subsequently, dilution and degradation phenomena cause the DNA loss in most cases. In fact, transient or stable transfections can be distinguished depending on the exogenous DNA integration or not into own chromosomes.

2.1.1 Mammalian Cell Transfection Techniques

In general, gene delivery into mammalian cells is inefficient per se, because it needs an abundant source of starting cells in order to assure an acceptable number of transfected

cells at the end of the experiment. For this reason, available cell lines able to continuously grow in culture can be employed for the routine assessment of new transfection procedures. An ideal transfection technique should ensure the following characteristics:

1. High transfection efficiency;
2. Low toxicity;
3. Reproducibility of the experiments *in-vitro* and *in-vivo*.

Nowadays, different techniques are used to deliver exogenous DNA into cells complying with the above requirements with peculiar advantages and showing specific drawbacks. In general terms, these techniques can be divided into four categories: (1) viral-mediated processes and (2) chemical, (3) mechanical or (4) physical approaches. The first group involves biological vectors such as adenoviruses and retroviruses in a process corresponding to cell infection [Anson 2004]. Preparation difficulty, immunity rejection and viral toxicity represent the main disadvantages [Chuah 2003]. Among the second category, chemical reagents exploit the DNA co-precipitation with calcium phosphate [Graham 1973] or the complex generation between DNA and a variety of polycations in polyfection (e.g. DEAE-dextran [McCutchan 1968]) or cationic lipids in lipofection [Felgner 1987]. They are not very expensive and the experimental procedure is simplified. Nevertheless, they do not guarantee a good transfection efficiency and they are prone to a certain variability. As a matter of fact, the DNA transfer is not direct, thus limiting the internalization and expression because of essential intermediate steps (i.e. cell attachment, endocytosis, complex dissociation). On the contrary, direct transfection techniques are represented by mechanical (microinjection, particle bombardment - *gene gun*) and physical (sonoporation, laser irradiation, electroporation) approaches. Mehier-Humbert et al. have highlighted their working principles, employed materials, advantages and limitations providing a complete summary according to the following performance criteria: transfection efficiency, toxicity, targeting and practicality [Mehier-Humbert 2005]. Microinjection represents the most direct method allowing the selective DNA delivery into specific cell compartments (e.g. cytoplasm or nucleus) by employing a glass needle controlled by a micromanipulator with the highest efficiency (up to 100%). However, it is too laborious. Moreover, the high cost, the application difficulty and the possibility to transfect only one cell at a time make it impractical for most researchers. In the so-called *gene gun* or *biolistic* technique (coming from biological and ballistic contraction) heavy metal particles carriers of sub-microgram quantities of

DNA per dose are accelerated to the sample. Thus, the transfection can indiscriminately occur in each cell compartment, interfering whether with cell structure or function. In general, physical approaches are well tolerated. By applying ultrasounds, sonoporation forms small transient pores mainly due to acoustic cavitation mechanism and improving cell permeability. The technique can be employed for the transfection of different tissues. In laser irradiation, the thermal effect changes the cell permeability in the laser impact region. This technique suffers from appropriate know-how requirement, expensive and cumbersome laser sources.

Among the physical methods, electroporation, also called electropermeabilization, represents one of the most employed transfection techniques. The traditional bulk electroporation generates transient nanopores in the plasma membrane of suspended cells by applying a homogenous electric field between two large electrodes at a distance in the range from mm to cm [Weaver 1996, Ho 1996].

2.1.1.1 Pore Formation and Resealing

Different models try to find the right explanation of the electroporation mechanism. Lipid membrane instability could be due to macroscopic factors, such as thinning and compression, or to the transition from hydrophobic to hydrophilic pores, more stable above a critical pore radius [Weaver 1993, Neumann 1999].

Nevertheless, there is a commonly accepted concept: nanoscale pores form as a consequence of the transmembrane potential increase which follows the application of a high voltage. More precisely, under an external electric field both the natural resting potential ($\Delta\Psi_0$, typically about -70 mV) and the induced membrane potential ($\Delta\Psi_E$) contribute to the potential difference across the membrane ($\Delta\Psi_m = \Delta\Psi_0 + \Delta\Psi_E$). In this context, electroporation occurs when $\Delta\Psi_m$ exceeds a critical threshold value ($\Delta\Psi_c$). Experimental procedures have determined this value to be in the range of 200 mV–1V and the relative critical electric field E_p from 100 Vcm^{-1} up to 10 $kVcm^{-1}$ depending on the cell type [Neumann 1972, Zimmermann 1974, Teissie 1993, Weaver 1993, Rols 2006].

The membrane permeabilization initially occurs at the cell pole facing the positive electrode. In fact, because of the negative interior of the cell membrane, that is the region

where the capacitance of the membrane is first exceeded when an external field is applied. The area of the membrane which is permeabilized depends on the pulse amplitude, whereas the degree of permeabilization can be controlled by pulse duration and pulse number [Gabriel 1997].

Nowadays, five steps are considered to be involved in pore generation mechanism: (1) Pores induction (< 1µs, ns range [Beebe 2003, Vernier 2006]) due to the application of the external electric field; (2) Expansion (µs-ms range) during which the pore density increases depending on the pulse duration. The higher the permeability, the higher the cell conductivity; (3) Stabilization or membrane reorganization. It occurs when the electric field decreases; (4) Resealing (from seconds to minutes). In absence of field the impermeability of cells is spontaneously recovered. Nevertheless, physical settings sensitively influence the electroporation result. Pores can be distinguished in transient (reversible/self-repairing) or not (irreversible) depending on parameters of external electric field, characteristics of the electroporation medium (conductivity) and of the cell (electric properties and shape) that is exposed to the electric field [Canatella 2001]. If these parameters are not suitable and accurately evaluated, irreversible electroporation takes place and cell death is inevitable.

2.1.1.2 Bulk/Batch Electroporation vs Single-Cell Electroporation

As for most of the traditional transfection procedures, one of the main limitations of bulk electroporation is the lack of spatio-temporal control over the process: it does not allow to select single cells (desirable requirement especially in highly heterogeneous tissues and primary cultures), and to monitor the transfection result in real-time. To circumvent these disadvantages, alternative microscale approaches are increasingly required. Single cell electroporation (SCEP) represents a promising tool in biochemical research, where manipulation and analysis at single cell level are required. Unlike bulk electroporation involving a homogeneous electric field applied to a whole cell population, SCEP is characterized by two possible working principles:

(i) Inhomogeneous electric fields focused near selected single cells;

(ii) Single cells isolation from their population in order to impose the electric pulses directly on them.

Moreover, the variety of outcomes typical of the bulk electroporation is replaced by the possibility to optimize the electroporation protocols (generally using pulses in the order of few volts) by directly looking into the single responses.
In the last years, different research groups have extensively reviewed the emerging SCEP techniques. A complete guidance comes from Wang et al. [Wang 2010]. Olofsson et al. have thoroughly discussed the multiplicity of systems employed to perform SCEP [Olofsson 2003]. Microfluidic single cell analysis has been also deepened with a brief introduction to SCEP chips [Chao 2008]. Moreover, Fox et al. have discussed electroporation by using microfluidic devices [Fox 2006].

2.1.1.3 Microfabricated Devices for the Electroporation of Target Cells

Currently, different methods are able to perform *in-situ* and *in-vivo* electroporation. Solid microelectrodes [Lundqvist 1998], modified Atomic Force Microscopy (AFM) silicon tips [Nawarathna 2008], electrodes filled with transfer material [Bestman 2006], Electrolyte Filled Capillaries (EFC) [Nolkrantz 2001, Agarwal 2009, Wang 2009] and micropipettes [Haas 2001 and Hewapathirane 2008 optimized the electroporation method for *Xenopus laevis Tadpodes*, Rae 2002, Rathenberg 2003, Pakhomov 2007, Uesaka 2008, Barker 2009] (also in combination with microelectrodes [Karlsson 2000, Ryttsen 2000, Alberg 2001, Tanaka 2009]) are employed as probes claiming a great spatio-temporal control over cell transfection.

Nevertheless, microfabricated devices are strongly emerging in this field for both manipulating selected cells in suspension or in adhesion.

Some of the most significant examples of microfabricated devices aimed at suspended cell electroporation are here reported. In 2001, Y. Huang and B. Rubinsky developed the first chip based on single cell trapping in microholes by pressure difference (between the top and bottom microfluidic chambers of a three-layered device) and electroporation by constricted field [Huang 2001]. In order to achieve high efficiency of gene transfection an improved device characterized by microfluidic channels was proposed by the same research group in order to handle cells in a flow-through manner [Huang 2003]. Electroporation using field constriction at micro-orifices was presented also by O.

Kurosava et al. in a more recent work demonstrating its application for the measurement of cell response to external stimuli [Kurosawa 2006]. In the integrated PDMS multiple patch clamp array developed by Khine et al. cells were laterally immobilized and electroporated at the end of microchannels [Khine 2005, Khine 2007, Ionescu-Zanetti 2008]. Channels and microholes are the main components of another successful example: gene transfer was performed in stem cells by employing a silicon glass device characterized by two channels connected by microholes acting as trapping sites [Valero 2008]. Single-cell electroporation by employing a planar micropore chip in combination with 2-D scanning vibrating electrode technology was also reported [Haque 2009].

Instead of entrapping cells at microholes or at microchannels opening smaller than the cells (as described up till now), in other systems electroporation occurs in channels or confined regions larger than the cells. A droplet-based microfluidic device was described: droplets containing cells flowed through two microelectrodes on the substrate [Zhan 2009]. The amplification of the electric field in the narrow region of a microchannel was exploited by Wang et al. for both lysis and electroporation [Wang 2006, Wang 2008]. Others performed cell lysis by electroporation, for example using 3D electrodes [Lu 2006] and a dielectrophoresis (DEP)-based chip [Ramadan 2006]. Ti/Pt electrodes deposited on a glass microscope slide were used to dielectrophoretically move and electroporate monocytes [MacQueen 2008]. Moreover, micropulsed radio-frequency was also employed in a chip allowing a 3D electric field distribution [He 2007]. Finally, among the most recent works, three groups have given great contributions in the microengineering field. Geng et al. improved the flow-through Wang's group electroporation chip described before with five narrow sections for the transfection of a large amount of cells [Geng 2010]. Andresen et al. proposed an injection molded chip comprising conducting polymer electrodes [Andresen 2010]. Moreover, both cell arraying and electroporation were carried out by Mottet et el. in a transparent LOC including 3D microfluidics and thick electrodes [Mottet 2010].

However, since most part of human body cells grows in adhesion and especially in case of mammalian cells there is an increasing cell line usage as model system similar to the *in-vivo* one, the development of microsystems well-suited for adherent cells electroporation is gaining more and more attention. A variety of mechanisms have been published. One of the first and easiest is represented by a defined cell culture cavity and thin-film electrodes parallel lines developed on a glass slide [Lin 2001, Lin 2003]. Moreover, gene transfection

was enhanced by employing an attracting field for DNA plasmids increasing their concentration close to the adherent cells [Jen 2004]. A porous membrane-based electroporation device was reported: cells were cultivated on a microporous alumina membrane and below it a polydimethylsiloxane (PDMS) film characterized by microholes was added. The electric field generated between two electrodes (one positioned above the cells and the other below the PDMS film) was concentrated in the areas defined by the holes allowing the selective electroporation of cells grown in those regions [Ishibashi 2007]. Alternatively, Vassanelli et al. proposed an array of planar cell-size microelectrodes (each one independently addressable) microfabricated in FBK facilities, allowing cells to be cultivated, randomly adhere and be selectively transfected [Vassanelli 2008]. Chang et al. employed pairs of thick and closely opposed microelectrodes to focus the horizontal electric field on targets (individual neuronal axons as reported example) in between them [Chang 2009]. PDMS was used also by Kim et al. for the development of a multi-channel electroporation chip able to generate multiple electric field gradients on the same device depending on the channel length were cells were cultivated. The high-throughput of the system (up to five channels) was exploited to simultaneously and easily analyze the cell response to increasing electric fields [Kim 2007]. Among innovative and extremely recent works, Koester et al. reported the new local micro invasive needle electroporation (LOMINE) carried out on the PoreGenic® chip consisting of DEP and needle electrodes array [Koester 2010]. Three-dimensional electrodes were employed also by Braeken et al. Their sub-cellular dimensions allowed to locally stimulate cardiomiocytes and single neurons *in-vitro* [Braeken 2009, Braeken 2010].

2.1.2 Cell-Substrate Interaction and Bioaffinity Requirements in Microsystems Field

Bioaffinity represents a fundamental parameter for the appropriate choice of the most suitable materials to develop BioMEMS-based devices aimed at *in-vitro* cell assays. The cell capability to recognize and interact with a substrate represents the first essential step allowing cell proliferation, migration and differentiation. In general tissue architecture and morphogenesis, cell adhesion follows a specific protein-mediated mechanism. These proteins are mainly integrins, a large family of heterodimeric transmembrane proteins that

transmit the signal from the cell surface to the thick network of cytoskeletal filaments that make up the cell scaffold. In particular, the interaction between cell surface integrin receptors and ExtraCellular Matrix (ECM) adhesion molecules generates a signal cascade followed by actin cytoskeleton reorganization and consequently the cell morphology change. The cell, initially round-shape (integrin inactivated state), then becomes spread (integrine activated state). This second morphological state represents an adhesion strengthening which involves focal adhesion junctions assembly and forces along the basal cell surface [Gumbiner 1996]. Also the complex nature of the interaction between cells and biomaterials has been studied and reviewed, giving a deep explanation about the molecular basis of this mechanism by means of transcriptomic and proteomic tools. The ECM composition is influenced by the substrate surface features. This aspect causes different integrins activation patterns and spatial arrangement, then reflected in the cell phenotype [Gallagher 2006].

In fact, it is well known that cell phenotypic behaviour and response strongly depend on the nature of the employed material. Its properties (i.e. roughness, chemical composition, wettability, surface functionalization or patterning, topographical features) cause specific cell response due to the direct contact of the cell culture with the substrate and altered phenotypes can also reveal altered cell functions, due for example to an incompatible substrate [Dewez 1999, Lampin 1997, Ito 1999, Berry 2004]. More specifically, the surface characteristics affect the serum protein adsorption layer which represents the real cell-substrate interface [Lynch 2007]. Cell-material interaction has been also studied by using microfabricated substrates [Petronis 2003, Digabel 2010].

As a consequence, microfabrication technology applied to cell culture is a topic constantly under study in order to develop enhanced system aimed at performing assays on cells grown in suitable conditions similar to the *in-vivo* microenvironment [Park 2003, Bhadriraju 2002].

In particular, the interest towards surface modifications for the development of biomimetic substrates aimed at cell culture and tissue engineering is more and more increasing [Healy 1999, Lan 2005]. Moreover, since *in-vivo* cells are surrounded by nanoscale topography, there is a strong attention towards nanotechnology for the development of biocompatible microsystems and also implantable biomedical devices [Sniadecki 2006, Polizu 2006]. In fact, nanoscale features are often integrated in order to influence cell adhesion and shape [Yim 2005, Bajaj 2007].

2.1.3 Moving beyond the State of the Art

A good biocompatibility and the possibility to perform multiple tests on the same chip represent necessary requirements, especially in perspective of high-throughput screening. Beyond the state of the art, the possibility to strictly control the delivery of different transfectant solutions toward specific areas of the same cell population represents one of the main goal. In fact, current methods usually allow the delivery of only one transfectant at a time. In this context, microfluidics is becoming an important feature in microdevices for cell analysis and system biology in general [Yi 2006, Szita 2010]. Beyond the multi-channel microsystem proposed by Kim et al. able to test different electrical protocols on the same chip (*Paragraph 2.1.1.3*), some other recent advances have been introduced in this field. From a structural point of view, Wang et al. developed a microfluidic cell array suitable for high-throughput cell screening. It is characterized by individually addressable chambers where different cells groups can be cultivated and different reagents can be delivered. However, they do not perform electroporation or gene transfection [Wang 2008]. Thus, the possibility to electroporate different cell groups with different transfectants represents a challenge for the development of real high-throughput Lab-on-Cell platforms.
In this context, the following thesis deals with a Lab-on-Cell for the electroporation of adherent cells. It is characterized by multiwells for cell confinement, a microfluidic structure based on independent channels and ns-TiO_2 functionalized electrodes for the improvement of cell adhesion specifically where the voltage is applied. *Chapter 3. Lab-on-Cell for Gene Transfection* is dedicated to this integrated platform.

2.2 Gene Sequence Analysis for Diagnostics

In the last decade the development of biological analysis systems has raised a great interest within the scientific community. Microsystems technologies are able to comply with the requirement of reduction of time, costs and increased sensitivity, by means of micro-Total Analysis Systems (μ-TAS). These integrated, miniaturized devices are capable to carry out different steps of an analysis technique all on the same chip [Lee 2004, West 2008]. In particular, a DNA-based μ-TAS, also called LOC, should perform the biological sample

treatment, amplify the DNA, and detect specific DNA sequences (oligonucleotides) on the same device [Anderson 2000, Campas 2004, Easley 2006]. Its main advantages are (1) improved performances related to higher sensitivity, throughput and automation of the analysis; (2) portability; (3) reduced costs because of minute sample and reagents volume consumption (microlitres); (4) integration of many analysis steps which allows, starting from a crude sample (whole blood or saliva), to rapidly provide a genetic profile. Among possible applications, the key one is the Point-of-Care (POC) diagnostics which opens up new perspectives in the field of personalized medicine and treatment. In particular, BioMEMS, with the integration of microelectronics and nanobiotechnology, are enabling the realization of biosensors able to perform sample handling and to detect specific bioaffinity reactions (DNA/DNA, antigen/antibody, enzyme/receptor) by means of suitable functionalization procedures (covalent binding, matrix entrapment, cross-linking and adsorption) [Bashir 2004].

In literature, several research works devoted to the development of integrated LOC devices for DNA analysis have been presented. For instance Dobson et al. have reviewed the state of the art with respect to commercial or semi-commercial systems for POC applications [Dobson 2007]. In particular, it can be evinced that the first generation of LOCs for molecular diagnostics at POC level is mainly based on (quantitative-fluorescent) Real Time Polymerase Chain Reaction (RT-PCR) [Zhang 2007]. This method allows also multiple detections per assay by means of the so-called multiplex PCR [Edwards 1994]. PCR based systems are usually employed for pathogen detection by identifying one or few target sequences [Dobson 2007, Malic 2007]. However, also real array technologies are available in this context, allowing to detect a large number of SNPs or DNA sequences thanks to their multiplexed structure. Among the most employed techniques, DNA microarray technology [Pritchard 2008] is characterized by high-throughput capabilities, but needs, like RT-PCR, sample labelling procedures.

2.2.1 Micro-ElectroMechanical Systems (MEMSs) for DNA Hybridization Detection: Cantilever-based Arrays

The detection of a specific DNA sequence can be performed by exploiting the DNA hybridization phenomenon. This is the chemical reaction during which a single-stranded

DNA (ss-DNA) binds its complementary by means of base pairing (adenine with thymine and guanine with cytosine). Thanks to its simplicity it is more commonly used than the direct sequencing of DNA. Moreover, the hybridization process is very efficient and specific. The working principle is the following: if two ss-DNAs perfectly match they can bind each other, otherwise the hybridization does not completely occur. Thus, this reaction can be sensitive also to small variations such as a single base mutation between two strands, allowing the detection of SNPs often responsible for genetic diseases.

In this context, a great interest is currently given to the development of label-free detection systems: electrochemical [Drummond 2003], waveguide [Bliss 2007] and Surface Plasmon Resonance (SPR)-based [Boozer 2006, Abdulhaim 2008] methods. Among the electrochemical systems, Ion Sensitive Field Effect Transistors (ISFETs) [Fritz 2002, Kim 2004, Ingebrandt 2007] and potentiometric systems [Numnuam 2008] have been reported in literature. In general, electrochemical methods are characterized by high sensitivity and SNPs detection capability. On the other hand, devices based on SPR have been also used to detect DNA hybridization with high sensitivity results. On the market some laboratory instrumentations are available, like the Biacore S51 [Myszka 2004]. However, SPR is difficult to implement in miniaturized portable systems because of the measurement principle requiring the precise alignment for the optical excitation and detection parts [Abdulhaim 2008]. Other approaches encompass optical biosensor Microsystems; they are based on the integration of highly sensitive Mach-Zehnder interferometer devices [Sepúlveda 2006].

Nowadays, among a large number of MEMS-based devices developed in order to detect the DNA hybridization event, most of them are constituted by cantilever array sensors [Sepaniak 2002, Ziegler 2004]. Microcantilevers are typically silicon suspended bars (less than 1μm thick, from tens to hundred of μm long and some tens of μm wide, thus 0.01 the size of their macroscopic counterparts Quartz Crystal Microbalances - QCM [Wang 1997]) able to detect the interaction between a specific functional layer and the analyte of interest. Depending on the functional layer, they are suitable for chemical or biological sensing. In particular, if the cantilever surface is properly functionalized with a specific probe, able to selectively bind a particular target molecule, the device can behave as a chemical or biochemical sensor. Different sensitive films are available, ranging from polymeric coatings (polyetherurethane - PEUT, phthalocyanines, etc.) for gas sensing applications to DNA oligonucleotide probes for detection of specific gene sequences. In fact, if the functional layer is a Self Assembled Monolayer (SAM) constituted by known ss-DNA probes, a spe-

cific oligonucleotide sequence, present in a unknown sample, can be easily detected. In case of complementary target, the following hybridization induces a differential stress between the top and the bottom surfaces of the cantilever, driving the deflection of the beam [Fritz 2000]. Cantilever-based sensors are extremely versatile; they can be operated in air, vacuum, or liquid. They can be mass-produced by means of micromachining as miniaturized sensor arrays increasing their potentiality as low cost devices with high performances, high level of integration and portability [Raiteri 2001, Baller 2000, Rasmussen 2003, Datskos 2004]. In spite of the large availability of cantilevers for AFM, silicon, silicon oxide, and nitride cantilevers for biosensing are rarely commercially available (e.g. CantiChip8 array of eight nanomechanical cantilevers with integrated electrical read-out [Cantion]). Cantilevers are present with different shapes, dimensions, and force sensitivities capable of measuring in the 10–11 N range at the levels of single molecular interactions.

The adsorption of target molecules on the microcantilever sensitive layer induces both an increase of cantilever mass and the generation of superficial stress. Therefore, two different working modes can be used for cantilever-based measurements: the dynamic and the static mode, respectively [Datskos 2004, Ziegler 2004, Lang 2005]. The former exploits the resonance phenomenon, the latter the deflection. However, both deal with beam bending and thus sometimes they can be contemporaneously exploited.

In dynamic mode a change in resonance frequency due to analytes adsorption is measured. In fact, the shift in the cantilever resonance frequency ($\Delta f = f_0 - f_1$ (Hz)) reveals the mass variations (with respect to the reference condition) due to the binding of target molecules ($\Delta f \rightarrow \Delta m$). The beam vibrates at its Eigen-frequencies generating a stress distribution and deformation typical for each resonance mode. In the first mode, the resonance frequency can be estimated by the simplified models reported in literature [Hansen 2001, Raiteri 2001, Datskos 2004, Ziegler 2004], where the structure is considered as a simple spring-mass oscillator. The mass variation with respect to the initial mass m_0 can be expressed as follows:

$$\Delta m = \frac{k}{4\pi^2}\left[\frac{1}{f_1^2} - \frac{1}{f_0^2}\right]$$

where k is the elastic constant

$$k = \frac{3EI}{L^3} = \frac{EWt^3}{4L^3}$$

with *E* that is the Young's modulus of Si, and *W*, *t* and *L* the width, thickness and length of the beam, respectively.

The resonance frequency f_0 for the first resonance mode is:

$$f_0 = \frac{1}{2\pi}\sqrt{\frac{k}{m^*}} = \frac{1}{2\pi}\sqrt{\frac{EWt^3}{4m^*L^3}}$$

where *m** is the effective mass that can be related to the mass of the beam, *m*, through the relation *m** = *nm*, where *n* is a dimensionless geometric parameter equal to 0.24 for a rectangular cantilever.

Therefore, both *m** and *k* are related to physical properties and geometry of the beam. Higher sensitivities can be achieved from thin, low-density devices.

Another important parameter is the quality factor Q which depends on the viscous damping of the cantilever vibration. The detection of the resonance frequency and the amplitude of the read-out for a given actuation intensity are strictly related to the quality factor, which can be estimated by $Q=f_0/\Delta f$ whose value increases when the measurement is carried out in vacuum. Q depends on the corrected cantilever mass, on the damping and on the natural circular frequency:

$$Q = \frac{\omega_0 \cdot m^*}{b}$$

where *b* is the drag coefficient for the beam motion and in first approximation it is proportional to the beam width and fluid viscosity. The efficiency of the resonance method is strongly affected in liquid environment, making the deflection mode more suitable for such applications. However, an improvement of the quality factor can be achieved by using a feedback system for the actuation, where the signal detected from the cantilever is fed to the actuator. This has been demonstrated to improve the read-out efficiency of orders of magnitude [Vidic 2003], making this approach usable also in liquid phase, although generally deflection mode can provide better performances in liquid. Actuation can be performed with several approaches, including integrated and discrete piezoelectric devices, electrostatic and magnetic induction set-up [Vidic 2003, Rogers 2003].

In deflection mode, bending of the cantilever δ, due to the chemical-physical reactions which specifically occur on one side of the beam, is measured. Nevertheless, the bending is related not only to the reaction-induced stress, but also to physical properties and geometry of the beam, according to the following equation:

$$\delta = \frac{3 \cdot L^2 \cdot (1 - \nu)}{E \cdot t^2} \cdot \sigma$$

where ν is the Poisson's ratio of the material and σ is the induced stress on the top side of the microcantilever.

Thin – low elastic modulus devices show best sensitivities in static mode, even if the thermal vibration noise increases by reducing the structure stiffness [Butt 1995]. In fact, compliant structures are preferred in deflection mode, while stiff and light structures are more suitable for the resonance one. This aspect must be taken into account when selecting the materials and technologies to realize a cantilever structure. Recently, polymeric beams (with Young modulus orders of magnitude lower then Si-based materials such as crystalline Si, SiO_2 and Si_3N_4) have been developed for static mode [Thaysen 2002, Calleja 2005, Johansson 2005]. Nevertheless, their stability in operative conditions should be investigated. Moreover, polymer-based technologies are not easily integrated with standard technologies and CMOS read-out with respect to other approaches.

Among the techniques employed to detect the cantilever bending (optical, piezoelectric and piezoresistive read-outs, electrostatic or electromagnetic based methods [Datskos 2004]), the most commonly used are the optical and piezoresistive read-outs [Carrascosa 2006], suitable for both the working modes.

In the optical read-out method it is possible to measure the absolute value of cantilever bending by means of a photodetector sensitive to the optical deflection of an incident laser beam. The need of a sophisticated alignment system for the optical beam makes this approach not really suitable in case of detection module with array architecture. The piezoresistive method needs a dc-biased Wheatstone bridge in order to measure the changes in resistivity of the cantilever material due to surface stress variations. For LOC applications where DNA-sensing properties are needed, the optical read-out is often employed because of its high sensitivity. Nevertheless, this method shows several significant drawbacks such as the possible beam refraction in liquid samples, high sensitivity to opacity and the difficulty to assure the collimation of the laser with the beam. The piezoresistive read-out reveals to be more suitable for the development of portable devices, due to its easiness of implementation into a microfabrication process [Mukhopadhyay 2005, Choundhury 2007].

Piezoresistivity is related to a carrier mobility change in semiconductors as a consequence of an induced stress. It can be exploited by different approaches [Creemer 2001] for sens-

ing events generating surface stresses: resistors, diodes and field-effect transistors with in general comparable sensitivities.

2.2.2 Moving beyond State of the Art

Nowadays, the feasibility of microcantilever-based DNA biosensors has been demonstrated for DNA detection in general and also for single-base mismatch identification [Fritz 2000, Hansen 2001, McKendry 2002, Alvarez 2004, Mukhopadhyay 2005, Stachoviak 2006, Yang 2008]. However, even if the integration of an electronic interface realized with a CMOS technology has been also proven [Verd 2005, Yu 2007, Yu 2008], this technique is not still consolidated for real diagnosis purpose. In fact, a real LOC with an integrated cantilever array is not yet available for this type of application. Moreover, the development of high density arrays, comprising from ten to thousands of differently functionalized cantilevers, represents one of the most important challenges in genomics. In fact, high-throughput platforms are becoming more and more requested in order to allow real-time, fast and simultaneous detection of a variety of DNA sequences, especially polymorphisms for diagnosis purpose. Compared to the current high-throughput DNA microarray technology [Pritchard 2008], cantilevers arrays are a promising alternative, because they permit the direct analysis of molecules without need of fluorescent labels. Since the labelling procedure is a compulsory step in almost all the routine tests, time consuming and very expensive, the cantilever-based technology will improve the genetic analysis in terms of time and cost effectiveness. The expected ultra-high sensitivity of the device (which can reduce or even avoid the need of DNA amplification, thus simplifying the structure of a LOC device), and the label-free detection mechanism could give a high added value to a diagnosis system.

However, apart from the intrinsic advantages coming from the development of cantilever-based systems, in literature less attention is given to the study of important preliminary phases such as the surface analysis and cantilever functionalization. For example, Tabard-Cossa et al. reported the study of the effect of morphology, adhesion, cleanliness of the sensitive layer on surface stress measurements [Tabard-Cossa 2007]. Also Desikan et al. evaluated the effect of nanometric morphology on the stress sensing properties [Desikan 2006]. Others analyzed the ink-jet printing method for the functionalization (immobiliza-

tion of probes) on microcantilevers [Bietsch 2004]. For this reason, a deeper knowledge of the immobilization layer (and how to optimize it) is still needed also in order to circumvent difficulties during the practical application.

Regarding these aspects, the thesis deals with the analysis of the immobilization layer of microcantilever arrays which will be integrated in a LOC for autoimmune diseases diagnostics. The necessity of further optimization and the functionalization procedure have been also discussed. *Chapter 4. Cantilever-based Sensors for Gene Analysis* is dedicated to these studies.

Chapter 3

3 Lab-on-Cell for Gene Transfection

3.1 Comparative Bioaffinity Studies for in-vitro Cell Assays on MEMS-based Devices

In order to choose the optimal materials for the Lab-on-Cell microfabrication bioaffinity studies were performed. Moreover, since there was an increasing attention toward nanoparticle-assembled materials for the development of biocompatible devices (see *Paragraph 2.1.2. Cell-Substrate Interaction and Bioaffinity Requirements in Microsystems Field*), a comparative analysis was carried out to check cell growth and morphology differences also on ns-TiO_2 films.

3.1.1 Candidate Substrates for Bioaffinity Tests

Different candidate substrates were chosen among those most employed for the development of MEMS-based devices [Maluf 2004, Beeby 2004] and deposited on Si wafers where an oxide layer (300 nm) was previously grown as adhesion interface. Both substrates and employed microfabrication technologies are listed in Table 3.1.

Table 3.1. Substrates and relative microfabrication technologies employed for bioaffinity study.

Substrates	***Microfabrication technology***
Ti (120 nm)	Sputtering
Si_3N_4 (100 nm)	Plasma Enhanced Chemical Vapour Deposition (PECVD)
SiO_2 (18 nm)	Plasma Enhanced Chemical Vapour Deposition (PECVD)
Au (150 nm)	Evaporation: electron beam deposition
Pt (150 nm)	Evaporation: electron beam deposition

More precisely, SiO_2 was deposited over a 100 nm Si_3N_4 layer and an intermediate layer of Cr (5 nm) was used as adhesion promoter for Au and Pt layers. These two substrates were also subjected to an hard bake (30 min, 190°C) in order to improve the metal adhesion.
Then, each wafer was treated with an oxygen plasma in order to remove organic compounds. Finally, the wafers were cut by means of a dicing saw.
As shown in the schematic sketch (Figure 3.1), a comparison between the materials reported in Table 3.1 (Zone 1), fabricated in FBK facilities, and ns-TiO_2 film (Zone 2) was carried out by depositing the last one on approximately one half of each substrate, while masking the other half. In Figure 3.2, two examples are presented.

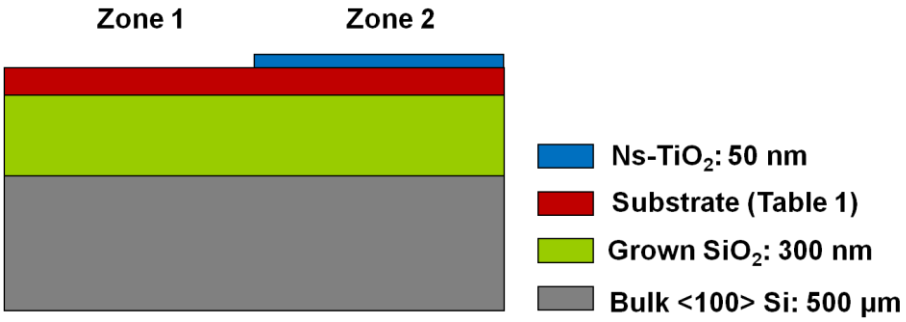

Figure 3.1. General cross-section of the deposited materials.

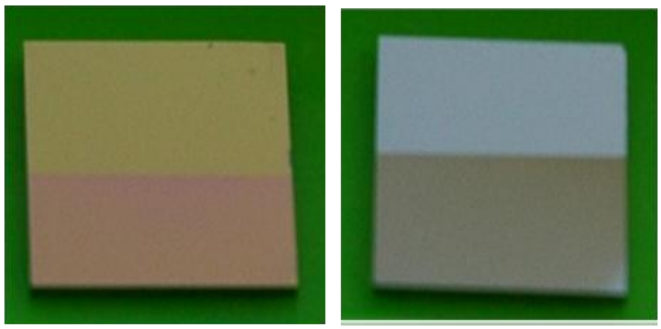

Figure 3.2. (*Left*) Au and (*Right)* Ti substrates (20 mm x 20 mm) functionalized with ns-TiO_2.

3.1.2 Cluster-assembled TiO_2 Film Deposition and Characterization

TiO_2 films were deposited by means of Supersonic Cluster Beam Deposition (SCBD) technique [Wegner 2006]. A Pulsed Microplasma Cluster Source (PMCS), developed by IFN-CNR (Trento) was employed and the same research group carried out the deposition [Toccoli 2003].

This method is suitable for the assembly of nanostructured and nanocrystalline metal oxides films in a Ultra High Vacuum (UHV) apparatus. The source, schematically shown in Figure 3.3, is based on the expansion of a neutral gas in vacuum with a fixed percentage of oxygen ($He+O_2$ 0.1%).

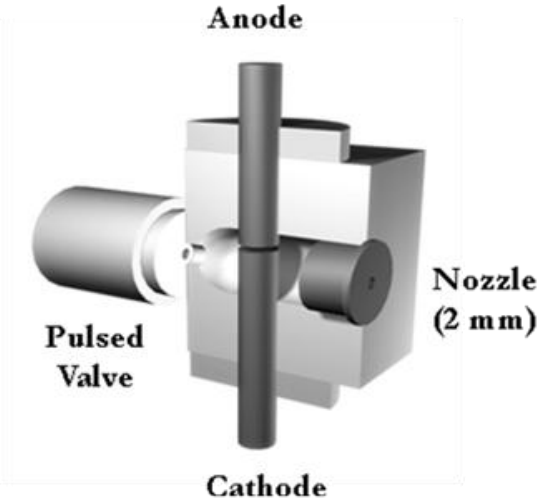

Figure 3.3. The Pulsed Microplasma Cluster Source (PMCS) employed for the substrate functionalization with ns-TiO_2 (IFN-CNR, Trento).

The gas mixture goes through a pulsed valve into a small chamber, where directly flows on two metal Ti electrodes. Between the electrodes a pulsed synchronized high voltage discharge causes the seeding of the beam by clusters of Ti that, combining with O_2, forms nanoclusters of TiO_2 of different shape and size. The distribution of clusters exits from the source forming a seeded beam that goes to hit the substrate in the deposition chamber generating a ballistic growth of clusters. The deposited film features strongly depend on the set-up conditions (i.e. expansion parameters and discharge characteristics).

Besides the deposition, IFN-CNR (Trento) and CNR-Licryl Laboratory-CEMIF.CAL (Department of Physics, University of Calabria) analyzed the obtained film. In detail, the optical, morphological and structural characterization of the TiO_2 was carried out by means of Spectroscopic Ellipsometry (UVisel, Jobin Yvone) [Vedam 1998, Losurdo 2002, Kaminska 2005], Scanning Electron Microscopy (SEM) [Goldstein 2003] and local micro-Raman analysis [Ferraro 2003] by means of a microprobe set-up (Labram, Horiba-Jobin-Yvon), respectively.

More precisely, an *in-situ* spectroscopic ellipsometer allowed to evaluate and control in real-time the film thickness (average thickness 50 nm) during the deposition or at defined

growth stages of the film (spectra not shown). Moreover, SEM technique gave information about grain structure and relative dimension. Figure 3.4 shows the typical morphology of the produced ns-TiO_2 films.

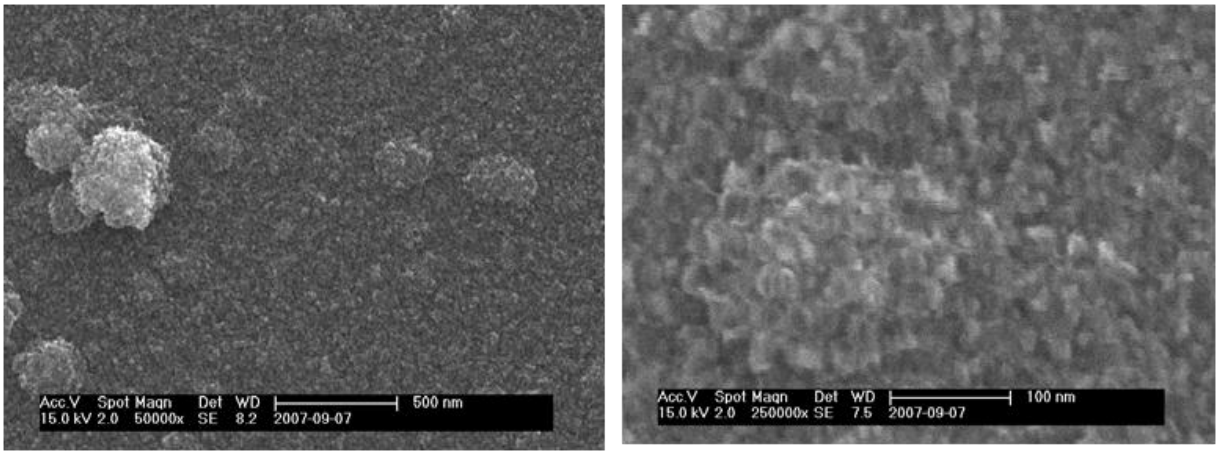

Figure 3.4. (*Left*) SEM micrographs of one TiO_2 sample grown by means of PMCS source; (*Right*) The high-resolution image shows the typical nanostructured morphology of the films with an average grain dimension of 10 nm (IFN-CNR, Trento).

The micrographs reveal that the assembling of clusters grows the film. At higher magnification grains dimensions can be clearly assessed: the morphology of ns-TiO_2 film is characterized by nano grains ranging from 8 to 20 nm in size, with the presence of distributed larger clusters in the micron scale. This kind of morphology presumes also a high porosity present in the films, confirming the result achieved with the data extracted by the ellipsometry where the films showed a porosity of about 50%.

CNR-LICRYL Laboratory - CEMIF.CAL (Department of Physics, University of Calabria) performed a micro-Raman analysis on the larger clusters revealing a crystalline structure of TiO_2 mostly in the Anatase phase. In Figure 3.5, a typical micro-Raman spectrum of the larger micrometric grains of TiO_2, showing a predominant Anatase phase.

In fact, the three E_g modes predicted for Anatase [Giarola 2010], a strong peak at 151 cm^{-1}, a shoulder at about 200 cm^{-1} and a broad band at 633 cm^{-1}, as well as one of the B_{1g} mode at 409 cm^{-1} are clearly observable. The one-phonon peak of the c-Si substrate, occurring at 520 cm^{-1}, prevents the observation of the two Anatase modes, B_{1g} and A_{1g}, usually expected in that frequency range [Giarola 2010]. Modes assignable to the other TiO_2 phase, Rutile, are also clearly detected: a weak band at about 240 cm^{-1}, usually defined as disorder-induced [Balachandran 1982] and the Eg mode, at about 450 cm^{-1}, as a shoulder of

the 409 cm^{-1} Anatase mode. Finally, two–phonon scattering from Si substrate generates two weak and broad peaks at about 300 and 970 cm^{-1} in the observed spectrum. The large bandwidths of the modes and the frequency shifts with respect to the values commonly reported in literature [Giarola 2010] could indicate small size crystal domains and strained structures in the deposited TiO_2.

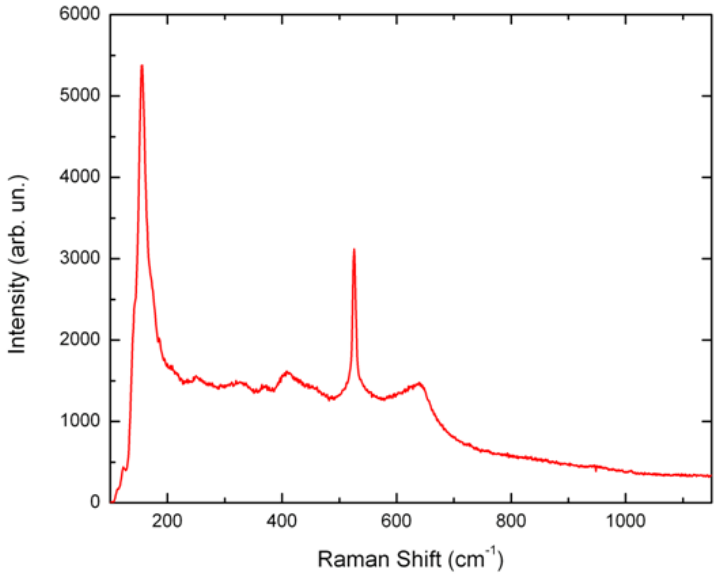

Figure 3.5. Micro-Raman spectrum on a grain of TiO_2 deposited on c-Si. Excitation source was the 633 nm line of He-Ne laser. A notch filter allowed the observation only above 150 cm^{-1} (CNR-LICRYL Laboratory , University of Calabria).

The deposition parameters were optimized in order to obtain the maximum of controlled crystalline Anatase phase. More precisely, the crystalline structure was maximized by setting 450 ms opening time and 1250 V discharge voltage.

3.1.3 X-ray Photoelectron Spectroscopy (XPS) Analysis of the Substrates

Before evaluating the substrates bioaffinity, a deep investigation about the surface nature was necessary. In fact, as explained in *Chapter 2* (*Paragraph 2.1.2. Cell-Substrate Interaction and Bioaffinity Requirements in Microsystems Field*), the phenotypic behaviour of cells strictly depends on material properties (i.e. hydrophobicity, charge, chemical composition, roughness) [Dewez 1999, Ito 1999].

In this context, besides the SEM analysis which clearly revealed the nanometric structure and porosity of the cluster assembled TiO_2 films, the analysis of the substrates chemical composition represented another relevant step before the biological response assessment.
The atomic concentrations of TiO_2 film and of the selected materials (Table 3.1) were determined by XPS [Barr 1994] (tilt 30°) analysis (Scienta ESCA 200 instrument equipped with a hemispherical analyzer and a monochromatic Al KR (1486.6 eV) X-ray source in transmission mode). A representative chemical composition of all analyzed ns-TiO_2 films deposited on the different substrates is reported in Table 3.2.

Table 3.2. Atomic concentration of TiO_2 film deposited by PMCS as determined by XPS surface analysis (tilt 30°), expressed in percentage (MiNALab-FBK).

N***anostructured film***	***O (%)***	***C (%)***	***Ti (%)***
TiO_2	44.4	39.7	15.8

Chemical composition of substrates resulted as expected in terms of atomic concentration (Table 3.3).

Table 3.3. Atomic concentration of the analyzed materials as determined by XPS (tilt 30°), expressed in percentage (MiNALab-FBK).

Substrates	***O (%)***	***C (%)***	***N (%)***	***Si (%)***	***Ti (%)***	***Au/Pt (%)***
Ti (Sputtering)	43.1	41.9	-	-	15.0	-
Si_3N_4 (PECVD)	33.9	16.4	12.3	37.3	-	-
SiO_2 (PECVD)	44.4	23.9	-	31.7	-	-
Au (Electron beam)	19.8	50.7	-	-	-	29.5
Pt (Electron beam)	22.7	42.3	-	-	-	35.1

However, XPS analysis revealed the presence of carbon contaminations with percentage values ranging from 16% to 50%. It is a common evidence that samples exposed to the air for a certain time before the XPS analysis can be affected by contaminations.

3.1.4 Materials Bioaffinity: Cell Viability and Morphology Studies

Once evaluated the chemical properties of the candidate materials (functionalized on one half with ns-TiO_2), the bioaffinity degree of the same substrates was studied.

Since each sample was characterized by both treated and non-treated areas, it was possible to contemporarily investigate the bioaffinity degree of the same cell culture on these two different surfaces.

After a deep cleaning of the substrates (sterilized in 70% EtOH and rinsed with deionised H_2O), bioaffinity was assessed by performing cell culture on different samples. For this purpose, the substrates were placed in a 12-well Tissue Culture PolyStyrene (TCPS) microplates (Falcon) and SKOV-3 human ovarian carcinoma cell line (American Type Culture Collection, ATCC) was cultivated in adhesion (5.000 cells/cm^2) following the standard procedure on polystyrene (*Biological protocols for SKOV-3 cell line maintenance and culture on substrates* are reported in *Appendix A, Paragraph 1*). As control experiment, the same polystyrene microplates were used and cells were directly cultivated on them. Samples and controls were maintained at 37°C in 5% CO_2 atmosphere.

Short-term viability assay (24 hours after plating) was performed by incubating cells with 0.5 µM Calcein AcetoxyMethylester (Calcein AM, Molecular Probes) for 10 min. Calcein AM is a cell viability marker. It is a non-fluorescent compound able to cross the viable cells membrane. Inside the cell it is hydrolyzed by endogenous esterase becoming a green fluorescent anion molecule retained in the cytoplasm.

The result was observed on opaque substrates by means of a direct fluorescence microscope (Leica DMLA), while an inverted microscope (OLYMPUS IX50) was employed for polystyrene control materials inspection. A CCD digital camera (Leica DFC 420C) was used in order to digitize images. Figure 3.6 shows the short-term viability assay result on a TCPS control.

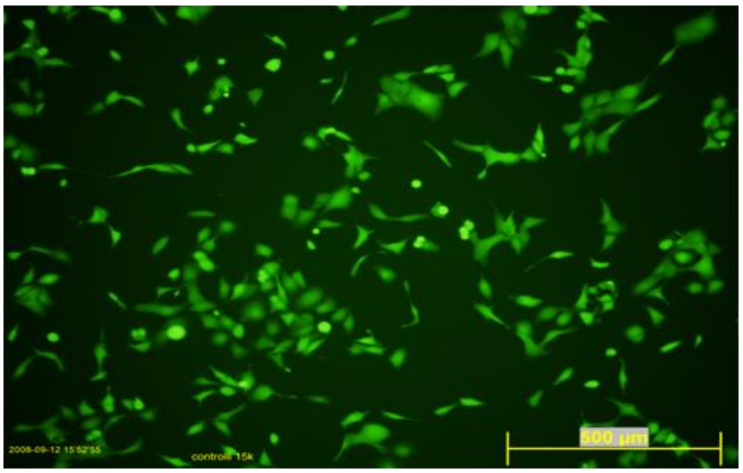

Figure 3.6. Fluorescence microscopy image of SKOV-3 cells grown for 24 h on TCPS as control, after staining with Calcein AM. 10X magnification.

Results of Calcein AM tests obtained on the microfabricated and functionalized materials are summarized in Figure 3.7. In general, these images reveal all a good bioaffinity of the employed materials, with a more evident higher cell density on Si_3N_4. Moreover, a homogeneous cell growth characterized every sample and no cellular debris were detected as sign of toxicity.

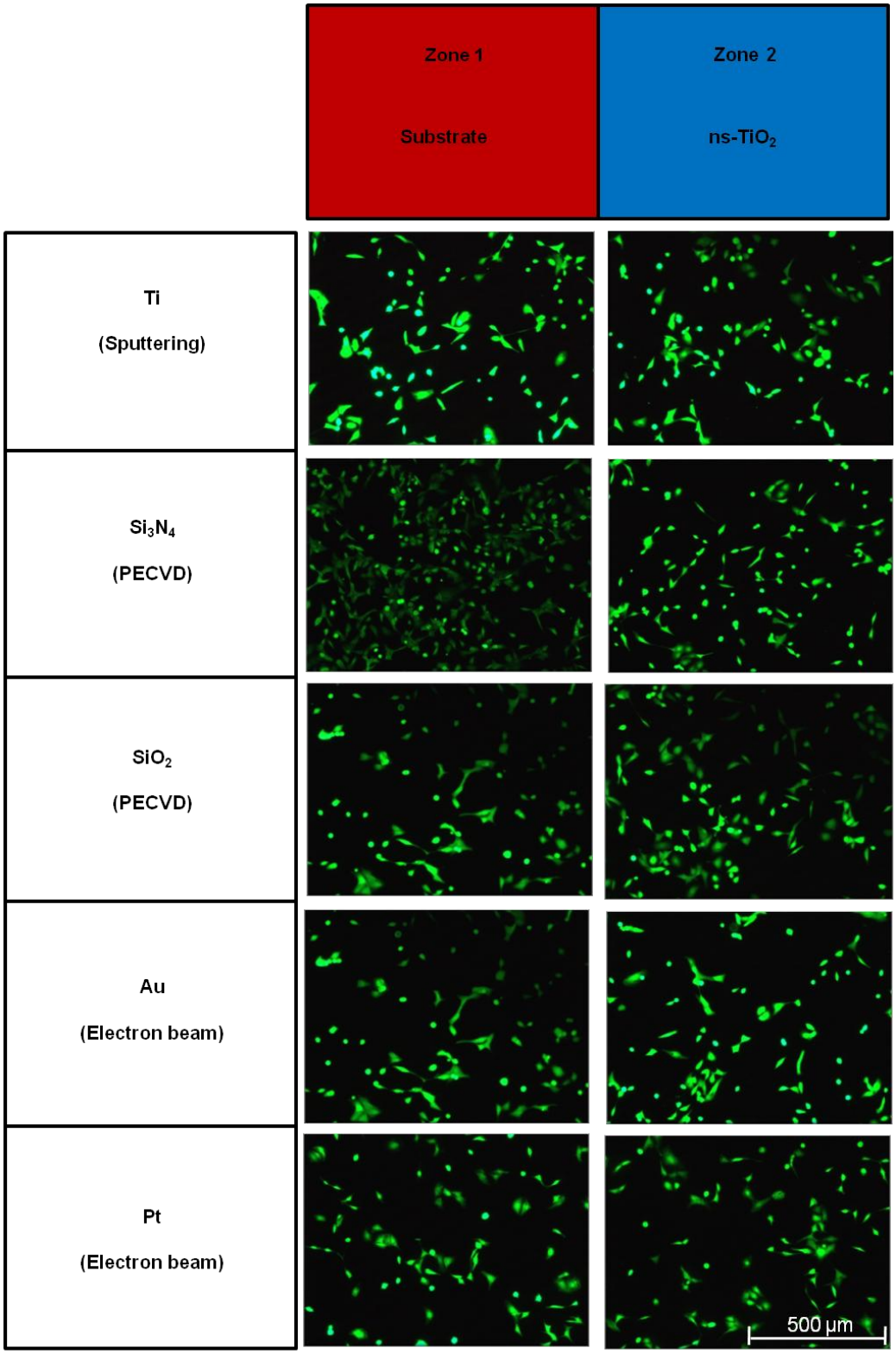

Figure 3.7. Fluorescence microscopy images of SKOV-3 cells cultured for 24h on Ti, Si_3N_4, SiO_2, Au, Pt, and on the same substrates functionalized with nt-TiO_2 films, after staining with Calcein AM. 10X magnification.

Since the Calcein AM assay is specific for the identification of viable cells, it represented a useful tool for a precise cell density evaluation. A direct counting of labelled cells on images allowed to calculate the *Viable Cell Density* for each type of substrate:

$$\textbf{\textit{Viable Cell Density}} = \text{total amount of viable cells/cm}^2$$

In particular, an average cell density was calculated considering six different regions per substrate: three in the ns-TiO_2 functionalized surface and three in the other one.
Moreover, in order to evaluate not only the best materials in terms of cell growth but also the effect of the ns-TiO_2 film on cell adhesion, a deeper analysis of the cells morphological appearance was carried out. Two main cell phenotypes were identified: round-shape and well adherent spread cells, as marked in the example of Figure 3.8.

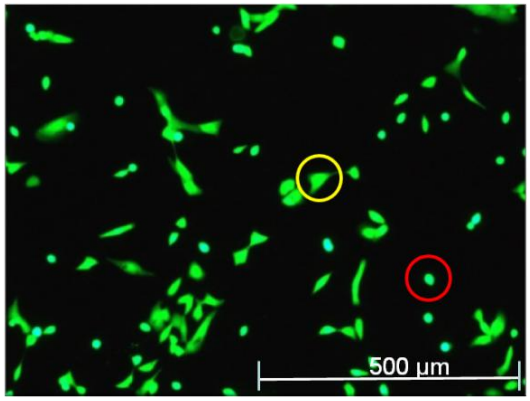

Figure 3.8. Cells morphological appearance: examples of round-shape cell (*red circle*) and well adherent spread cell (*yellow circle*).

The round-shape is typical of cells in suspension, while the spread one is characterized by a flat morphology due to the contact points generation among cells ECM and/or with the serum proteins adsorbed to the substrate surface [Lynch 2007, Eisenbarth 2002].
Given that the cell morphology reflects the cell response to the substrate (*Paragraph 2.1.2. Cell-Substrate Interaction and Bioaffinity Requirements in Microsystems Field*), the optimal condition was considered the spread one. The relative percentage was calculated as follows:

$$\textbf{\textit{\% Spread cells}} = (\text{Spread Cell Density}/\ \text{Viable Cell Density}) \times 100$$

Both quantitative (which considers the total *Viable Cell Density*) and morphological analysis (which considers only well adherent spread cells) are summarized in the histograms of Figure 3.9A and 3.9B, respectively.

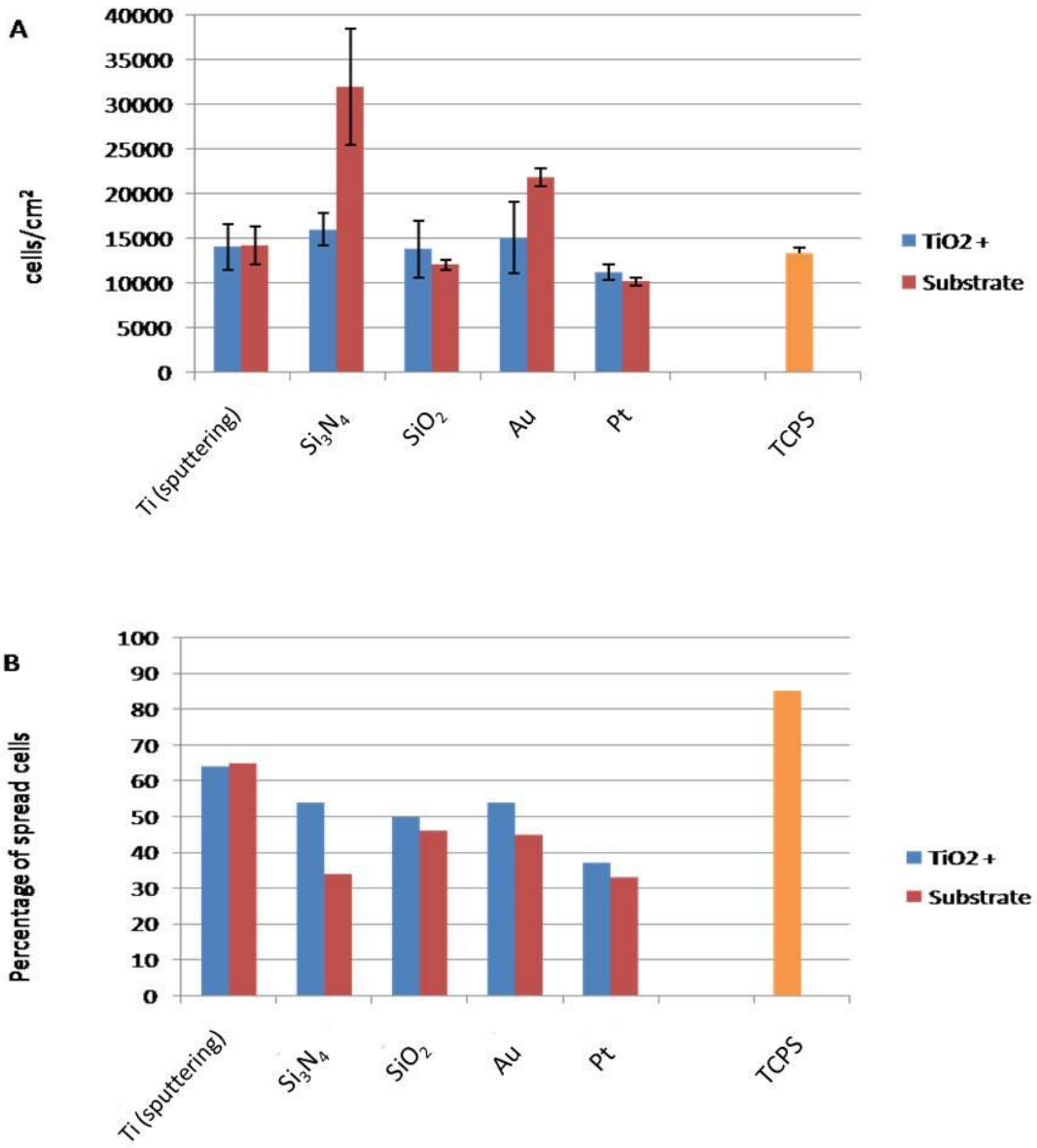

Figure 3.9. Quantitative (A) and morphological (B) analysis of SKOV-3 cells after 24 hours from plating. Cell density (cells/cm^2) and percentage of spread cells are represented.

After 24 hours cell densities on TiO_2 films and substrates were almost comparable or even higher (i.e. Si_3N_4 and Au) with respect to that observed on TCPS controls. However, if only well adherent spread cells were analyzed (Figure 3.9B), it was demonstrated that TiO_2 deposited by PMCS (TiO_2 +) increased the percentage of spread cells, suggesting that this

nanostructured material can promote cell adhesion, improving the bioaffinity of the candidate materials for MEMS-based devices.

3.2 Schematic Representation of the Integrated Platform for Cell Electroporation

The proposed integrated microsystem was designed in order to allow addressed cell electroporation and to control the delivery of different transfectants solutions into specific areas of the same cell population in perspective of high-throughput screening. The first requirement was satisfied by the development of a MicroElectrode Array (MEA)-based electroporation module, whose microfabrication substrates were chosen on the basis of the bioaffinity study results (*Paragraph 3.1.4. Materials Bioaffinity: Cell Viability and Morphology Studies*).

Secondly, the delivery of different transfectants was performed by pressure-driven flow through a microchannel-based fluidic structure integrated below the MEA and connected with it through crossing microholes. The working principle and structure of the Lab-on-Cell are summarized in Figure 3.10.

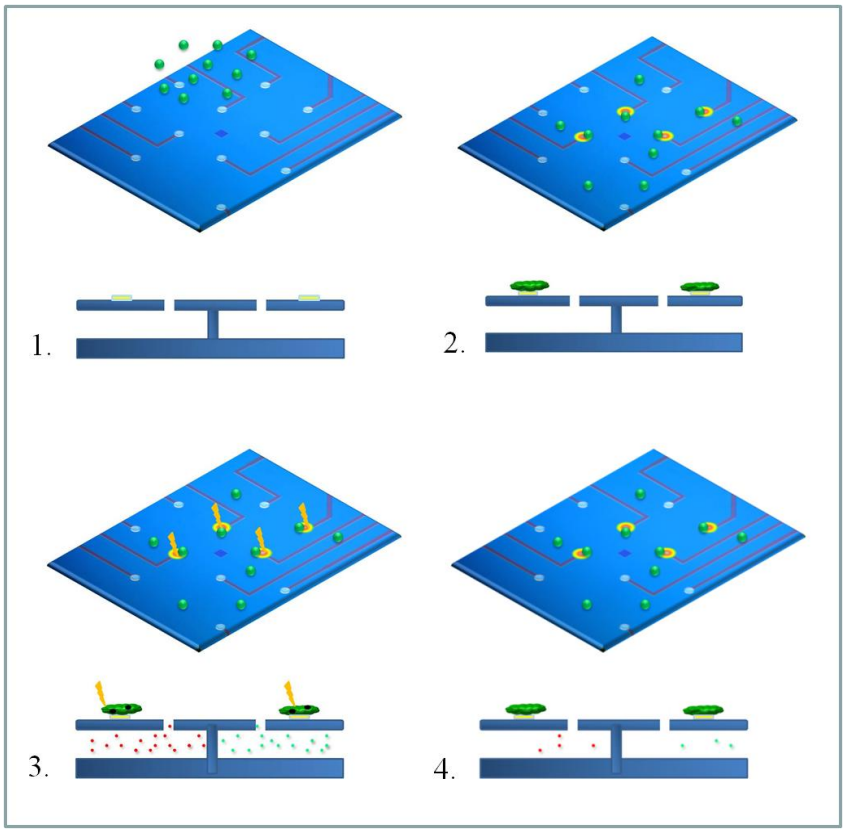

Figure 3.10. Schematic illustration of the Lab-on-Cell.

The device concept can be simplified in few steps: (1) Cell inoculum and plating; (2) Random adhesion of cells on MEA; (3) Transfectant solutions delivery through microfluidic channels and electroporation; (4) Pores resealing and electroporation result analysis by means of optical or fluorescence microscopy depending on the employed electroporation marker.

3.3 Electroporation Module Development

The comparative bioaffinity studies (*Section 3.1 Comparative Bioaffinity Studies for in-vitro Cell Assays on MEMS-based Devices*) allowed to choose the optimal materials for the device microfabrication, performed in FBK facilities. In particular, the selected materials suitable for the cell culture were:

- Au as electrodes metal
- Amorphous Si_3N_4 as passivation layer

  Both Au and Si_3N_4 had showed an optimal cell response in terms of viable cell density. In fact, the quantitative analysis (which considered the total viable cell density) had revealed a higher cell growth on these two substrates. Besides the great bioaffinity, Au is a good conductor and Si_3N_4 is completely impermeable to ions representing a suitable layer for the extracellular electrolyte insulation.
- Ns-TiO_2 for the functionalization of the electrodes active areas

  This type of functionalization was chosen in order to improve the cell adhesion specifically where the voltage was applied. In fact, the morphological analysis (which considered only well adherent spread cells) had demonstrated that TiO_2 increases the percentage of spread cells suggesting that this ns-material can promote cell adhesion. This parameter plays a key role in adherent cell electroporation, as it could improve the overall transfection efficiency.

3.3.1 MEA Microfabrication

The electroporation module consists in an array of planar microelectrodes. It was characterized by two levels of metal structures (buried connection lines made of Al 1% Si + Ti/TiN and Cr/Au electrodes) in order to reduce the fabrication costs, while improving the device electrical performances. Passing holes allowed the delivery of transfectants solutions from the microfluidic structure (integrated below the MEA) into desired areas of the chip (as anticipated in *Paragraph 3.2*). Wafer and chip layouts, and dimensions of each part are shown in Figure 3.11 and listed in Table 3.4, respectively.

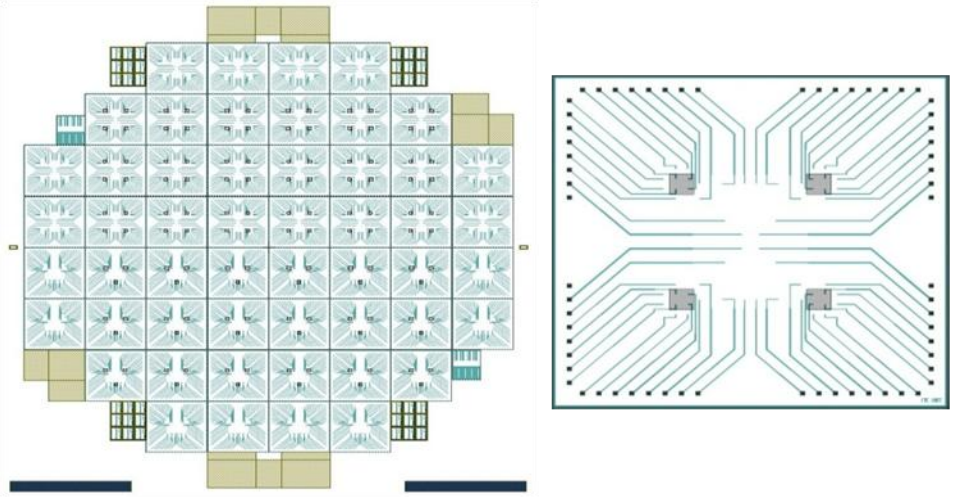

Figure 3.11. (*Left*) Wafer and (*Right*) chip layouts. Two structures were developed: with three or four groups of electrodes. On the right the example with four groups is shown.

Table 3.4. Geometrical parameters of the MEA-based module.

Parameter	***Value***
Electrode diameter	50 µm
Membrane dimension	20 - 60 µm
Holes dimension	3 - 4 µm
Chip dimension	1 cm x 1 cm

In detail, the microfabrication process, carried out by C. Collini, started from a 500 µm thick Si wafer (double side polished). A multilayer of dielectrics was grown and deposited on the top of Si ($SiO_2/Si_3N_4/SiO_2$ ~ 1 µm of thickness), in order to insulate the electrodes

and realize a tensile membrane for the injection system. An Al 1% Si + Ti (410/60 nm)/ TiN (140 nm) multilayer was deposited by sputtering and patterned by photolithography and plasma dry etching to define electrodes, lines and contact pin zones. A layer of Si_3N_4/SiO_2 (200/20 nm) was then deposited by PECVD for insulating the metal lines of the electrodes. Contacts were opened through the Si_3N_4/SiO_2 layer by a plasma dry etching. A layer of Cr/Au (5/150 nm) was evaporated and in order to define the electrodes photolithography and wet etching were carried out.

4 µm holes were opened across the electroporation module, more precisely in the middle of each well containing the transfectant solutions (see *Paragraph 3.4 Microfluidics Development and Final Packaging of the Integrated Platform*). In particular, the back multilayer of $SiO_2/Si_3N_4/SiO_2$ was patterned by photolithography and plasma dry etching to define the inlet regions, whereas the Si_3N_4 layer was patterned by photolithography to define the inlets on the dielectric membrane. A tetramethylammonium hydroxide (TMAH) wet etching step from the wafer back side was used to form the inlet zones. Then, the remaining multilayer membranes (with width varying from 20 to 60 µm and thickness of 1.2 µm) was etched by means of plasma dry etching to completely dig the holes (Figure 3.12).

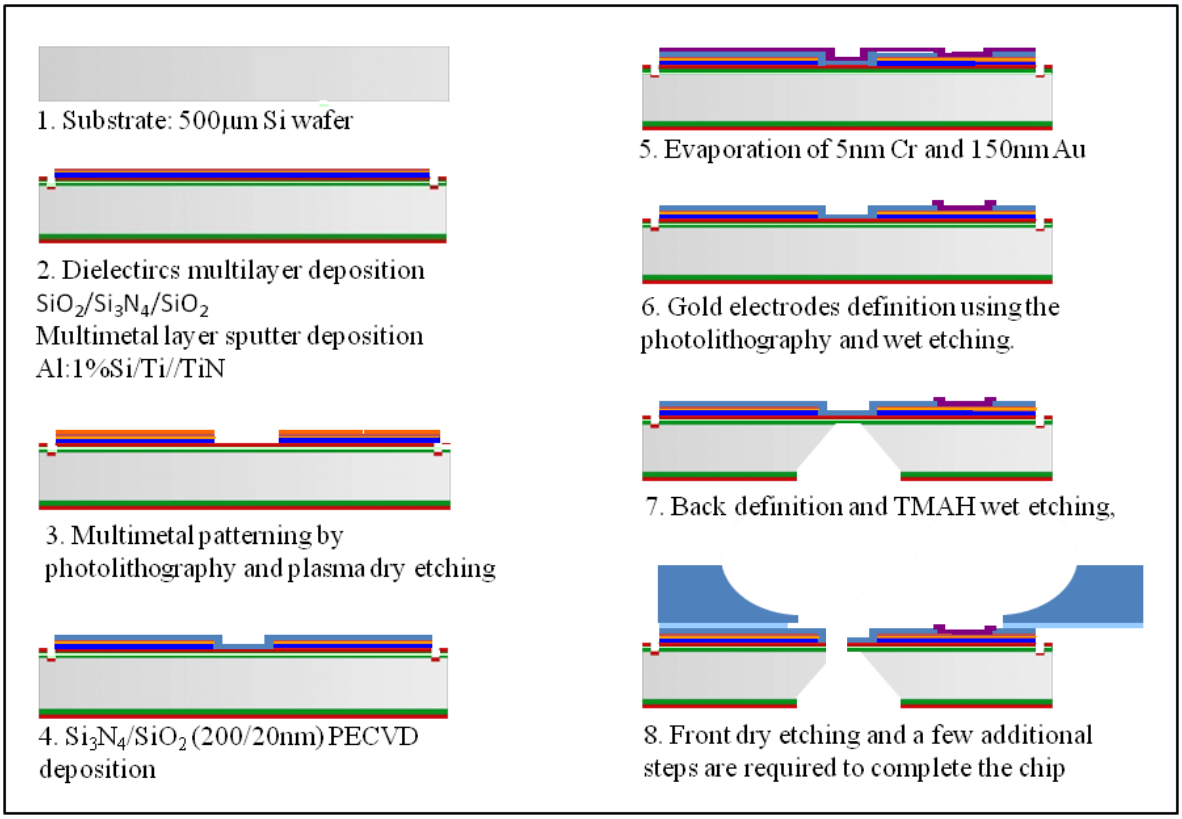

Figure 3.12. Fabrication process of the MEA-module. Only the main steps are here reported.

The result of the microfabrication process is shown in Figure 3.13.

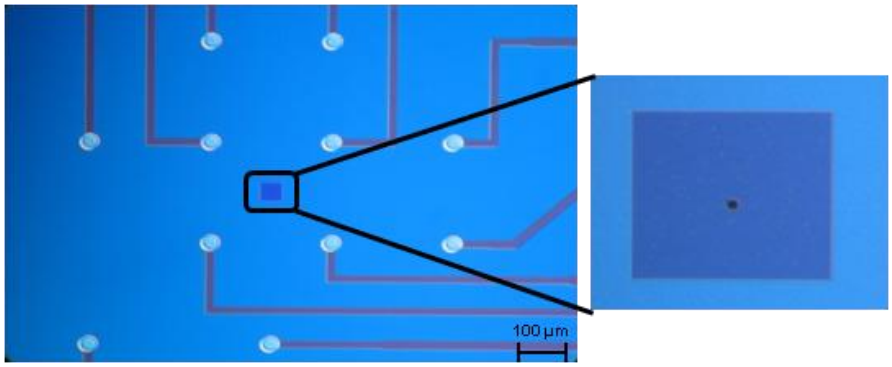

Figure 3.13. Microphotograph of the Au circular electrodes array (more precisely one region) and (*Inset*) the membrane of dielectric multilayer with passing hole.

3.3.2 Electrodes Functionalization with ns-TiO_2

After the fabrication of the microelectrode array (dry etching shown in Figure 3.12 (8)) additional steps were carried out. Amongst them, the electrodes functionalization with ns-TiO_2 by means of PMCS technique (*Paragraph 3.1.2. Cluster-assembled TiO_2 Film Deposition and Characterization*) in order to improve cell adhesion. The peculiar properties of PMCS make this technique suitable for the functionalization of microelectronic biocompatible devices, like the planar MEA. The films were deposited at room temperature (RT), without requiring any annealing post treatment which could damage the matrix of electrodes.

A fabrication step based on lithography [Levinson 2005] and lift-off was implemented in order to allow the functionalization of the Au electrodes, specifically in the active zone, where the voltage is applied to adherent cells. In particular, the whole device was covered with negative photoresist (MaN 1420, Microresist Technology GmbH) patterned in such a way to leave the active areas of the electrodes exposed to the beam. After the PMCS ns-TiO_2 deposition on the whole array surface, a lift-off procedure was carried out in order to remove both photoresist and unwanted TiO_2. The main steps and functionalization result are shown in Figure 3.14.

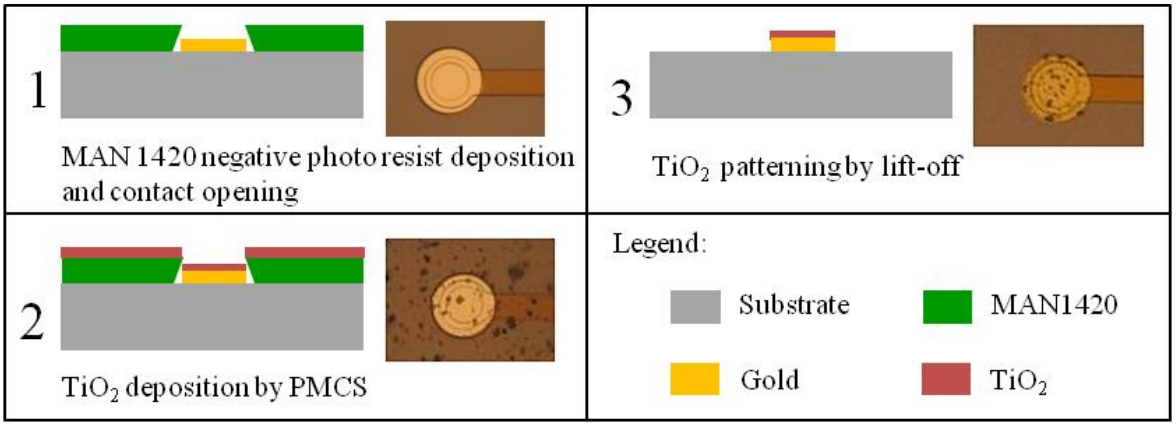

Figure 3.14. Lithography and lift-off combined process for the ns-TiO_2 functionalization of the electrode active areas: (1) microelectrode with patterned photoresist before ns-TiO_2 deposition; (2) TiO_2 deposition by means of PMCS on the whole electroporation array; (3) photoresist removal together with the unwanted TiO_2.

In Figure 3.14 (3), the TiO_2 deposition is visible only on the electrode, while the remaining regions are clean. The presence of microscopic droplets was due to characteristic process of the cluster formation, where the gas dynamic of the supersonic expansions allowed the aggregation of larger micrometric clusters, together with others in the nanometric range.

3.4 Microfluidics Development and Final Packaging of the Integrated Platform

The microfluidic channels were realized using a PDMS/Si hybrid structure. The fluid inlets were formed on a PDMS layer by using soft lithography techniques. This layer was then bonded on the back side of the Si electroporation device using oxygen plasma activation. Figure 3.15 (*Left*) shows a cross section of the microfabricated device with a detailed view of the employed materials, one hole and the relative microchannel. In order to complete the fluidic connections fused silica tubes were added. Finally, the chip was inserted in a custom Printed Circuit Board (PCB) and the packaging was completed with the addition of two different three-dimensional chambers:

1. An inner quartz multi-well chamber to contain small amounts of different transfectant solutions (each well of 2-3 mm diameter, ~ 20 µl total capacity). This chamber was realized by isotropically etching a 500 µm thick- quartz wafer. The glass wafer

was masked with 500 nm of undoped polysilicon and etched with 40% HF at an etching rate of 37.5 µm/hour. Then, it was glued on the chip with epoxy resin.

2. An external polystyrene chamber/plastic cap for the whole cell culture and medium confinement (27 mm diameter, 1 ml capacity).

Figure 3.15 (*Right*) shows a picture of the final packaged device. Some details of the packaging components are reported in Table 3.5.

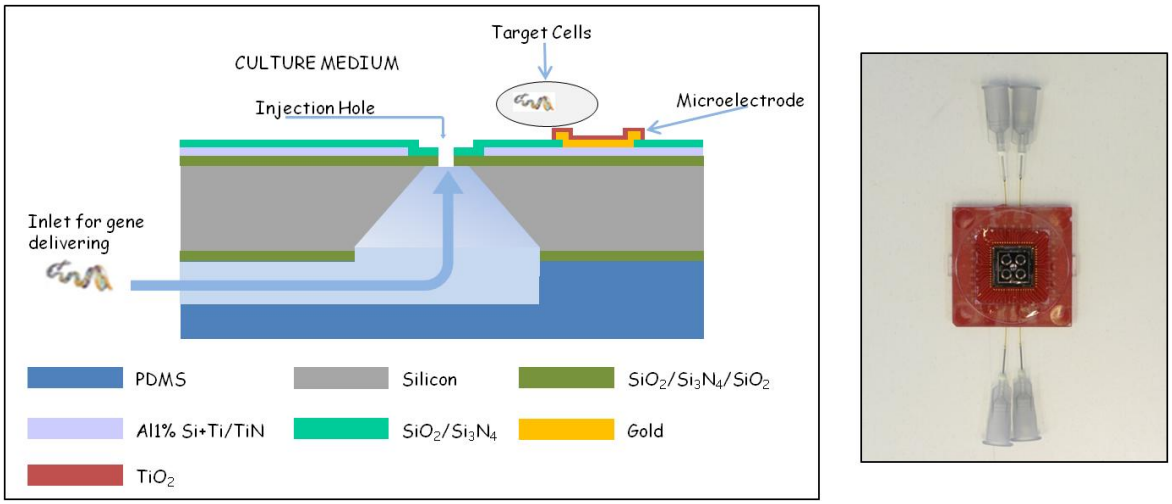

Figure 3.15. The integrated platform: (*Left*) Schematic cross section of the integrated system; (*Right*) Example of final packaged device with a 4-well inner chamber.

Table 3.5. Details of the packaging components and of the final device.

PCB dimension	~ 3 cm x 3 cm
Chip dimension	1 cm x 1 cm
Fused silica capillary tubes - inner diameter	150 µm
Fused silica papillary tubes - outer diameter	360 µm
Number of electrodes per well	12-18

3.4.1 Testing of the Microfluidics Structure

The robustness of the membrane and the effectiveness of the microfluidic approach feasibility were initially evaluated by using deionised H_2O fluxed through the capillary tubes. Figure 3.16 shows the electroporation chamber filling phases through the 4 μm hole. The membrane robustness was characterized upon different operating conditions.

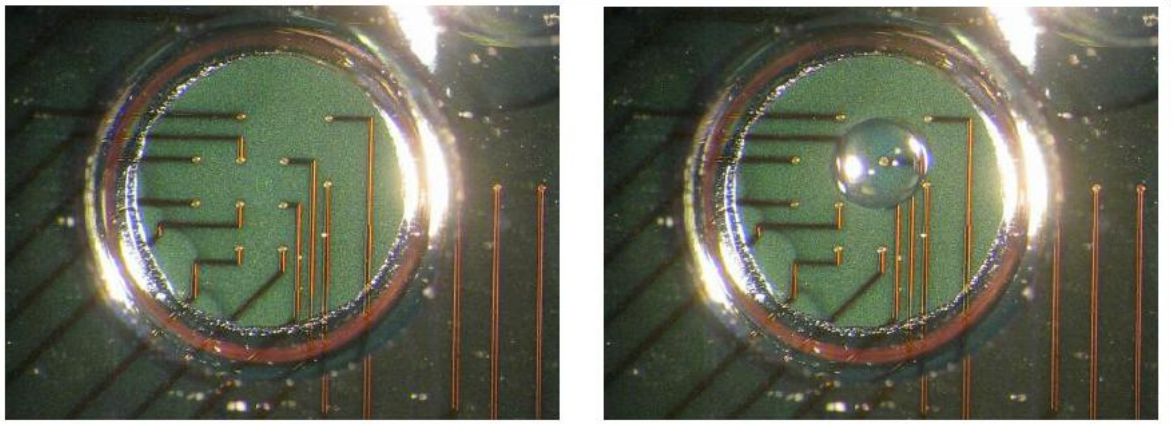

Figure 3.16. Microphotographs showing the chamber before (*Left*) and during (*Right*) the filling phase through the 4 μm hole.

Since the pressure-driven flow was generated by means of a syringe pump, it was quite difficult to ensure a fine control of both flow pressure and rate. However, no membrane breaking effects were observed during the procedure as well as after the complete filling of the microchamber.

3.5 Experimental Method for Cell Electroporation

Before starting the electroporation experiments, each chip status was checked under the stereoscopic microscopy (OLYMPUS SZX7). Moreover, since the wire bonding is manually performed and some defects can occur each chip was electrically characterized. An electrode addressing system and a PCB board with a PLCC (Plastic Leaded Chip carrier, Yamaichi) in which each integrated platform was mounted were employed. A standard solution with known conductivity (1413 μS/cm KCl, Crison) was used and each electrode connection signal was checked by means of 419A LF Impedance Analyzer (Hewlett Pack-

ard). Measurements were performed at 100 kHz frequency. An external Pt electrode was used as reference. Figure 3.17 shows the components of the experimental set-up for the electrical characterization of the devices.

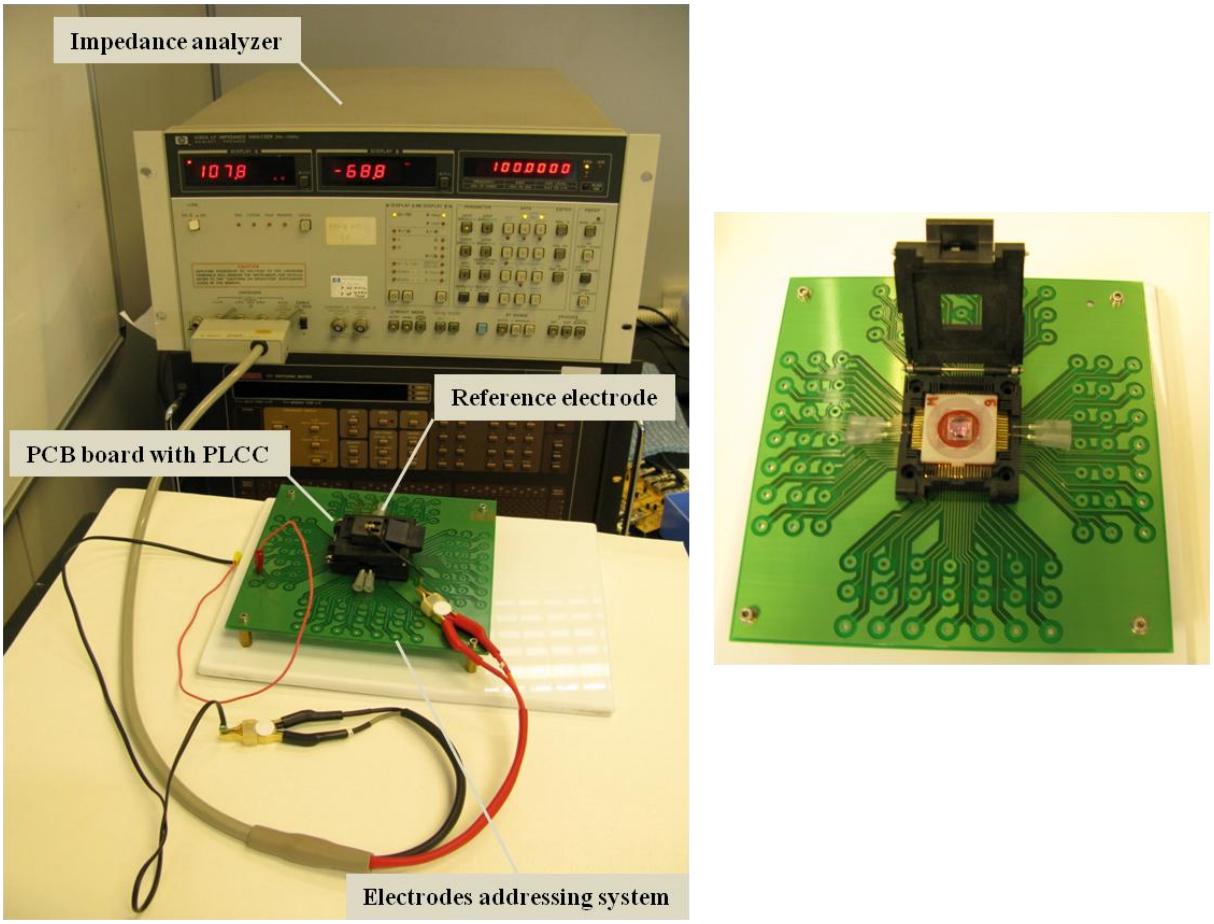

Figure 3.17. (*Left*) Complete experimental set-up for the electrical characterization of the devices: impedance analyzer, PCB board with PLCC, electrodes addressing system and a Pt reference electrode; (*Right*) Enlarged picture of an integrated platform placed on the PLCC and the electrodes addressing system.

Electrodes which gave open circuit were marked as not working and were not used in further electroporation experiments. A reference system was created in order to make the electrodes identification easier also for the subsequent electroporation choice and observation. In Figure 3.18 are shown two pictures employed for the identification of electrodes on 4-wells and 3-wells devices, respectively. They represent the electrodes addressing system with specified electrode numbers. The position of the respective electrodes on the chip is indicated in the inset. This system allowed to associate the signal reading or the voltage application (during the electroporation) to precise electrodes on the chip.

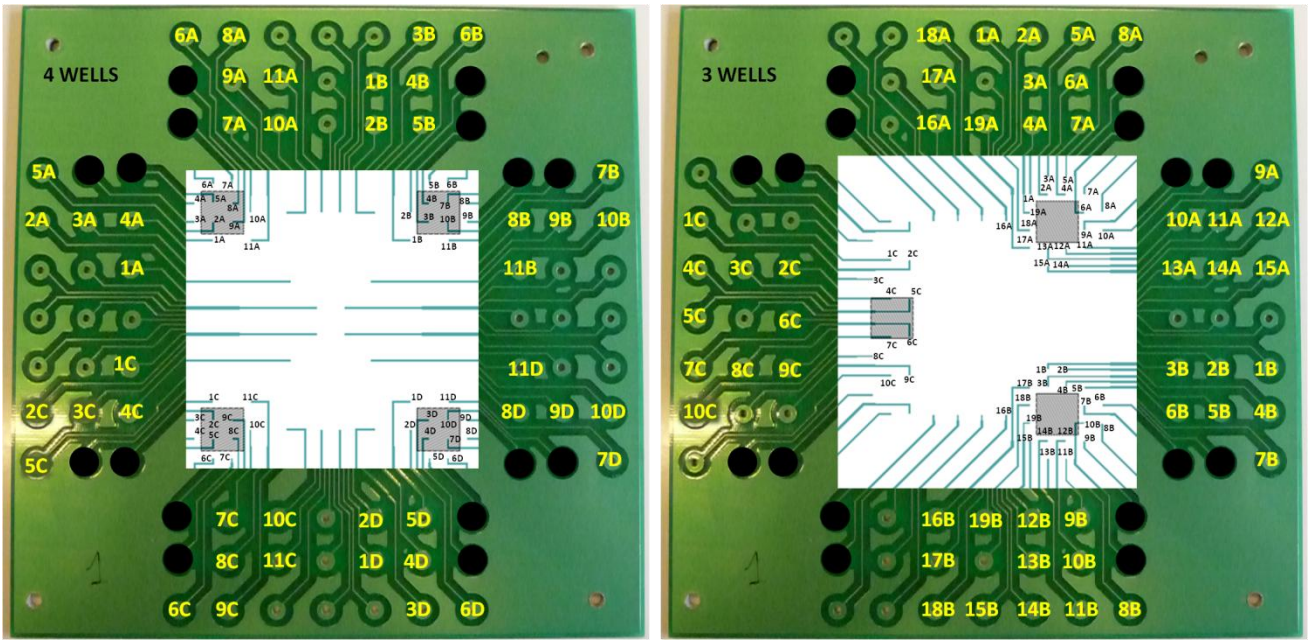

Figure 3.18. Electrode identification system on the addressing system.

Once electrically characterized the chips, and after a deep cleaning (Extran Soap, absolute EtOH and milli-Q H_2O), U.V. light sterilization and overnight equilibration of the biochip surface with culture medium, human cervical cancer HeLa cells (ATCC) were cultivated on the integrated platforms at CIBIO (University of Trento) (*Appendix A, Paragraph 2. Biological Protocols for Hela Cell Line Maintenance and Culture on Lab-On-Cell Integrated Microsystem*). 24 hours later, cell monolayer was rinsed with warm PBS in order to remove the not well adherent cells and it was carefully observed under the microscope in order to evaluate both cell distribution over the MEA and general morphology. Only the well working electrodes in presence of adherent cells were selected for the electroporation experiment. This analysis was performed in order to have a better control on the statistical evaluation of electroporation yield (see *Paragraph 3.6.1. Electroporation Efficiency*) and to identify after electroporation the following unwanted effects:

- False positives (labelled cells on not selected electrodes);
- Cell detachment in response to an excessively invasive electroporation protocol.

3.5.1 Electroporation Set-up

The electroporation set-up consisted of the same electrode addressing system (shown in Figure 3.17), a wave generator (Tektronix AFG3102) and a fluorescence microscope (Nikon Microscope Eclipse 90i) for the result analysis. For the optical inspection of the chip and cell culture status before the electroporation tests the OLYMPUS BX51M microscope was employed (Figure 3.19).

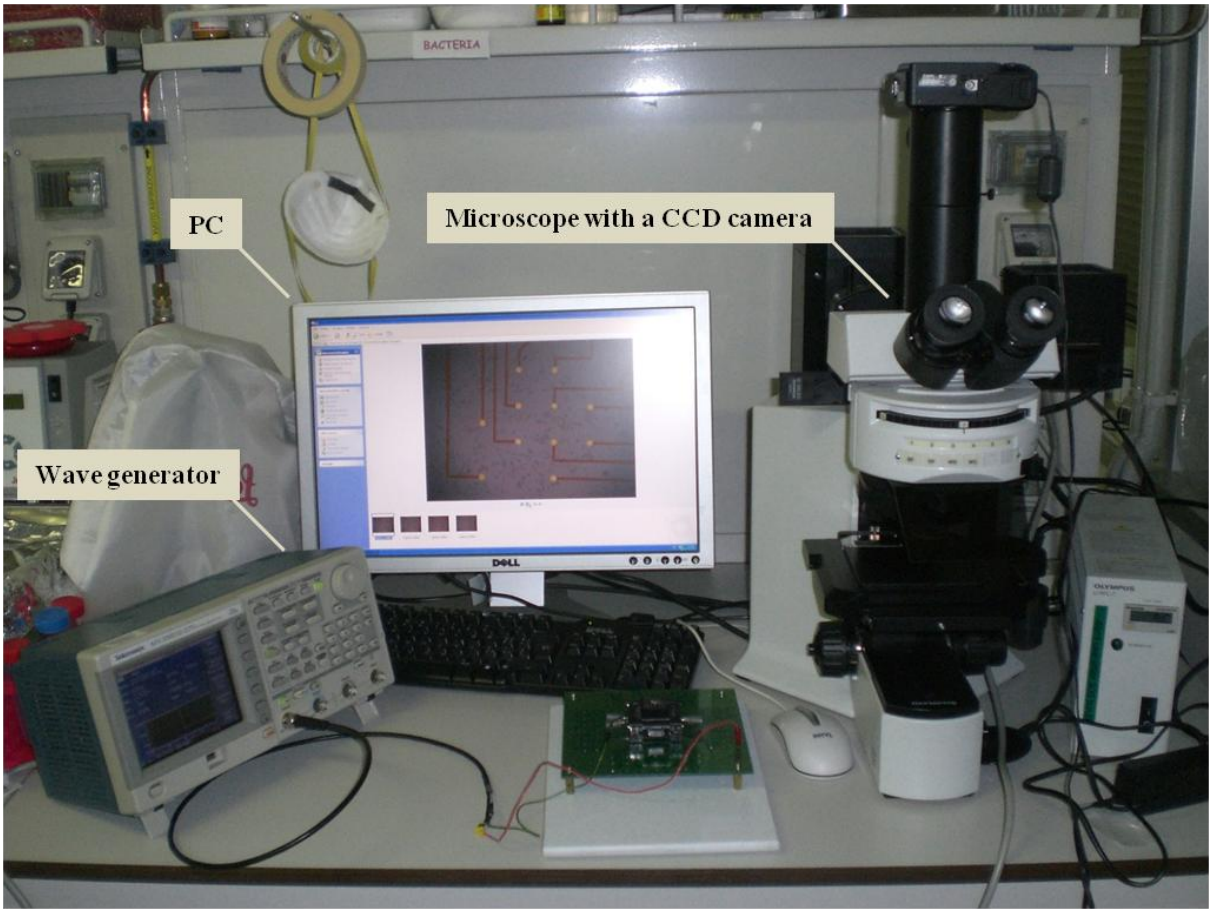

Figure 3.19. Complete set-up for the electroporation experiments.

3.5.2 Choice of the Electroporation Protocol

Starting from previous studies and acquired knowledge at BioSiLab S.r.l, different biological and physical factors were investigated in order to determine the optimal electroporation protocol for the specific HeLa cell line.

Biological factors:

- Cell density

  An adequate cell density is required in order to assure efficient signal pathways amongst cells. In fact, when the number of cells is too low and cells are distributed far from each other they are not able to communicate amongst themselves with negative consequences on the metabolic activity of the whole cell population. On the other hand, an excessive cell density implies the culture growth in bilayer making difficult both the initial electrode selection and electroporation result assessment.

  50.000 cells/cm^2 was identified as the optimal plating condition, considering that the experiments were performed 24 hours after the seeding and required a good cell monolayer over the microelectrode array.

- Transfectants concentration and incubation time after electroporation

  Before considering the parameters cited above, the employed transfectant are listed here:

  1. Lucifer Yellow (Sigma-Aldrich, St. Louis, MO, U.S.A.), a small (475 Da) fluorescent dye used in order to evaluate the feasibility of the proposed approach;
  2. pEGFP-N1 plasmid (Mountain View, CA, USA), a 4.7 kb plasmid for the enhanced expression of the Green Fluorescence Protein (GFP). The possibility to perform gene expression and the viability of cells after electroporation were verified by transfecting this plasmid.

  Their optimal concentrations were identified in order to save reagents but obtaining at the same time a good result. For instance, when the concentration is too low, consequently also the fluorescent signal is low as well, making the electroporation result difficult to be identified. Moreover, also an excessive concentration is unfavourable. It can affect the cell viability because of toxic effects or generate high background, thus limiting the optical detection.

  Finally, the selected concentrations were:

  1. Lucifer Yellow: 0.5 mM (diluted in PBS);

2. pEGFP-N1 plasmid: 0.5 µg/µl (diluted in TRIS-EDTA - TE - buffer solution, Sigma-Aldrich, St. Louis, MO, U.S.A.,DNAse/RNAse free).

The incubation time was also adjusted depending on the transfectant type:

1. Lucifer Yellow: 5 minutes, light protected, in order to ensure the pores resealing after the electroporation and to avoid the fluorophore photobleaching.
2. pEGFP-N1 plasmid: ~ 6-10 hours in order to allow the gene expression; ~ 24 hours for the cell viability assessment after electroporation. In both cases the chip were maintained at 37°C in a 5% CO_2 environment until the observation result.

Physical factors or electric pulse features:

- Pulse shape

  Rectangular pulses were tested for all the electroporation experiments. This shape is usually employed also in bulk electroporation.

- Amplitude/Electric field strength

  The amplitude was changed from 5V to 9V in order to define a right compromise between electroporation result and HeLa cell viability maintenance. The value was decided in order to (a) identify a threshold voltage, higher than the rest membrane potential (0.7 V, as explained in *2.1.1.1 Pore Formation and Resealing*) and below which no electroporation occurs and to (b) avoid cell damaging, detachment from the substrate or even death due to the excessive voltages.

- Pulse duration

  A constant duration was chosen (200 µs period - 50% duty cycle – 100 µs pulse width).

Once chosen the experimental protocol, single-site electroporation was performed. In detail, after the positioning of the platform in the PLCC socket, the transfectant solutions were injected by pressure-driven flow through microchannels. Then, a single pulse with specific features was applied independently to each microelectrode. In order to assure a

better distribution of the electric field, also the electroporation tests were carried out using the external Pt electrode as reference. It was inserted above the chip in contact with the whole medium and connected to the signal generator.

3.6 Single-Site Electroporation Results: Lucifer Yellow (LY) Uptake and Gene Expression

Successful LY delivery was obtained by applying a 100 µs wide and 6V amplitude electric pulse to the electronic circuit. After 5 minutes incubation (light protected) and washing with PBS, the electroporation was monitored by means of fluorescence microscopy. Figure 3.20 demonstrates the specificity of the transfection: only the four cells positioned on the selected electrode have been specifically stained, thus demonstrating, in that region, the permeabilization of the membrane due to the opening of transient pores.

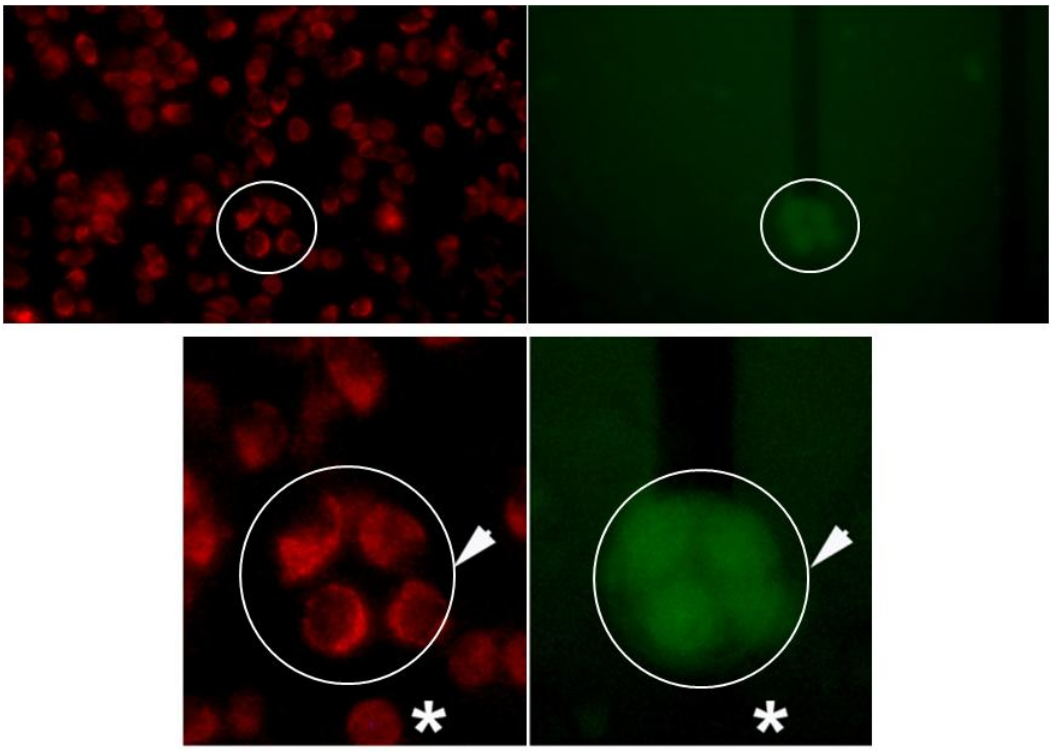

Figure 3.20. Fluorescence micrographs of HeLa cells electroporation with Lucifer Yellow (0.5 mM): (*Left*) autofluorescence view of the cell population; (*Right*) specific uptake of the fluorescent dye. 10X magnification.

In order to deliver pEGFP-N1 into cells a higher electric pulse (7 V, 100 µs) was applied and the chips were maintained in fresh nutrient DMEM medium at 37°C in 5% CO_2 atmosphere. Cells were observed 10 and 24 hours after electroporation in order to evaluate gene expression and cell viability, respectively.

The successful expression of the fluorescent protein after 10 hours demonstrated the plasmid uptake (Figure 3.21).

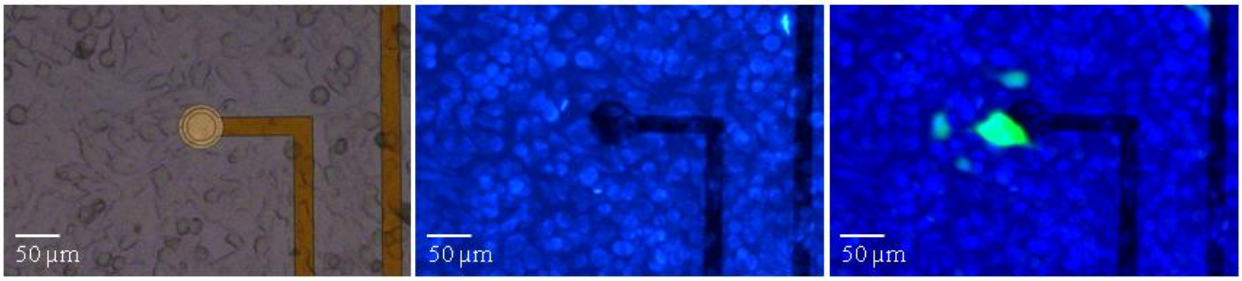

Figure 3.21. HeLa cells electroporation with pEGFP-N1 (0.5 µg/µl): (*Left*) pre-electroporation; (*Middle*) autofluorescence view of the cell population; (*Right*) specific uptake of the plasmid with consequent expression of GFP. 10X magnification, @10h after electroporation.

Moreover, the maintained well spread morphology over time (after 24 hours) proved that the electroporation protocol was not invasive and did not affect cell viability (Figure 3.22).

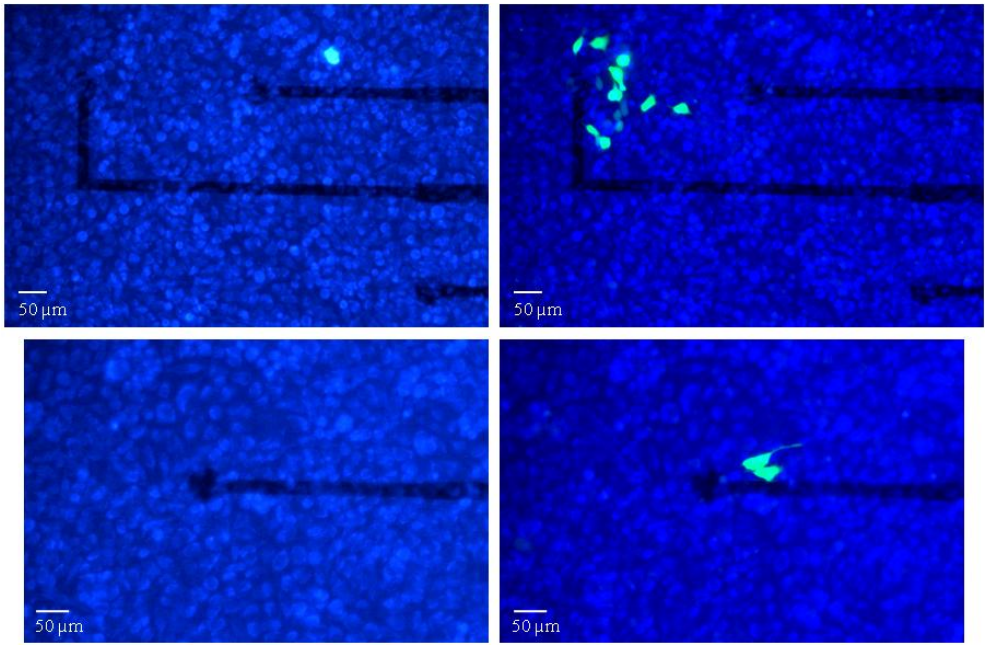

Figure 3.22. Two examples of HeLa cells electroporation with pEGFP-N1 (0.5 µg/µl): (*Left*) autofluorescence view of the cell population; (*Right*) specific uptake of the plasmid with consequent expression of GFP. 10X magnification, @24h after electroporation.

With respect to the case at 10 hours from the electroporation event, after 24 hours cells were closed to the selected electrodes, but not exactly over them. This aspect does not represent a sign of aspecific electroporation, but it is due to the evolution of the cell culture itself (cell replication/mytosis) and in particular to the different localization of the same cells over time (cell migration).

3.6.1 Electroporation Efficiency

In general, the Electroporation Yield is expressed as follows:

EP Yield (%) = (n° of electrodes with labelled cells/total number of selected electrodes) x 100

In case of gene transfer this value is called **EP Efficiency (%)** because it considers both the Electroporation Yield und cell viability after the electroporation event. Only not damaged cells are able to express the proteins. Preliminary gene transfection experiments allowed to approximately measure this value. The protocol characterized by a 7V pulse gave a maximum EP efficiency value of 50%.

3.7 Conclusions

Summarizing, this research activity concerns an improved platform for cell electroporation, whose main features are the electrodes functionalization and controlled transfectants delivery.

At first, bioaffinity studies were performed in order to choose the best materials for the device microfabrication. The candidate substrates were Ti, Si_3N_4, SiO_2, Au and Pt. Moreover, since there was an increasing attention towards nanoparticle-assembled materials in the fabrication of biocompatible microsystems, a comparison between these materials and ns-TiO_2 film deposited by PMCS was performed. To explore the differences, SKOV-3 cell line was cultivated over them and a short-time (24h) Calcein AM-based viability assay was carried out. By calculating the total viable cell density (quantitative analysis), Si_3N_4 and Au

demonstrated an higher cell growth with respect to both TCPS control and the other materials. The morphological analysis (which considered the only well adherent spread phenotype) showed that TiO_2 film increased the percentage of spread cells suggesting that this ns-material could promote cell adhesion.

According to the bioaffinity results, the MEA-based electroporation module was microfabricated by employing Si_3N_4 and Au as materials exposed to the cell culture: Si_3N_4 as passivation layer and Au as metal for microelectrodes. In addition, in order to improve the cell adhesion only on the active areas of the electrodes, specifically were the voltage is applied during the electroporation event, a microfabrication process based on lithography and lift-off was studied. A microfluidic structure and silica tubes were integrated to inject different transfectant solutions into desired areas of the chip, through passing holes previously opened on the MEA (single-site delivery). Two different chambers were also added for tranfectants and cells confinement, respectively.

Besides the substrates bioaffinity, also the complete Lab-on-Cell biocompatibility was demonstrated. In fact, HeLa cells were successfully cultivated using traditional protocols and single-site electroporation was performed. In order to evaluate the feasibility of the technique LY was employed demonstrating the specificity of the transfection. Moreover, gene expression and maintained cell viability after electroporation were assessed transfecting pEGFP-N1 plasmid. In both cases the electroporation protocols were optimized by investigating both biological and physical factors (i.e. cell density, transfectants concentration and incubation time, electric pulse features with particular attention to the amplitude). Finally, preliminary results allowed to obtain a rough estimation of 50% electroporation efficiency.

Chapter 4

4 Cantilever-based Sensors for Gene Analysis

As described in *Chapter 2. State of the Art*, nowadays there is an increasing attention towards integrated systems for gene analysis. In particular, beyond methods able to perform gene transfection (*Chapter 3. Lab-on-Cell for Gene Transfection*), others can detect mutations at DNA sequence level.
The main target of this research activity was the immobilization layer and functionalization procedure study of a microcantilever-based module developed in FBK facilities. The following detection system was microfabricated with the future aim to be integrated in a LOC for the early diagnosis and screening of autoimmune diseases. In particular, the diagnosis of chronic autoimmune diseases such as Multiple Sclerosis (MS) and Rheumatoid Arthritis (RA) will be based on the label-free detection of Human Leukocyte Antigens (HLAs). These genes are the major determinants used by the body's immune system for recognition and differentiation of self from non-self (foreign substances). Since many HLA molecules exist, but some of them are more common in certain autoimmune diseases, the HLA detection by DNA hybridization (with SNPs resolution) would be very useful in diagnostics. However, a system like this could be extended to many others applications in diagnostics by only considering different DNA probes specific for a genetic disease or the detection of pathogens. In fact, the working principle will be the same.

The proposed detection module will work in bending mode (i.e. stress-detection mode) with a piezoresistive read-out system. The choice of the bending working principle is due to the fact that in dynamic mode the resonance frequency depends not only on the absorbed mass, but also on environmental parameters, such as density and viscosity of the medium. Since DNA hybridization is an analysis to be performed in liquid (were the resonance frequency is reduced, making the dynamic mode less sensitive), the static mode is preferred. In addition, since the laser light can be absorbed by a liquid, while the piezoresistive read-out is efficient in any liquid medium, this last read-out method was considered (as ex-

plained also in *Paragraph 2.2.1 Micro-ElectroMechanical Systems (MEMSs) for DNA Hybridization Detection: Cantilever-based Arrays***)**.

As a first approach, the detection and read-out electronics will be created in a hybrid integration structure. One chip will constitute the sensing module made by a MEMS-based cantilever array, and another one will be represented by an Application Specific Integrated Circuit (ASIC) able to manage and process the analog signal coming from the cantilever array. Then, the full integration of both the sensing and read-out modules will be performed in order to comply with the demand of portability of the LOC. The final LOC systems will also include a PCR chamber for the amplification of the DNA target before the detection. The system will be integrated with Personal Digital Assistants (PDAs) and diagnostic software for the realization of an automated and portable diagnostic system (Figure 4.1).

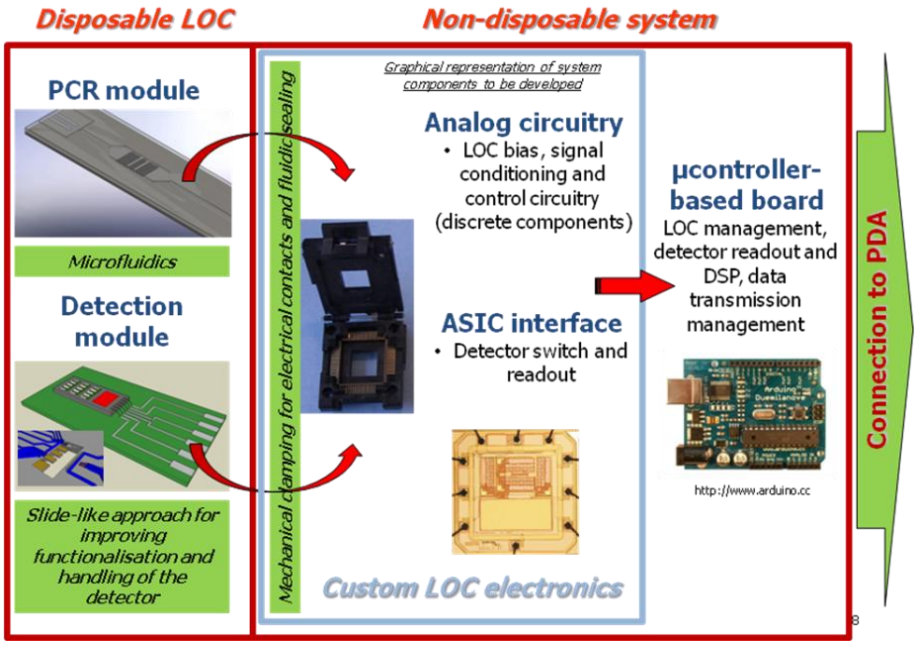

Figure 4.1. LOC system approach.

4.1 Design of MEMS-based Cantilever Arrays

When high sensitivity is required, a proper technology is needed in order to reduce the beam thickness to sub-micron scale [Ziegler 2004]. Since the sensitivity of microcantilever devices operated in static mode is proportional to the beam curvature due to surface inter-

action, selection of materials and device thickness were the major design and technical points. As described in *Chapter 2. State of the Art* (*Paragraph 2.2.1 Micro-ElectroMechanical Systems (MEMSs) for DNA Hybridization Detection: Cantilever-based Arrays*), different read-out methods are available. However, for POC applications piezoresistive read-outs take advantage of the good sensitivity, high robustness, simple read-out principle and easy integration for large arrays. This choice was anticipated also in the previous introduction.

Both analytical and Finite Element (FE) analysis were performed by the BioMEMS group and focused on the evaluation of expected sensitivity and response with different technological approaches.

In Table 4.1, simulated responses to the typical concentration of 400 nM 12 bp-DNA with single mismatch are reported for single crystal beams (thickness 340 nm Si, 200 nm SiO_2: "SOI") with implanted resistors (100 nm junction depth), SiO_2 beams with single crystal piezoresistors etched in the device layer of a SOI wafer (thickness 400 nm SiO_2, 100 nm Si: "SiO_2-SOI"), SiO_2 beams with poly-Si piezoresistors (thickness 400 nm SiO_2, 100 nm poly-Si, 200 nm SiO_2: "SiO_2-poly") and single crystal beams (thickness 340 nm Si, 200 nm SiO_2: "SOI") with poly-Si resistors (100 nm thickness poly-Si, with 200 nm SiO_2 for device passivation), "SOI-poly".

Table 4.1. Result of analytical evaluation of performances achievable with different technologies. Pls. see the main text for the description of the technologies.

Device type	***Expected sensitivity (ΔR/R) [M^{-1}]***	***Response @ 400 nM [ppm]***
SOI	**13.7**	**5.5**
SiO_2 – SOI	11.1	4.5
SiO_2 - poly	7.5	3
SOI – poly	11.7	4.7

The reported thicknesses are the result of an optimization based on analytical models including the mechanical properties of the structures and an applied surface stress equivalent to DNA interaction. The optimization was performed in terms of detector response for each

technology by taking into account technical constraint and device suitability. The analytical model was developed on the basis of data extracted from [Fritz 2000] and preliminarily compared with results described in [Mukhopadhyay 2005].

As shown, the highest response can be achieved with implanted resistors on single crystal Si. Moreover, the optimal design of devices was considered by FE simulations. Results of read-out sensitivity for different implants types as a function of position along the beam are shown in Figure 4.2, reporting the n-type implant largely outperforming p-type resistors for planar stress condition, which are the ideal conditions for long beams working in static mode.

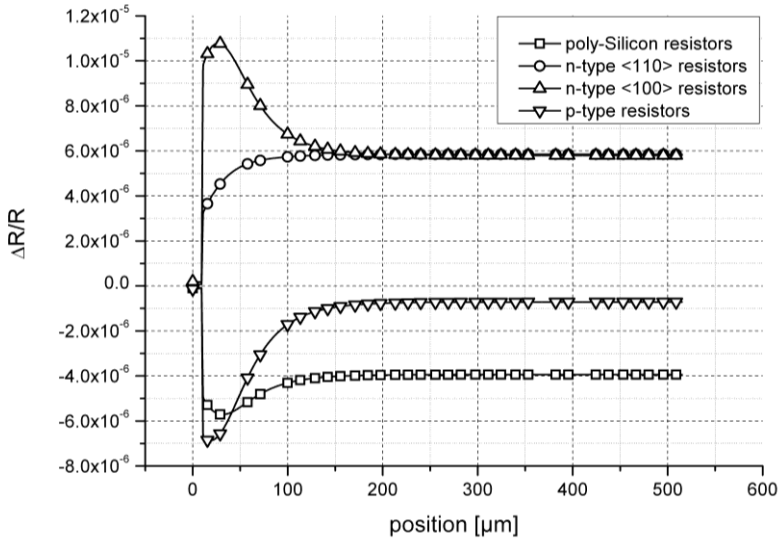

Figure 4.2. Simulated response of piezoresistive element to single-base mismatch at 400 nM DNA concentration, as a function of position along the beam.

As reported in Figure 4.2, the graph demonstrates that the maximum response values can be achieved by positioning the resistors near the microcantilevers anchorage point.

The final microcantilever structure is described in Figure 4.3. Resistors are placed near the anchorage point of the cantilever because in that region the structure is subjected to the highest stress. In particular, a Wheatstone bridge will be integrated. Its structure will be based on four equal resistors: two reference resistances on the bulk, one resistance on the reference microcantilever and one on the test microcantilever. The full Wheatstone bridge configuration allows an increased reference potential control and larger area and pad number.

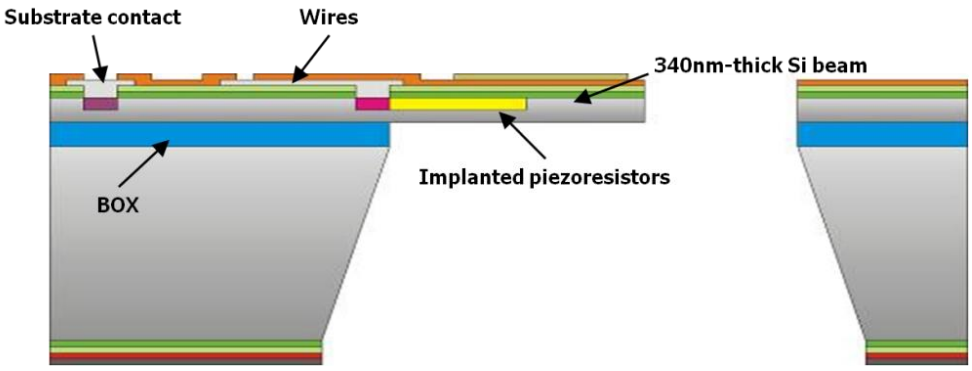

Figure 4.3. Structure of a complete microcantilever with integrated read-out.

Silicon-On-Insulator (SOI) approach for the realization of suspended thin beam:

- SOI wafer, device layer: 340 nm thickness
- Buried oxide (BOX): 400 nm thickness
- Structure definition: dry and wet bulk micromachining
- Passivation SiO_2 layer: 200 nm (on beam)
- Doping (from implant test):
  Substrate doping: p ~1e17at/cm^3
  Piezoresistors doping: n ~8e18at/cm^3, junction depth ~75nm, R ~2kΩ/sq.

For details see A. Adami's Thesis [Adami 2010].

4.2 Sensor Microfabrication: SOI-MEMS Cantilevers

Starting from Figure 4.3 and details listed in the previous paragraph, the proposed technological approach was based on SOI substrates, allowing an extreme reduction in beam thickness (380 nm) - parameter that is related to the sensitivity of the overall biosensor - and n-type implanted piezoresistors with low junction depth. Besides high sensitivity, the SOI approach is characterized by high reproducibility. Nevertheless, in order to perform the surface studies and to choose the optimal functionalization procedure, the read-out integration was not necessary. For this reason, the technological development was initially focused on the realization of just the device mechanical structures without implanted resistors. A technological process was developed and performed by the M. Decarli in the micro-

fabrication laboratory of FBK. Each mechanical structure of the devices was based on crystal Si and PECVD deposited SiO_2 as adhesion layer. Moreover a Au layer was added for promoting the covalent binding of DNA probes with thiol-based chemistry (probes with –SH as functional group).

In detail, the CMOS-compatible fabrication process started with a multilayer mask deposition on both sides of the SOI wafer (Soitec). The substrate had a 340 nm thick crystal Si device layer, a 400 nm thick BOX layer and a 525 µm thick handle layer. The lithographic definition of the geometry of the cantilevers arrays was performed. Then, the beams were etched through the device layer with a standard Reactive Ion Etching (RIE) step, in which the BOX layer acted as an etch stop. Since in static mode the biochemical reaction must selectively occur only on one side of the cantilever, the top area was covered by a Au film (20 nm) by employing a PECVD SiO_2 as adhesion layer. Moreover, an interface of Cr was also used. In particular, the immobilization layer consisted in the e-beam evaporation of Cr/Au (3/20 nm) on top of each beam and lift-off definition of the geometrical pattern on the beams. Bulk micromachining was the last step of the fabrication process and the most critical in terms of yield of the cantilevers arrays. Tetramethylammonium hydroxide (TMAH) was employed as a wet anisotropic etchant, in order to remove Si from the handle layer (backside). Finally, microcantilevers were released by oxygen plasma. The process flow is depicted in Figure 4.4.

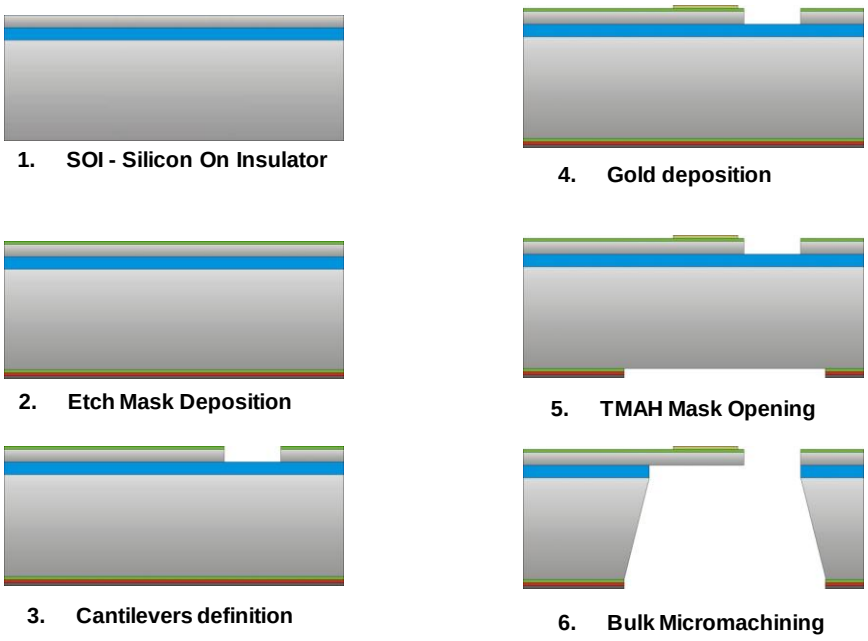

Figure 4.4. Simplified schematic process flow for cantilever detector array fabrication.

In addition to favourable sensing properties of single devices, an array configuration can be easily implemented with MEMS technologies, as shown in the SEM picture of Figure 4.5. The obtained configuration could allow the detection of multiple species at the same time, as well as the implementation of reference sensors to reject both physical and chemical interfering signals. Repetitions necessary for statistical confirmation could be also considered.

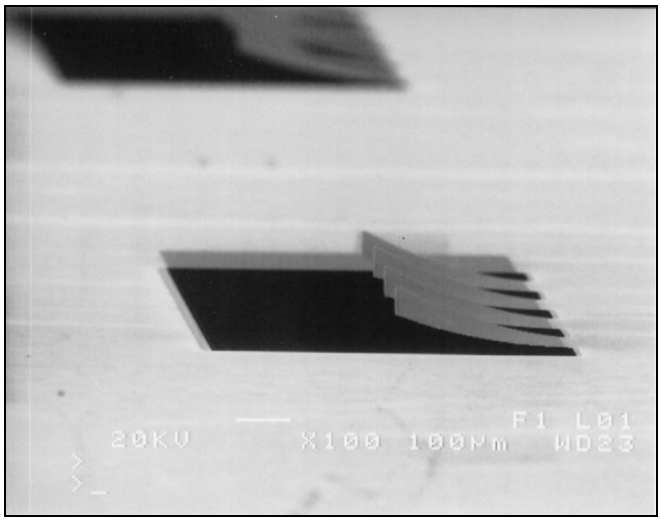

Figure 4.5. SEM picture of fabricated devices: an array of four 380 nm thick microcantilever structures is shown (JEOL JSM-6100, MTLab-FBK).

As it can be clearly seen, the beams are deflected upwards (~ 30 µm) due to an unbalance of the residual stresses of thin films deposited on the cantilevers.

4.3 Microcantilever Material Characterization: Gold Layer Analysis

Since the functionalization procedure and hybridization event occur exactly there, the application under study required an optimal immobilization layer in terms of Au uniformity and content (%). The uniformity is a key parameter governing the suitability of the SAM to sufficiently sense the stress resulting from the hybridization reaction. On the other hand, the Au percentage represents the amount of linkage points for the binding of thiolated DNA probes onto Au. In fact, the immobilization efficiency is requested also in terms of surface grafting density of the probe molecules and uniformity of coverage, which must be high enough to generate a surface stress as large as possible. A low probe density and a bad

coverage (for instance non uniform) would drastically decrease the sensitivity of the device.

Initially, the surface layer (Cr/Au – 3/20 nm) was characterized in terms of roughness by means of AFM (NT-MDT Solver Pro.). Moreover, also XPS (Scienta ESCA 200 instrument equipped with a hemispherical analyzer and a monochromatic Al KR-1486.6 eV-X-ray source in transmission mode) was employed in order to better understand the chemical composition and thus the quality for the subsequent functionalization process. For both the analysis, macro substrates (1x1 cm^2) with the following features were employed:

1. Same Si substrate used for the cantilevers microfabrication;
2. SiO_2 deposited by means of PECVD;
3. Evaporation of Cr/Au (3/20 nm): interface/immobilization layer respectively.

Before the analysis, the substrates were subjected to annealing (210°C, 1h, N_2 atmosphere) in order to simulate the thermal treatment of real microcantilevers and oxygen plasma (process also used to release the structures).

Figures 4.6 and 4.7 show the AFM analysis on a 15x15 μm^2 surface and a narrow 2x2 μm^2 area, respectively.

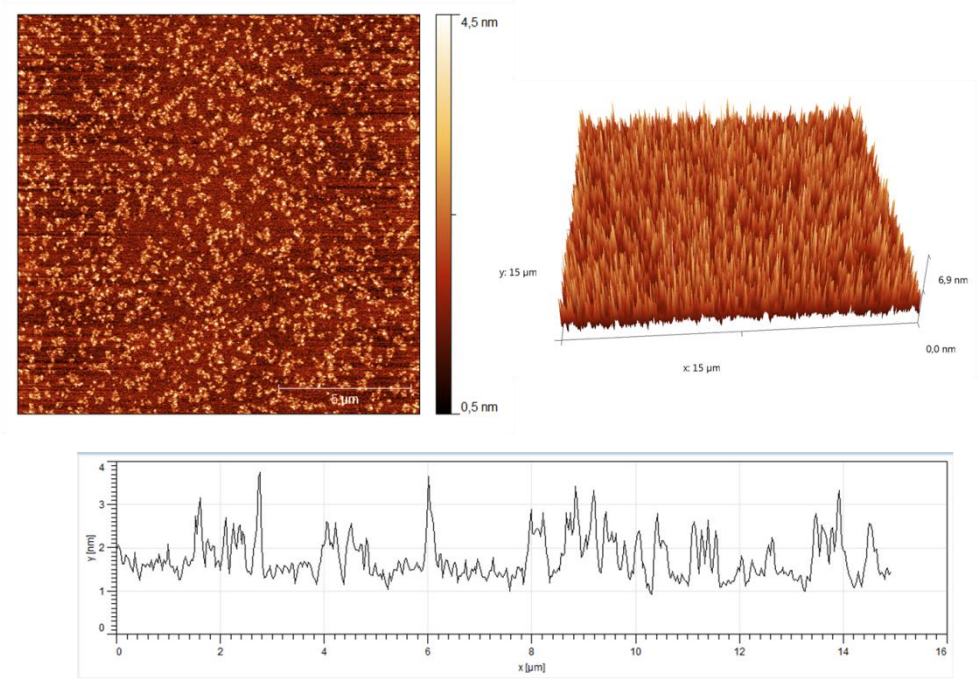

Figure 4.6. AFM analysis: (*Top left*) image of 15x15 μm^2 area; (*Top right*) 3D representation; (*Bottom)* Roughness profile, Ra= 0, 468 nm (BioSint-FBK).

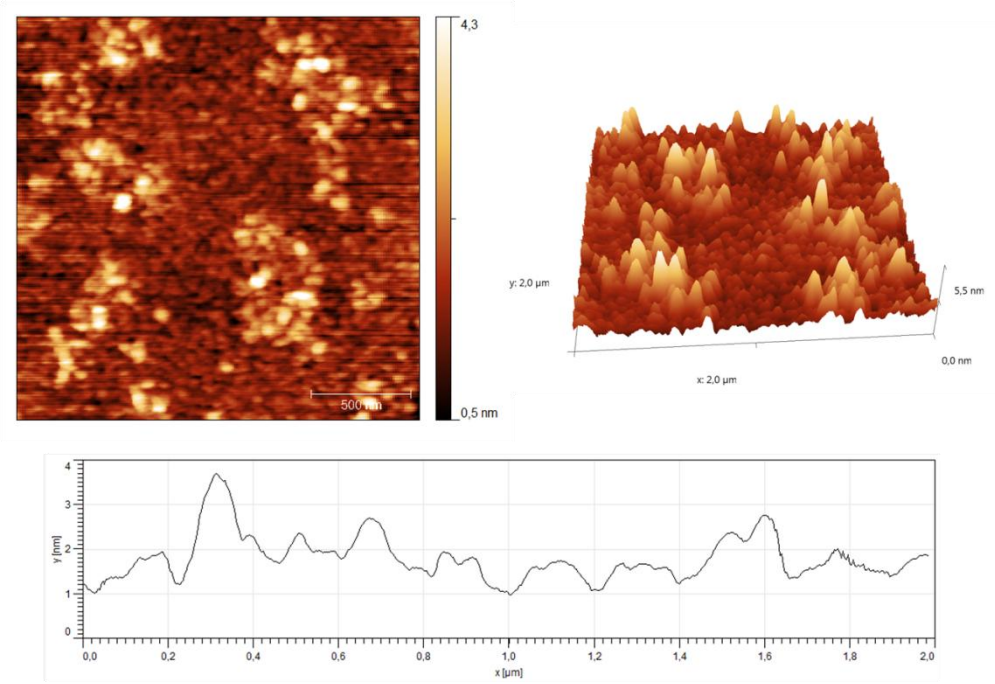

Figure 4.7. AFM analysis: (*Top left*) image of 2x2 µm^2 area; (*Top right*) 3D representation; (*Bottom)* Roughness profile, Ra= 0, 430 nm (BioSint-FBK).

The results demonstrate that the top layer is almost flat (Ra=0,430 nm). However, the Au surface is not very uniform. Especially the 2x2 µm^2 analysis shows scattered Au islands over the surface.

Au atoms seem not to generate a uniform layer and above all Au is insufficient to allow a suitable SAM generation.

In order to assess the chemical composition of the Au layer characterizing the cantilever array, an XPS analysis was performed on substrates without treatments, after annealing and after both annealing and oxygen plasma. The study was carried out at two different tilt angles. The analysis at 90° corresponds to about 10 nm deepness into the layer, while the analysis at 15° is focused on 3-4 nm of surface. This last measurement is more sensitive to the surface composition, thus possible contaminants become important. XPS analysis confirmed the non-homogeneity observed by AFM. Moreover, it revealed a very low percentage of Au (8.6%) after the treatments, together with high levels of O and C contaminants and evidence of Cr also on the upper surface.

In detail, as evinced from Table 4.2, also samples without treatment revealed on the surface of interest (15° tilt angle) a not very high content of Au (31.6 %) and significant contaminations, especially of C (56.2 %). Annealing procedure decreased the Au percentage to 25.1 % and C contamination to 45.1 %, whereas it increased O contamination (from 12.2

% to 24.1 %) and Cr release from the interface layer. The last step of oxygen plasma decreased once again Au until 8.6 %, and caused an increased in C contamination and Cr presence on the surface. Moreover, as expected, oxygen plasma revealed further undesired Au oxidation (O content 33.3%).

Table 4.2. Atomic concentration of Cr/Au film after specific microfabrication steps, as determined by XPS surface analysis (tilt 90° and 15°), expressed in percentage (MiNALab-FBK).

Cr/Au sample (90°) and (15°)	***O* 1s *(%)***	***C* 1s *(%)***	***Cr* 2p *(%)***	***Au* 4f *(%)***
Without treatments (90°)	4.7	19.9	-	75.3
Without treatments (15°)	**12.2**	**56.2**	-	**31.6**
After annealing (90°)	15.9	17.6	3.7	62.9
After annealing (15°)	**24.1**	**45.1**	**5.7**	**25.1**
After annealing and oxygen plasma (90°)	27.3	17.3	21.8	33.6
After annealing and oxygen plasma (15°)	**33.3**	**50.6**	**7.5**	**8.6**

The surface changes after the treatments can be easily observed in the following histogram (Figure 4.8).

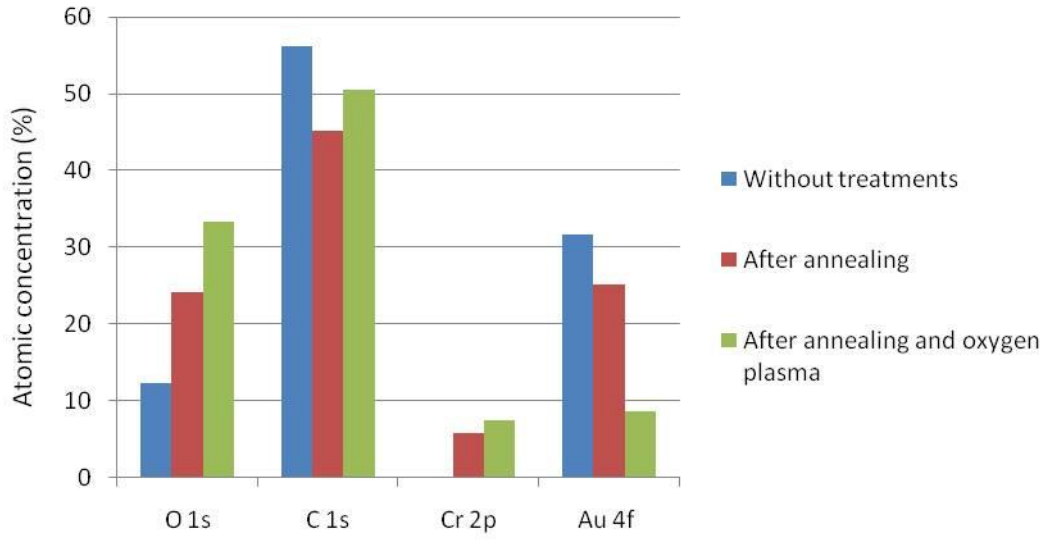

Figure 4.8. Histogram representing the atomic concentration variations of the Cr/Au film after the treatments.

4.3.1 First Improvement: Ti (instead of Cr) as Adhesion Layer

The Au conditions revealed by XPS and AFM analysis described in the previous paragraph were not suitable to obtain a good SAM, that means a uniform and high density probe deposition. For this reason, another interface was evaluated, Ti instead of Cr (Table 4.3 and Figure 4.9). Also this analysis showed that annealing and oxygen plasma caused a release of interface layer (atoms of Cr or Ti) on the surface, even if with different percentages. However, the substitution of Cr with Ti as adhesion layer revealed a lower Au degradation whose final percentage value corresponded to 28.1%. Regarding the contaminations, the O one was less invasive with respect to the previous case. Thus, for the further fabrication process, Ti was employed as adhesion layer. However, C content was still too high and a specific cleaning procedure was required.

Table 4.3. Atomic concentration of Ti/Au film after specific microfabrication steps, as determined by XPS surface analysis (tilt 90° and 15°), expressed in percentage (MiNALab-FBK).

Ti/Au sample (90°) and (15°)	***O* 1s *(%)***	***C* 1s *(%)***	***Ti* 2p *(%)***	***Au* 4f *(%)***
Without treatments (90°)	1.5	14.7	-	83.8
Without treatments (15°)	**3.8**	**50.6**	-	**45.7**
After annealing (90°)	6.9	23.2	Traces	69.9
After annealing (15°)	**14.3**	**54.4**	**8.8**	**22.5**
After annealing and oxygen plasma (90°)	9.1	20.5	Traces	70.4
After annealing and oxygen plasma (15°)	**15.5**	**53.5**	**2.9**	**28.1**

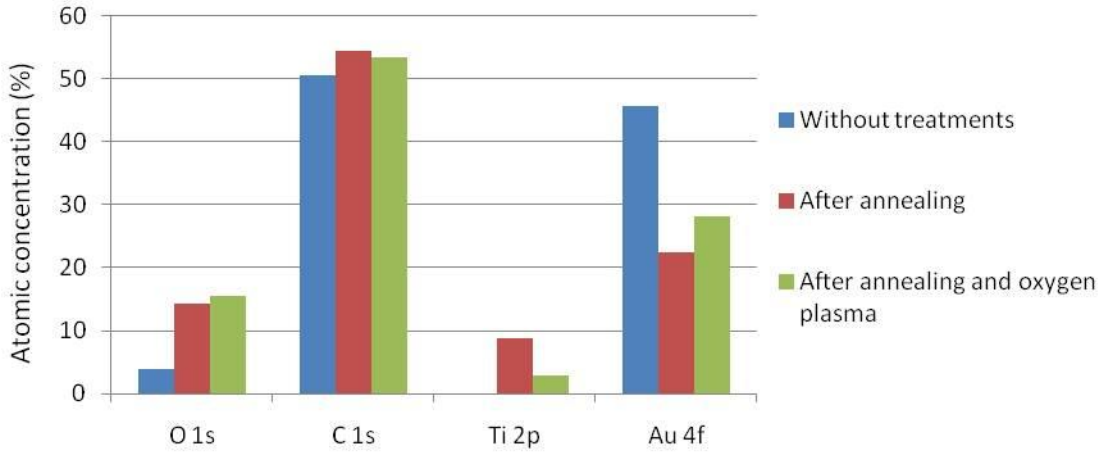

Figure 4.9. Histogram representing the atomic concentration variations of the Ti/Au film after the treatments.

4.3.2 Second Improvement: Ar Plasma Treatment

Standard wet chemical procedures were not compatible with microcantilevers arrays, mainly because the piezoresistive read-out Al connections could be etched by solutions like piranha (H_2SO_4 (98%) and H_2O_2 (30%)). In order to decrease the C contamination, while improving the Au layer, Ar plasma treatment was chosen as cleaning procedure. Different treatment parameters were changed (power, duration and gas flow) to select the protocol giving the best result. The optimal conditions allowing the best surface cleaning without surface damage were obtained by applying an Ar plasma treatment with these characteristics: 30% flow, 15 Watt, 3 minutes. The XPS results are listed in Table 4.4.

Table 4.4. Atomic concentration of Ti/Au film after Ar plasma treatment as determined by XPS surface analysis (tilt 90° and 15°), expressed in percentage (MiNALab-FBK).

	O* 1s *(%)	***C* 1s *(%)***	***Ti* 2p *(%)***	***Au* 4f *(%)***
Ti/Au (90°)	9.8	16.8	traces	73.4
Ti/Au (15°)	**18.7**	**45.5**	**4.1**	**31.7**

Au percentage increased from 28.1 % to 31.7 %, whereas the C contamination decreased from 53.5 % to 45.5 %. Ti percentage increased, as well as O content. The comparison be-

tween the Ti/Au film analysis before and after the Ar plasma treatment is shown in Figure 4.10. The surface changes coming from the Ar plasma treatment seemed not to significantly improve the Au content. Further treatments should be considered (*Chapter 5. Conclusions*).

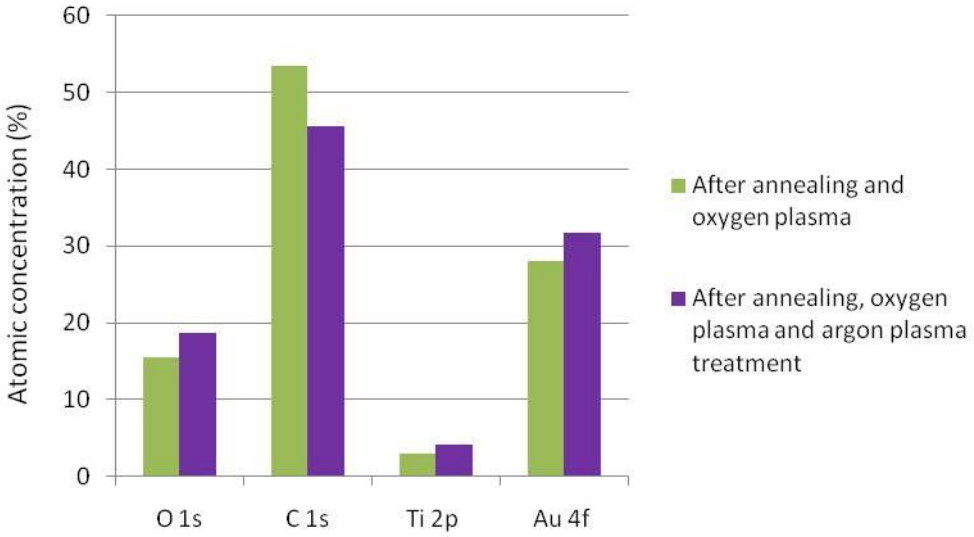

Figure 4.10. Histogram representing the comparison between the Ti/Au film before and after the Ar plasma treatment.

4.4 Cantilever Functionalization

A consistent part of the success of bioaffinity detectors is related to the availability of proper functionalization techniques, allowing the immobilization of high-quality SAMs of DNA probes on the structures, especially on high-density devices. In general, bioreceptors immobilization on the sensor surface strongly affects the quality of microcantilever analysis, since it influences not only the efficiency of DNA attachment, but also the degree of the subsequent specific or not binding. The immobilization process should:

- avoid any change in the mechanical properties of the cantilever;
- be uniform, in order to generate a surface stress as large as possible;
- be stable and robust, with molecules covalently anchored to the surface;
- allow accessibility by the target molecules.

For this reason, suitable procedures for suspended structures were investigated. The main techniques generally used to deposit DNA probes on cantilevers consist in the ink-jet spot-

ting and the incubation in dimension-matched glass capillaries (each one filled with a specific oligonucleotide solution) [Lang 2005] (Figure 4.11).

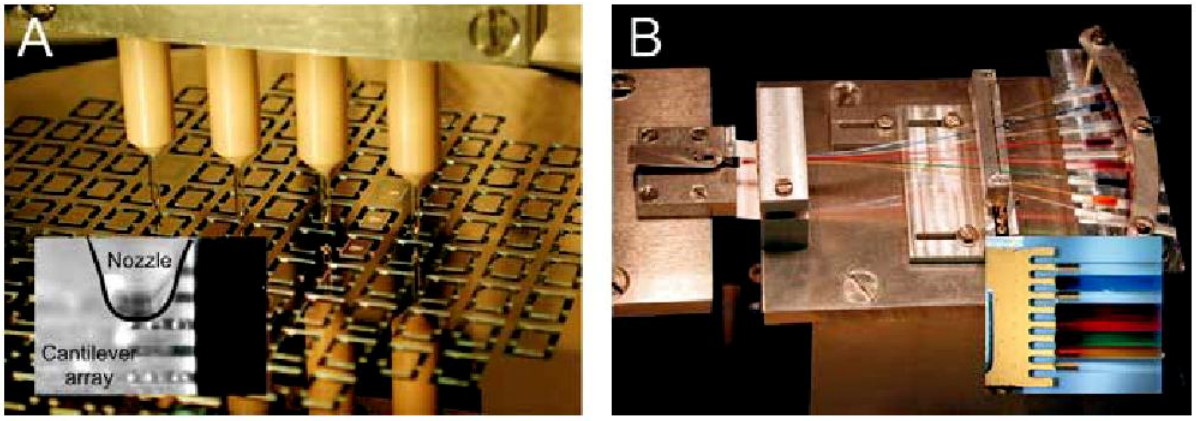

Figure 4.11. Deposition techniques for cantilevers: (A) coating by ink-jet spotting; (B) incubation in microcapillaries [Lang 2005].

Since the second system is stiff to be applied for high density arrays functionalization, the ink-jet spotting technique was chosen. Nevertheless, a contact spotter was available. Like the ink-jet spotting, also the mechanical microspotting method is frequently employed to produce DNA microarrays and can deposit precise volumes of reagents in desired regions of a substrate by performing direct contact of solid or capillary pins. A system of x, y, z movement guides the spot localization. Moreover, in general the coating by means of a spotter is faster than incubation in microcapillaries (1-5 min vs. 15-30 min). It is versatile and permits to functionalize only the upper side of the cantilever without contaminate the other one. In addition, a spotter requires lower sample volumes with respect to the microcapillary-based method. Others techniques employed for DNA functionalization belong to the class of the so called contact printing [Yu 2005].

4.4.1 Evaluation of Spotting Technique Feasibility and Microcantilever Mechanical Resistance: Phosphate Buffer Deposition

Initially, the spotting feasibility and the mechanical resistance of microcantilevers at pin contact had to be assessed. In order to achieve this purpose the custom BioRad VersArray Chip Writer Pro System (Biorad) was employed at CIVEN (Coordinamento Interuniversi-

tario Veneto per le Nanotechnologie, Venezia – Marghera) (Figure 4.12).

Figure 4.12. (*Left*) VersArray ChipWriter Pro Systems (Biorad) employed for technique feasibility and cantilever resistance assessment; (*Right*) Telechem pin used for the deposition.

More precisely, the spotting technique was tested on a chip consisting of 4 arrays of 4 cantilevers (i.e. a total of 16 beams) stuck on a typical microscopy glass (25x75 mm^2) fixed in turn in a specific position under the spotter by means of a magnet. Array geometrical parameters and photograph are shown in Figure 4.13.

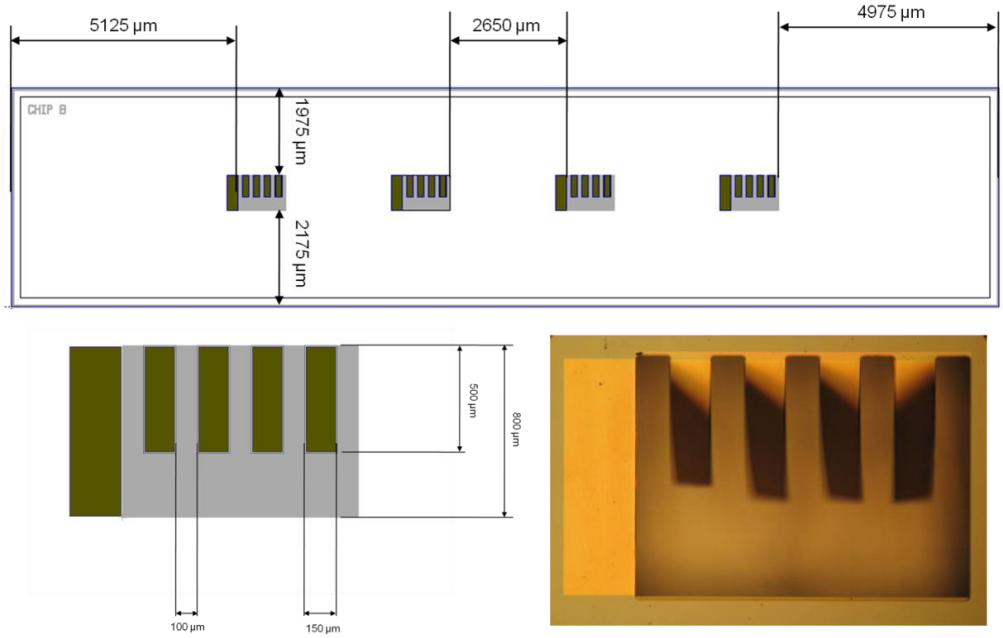

Figure 4.13. (*Top*) Chip layout (4 arrays of 4 cantilevers); (*Bottom left*) 4 microcantilevers array layout; (*Bottom right*) Optical microscopy photograph of the microfabricated array.

In order to demonstrate the feasibility of the deposition method potassium phosphate monobasic solution (KH_2PO_4, 1 M, pH 3.8) was employed (Sigma-Aldrich). As frequently described in literature [Alvarez 2004, Calleja 2005, Mukhopadhyay 2005] it is a solution commonly used as immobilization buffer for the deposition of DNA probes, also in microarray technology. Technical difficulties were considered. Since the quality of cantilever analysis is strongly influenced by the functionalization process, x, y, z pin directions and volumes were optimized in order to ensure a good coverage avoiding cantilever breaking. At first, the movement of the spotter pin and drop localization were precisely determined adapting the parameters to the array structure reported in Figure 4.13. More precisely, these parameters correspond to the position of the spots along the microcantilevers (x), the distance between deposition points (y) and pin height (z) relative to more or less contact with the cantilevers surface. For the z direction the upwards deflection of microcantilevers (~ 30 µm) was taken into account. Also the right pin contact time was established in order to limit the breaking possibility. Regarding the spotting machine, humidity, temperature and pin type were selected to avoid the sample evaporation, while using environmental temperature with a small amount of reagent consumption, respectively. In Table 4.5 the set parameters are listed. It must be noticed that the spot diameter refers to the case of deposition on a planar surface as in classic microarray development.

Table 4.5. Spotting machine setting: humidity and temperature parameters; pin type with relative drop volume and spot diameter.

Internal humidity of the spotting system	~50%
Plate temperature	RT
Pin external diameter ***TeleChem SMP3 Stealth quill pin***	~50 µm
Sample total volume inside the pin	65 nl
Drop volume	0.65 nl
Spot diameter *(depending on the pin contact time: 0.03 sec)*	~100 µm

The evaluation of procedure suitability was performed by SEM investigation; a picture of microcantilevers with KH_2PO_4 deposition is shown in Figure 4.14. No washing step was employed, because the aim of this study was just to find out the right deposition conditions to cover most part of the microcantilever avoiding microcantilever breaking.

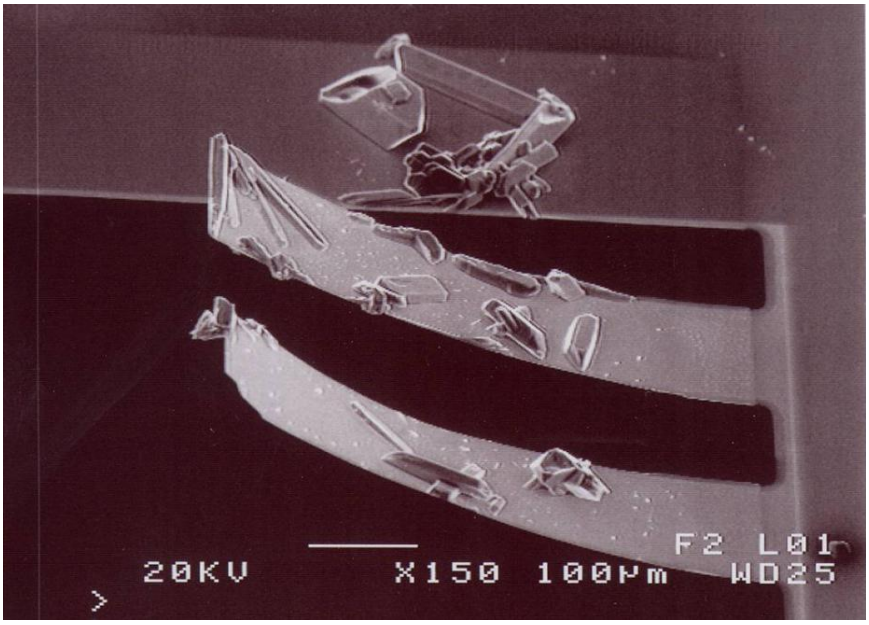

Figure 4.14. SEM picture of microcantilevers after spotting of KH_2PO_4 buffer solution (1M, pH 3.8) (JEOL JSM-6100, MTLab-FBK).

The result revealed a clear coverage of the upper surface of each beam, which can be inferred from the crystallites present along the cantilevers after the spotting procedure. Another key aspect was the yield of the adopted spotting procedure. Microcantilevers are fragile structures and they can be easily broken if they are touched by the tip of the spotter. The micrometric control on x, y, z movement allowed to obtain a 100% yield of the deposition method. The best approach involved the deposition of a single drop spotted on the non-clamped edge of each beam, allowing the coverage of the complete beam depending on both the upwards curvature of the beams and the surface wettability, as clearly evinced from the distribution of potassium-phosphate crystals on almost the whole top surface.

4.4.2 Avoiding Contaminations: Fluorescein Deposition

For the application described in the introduction of this Chapter (LOC for autoimmune diseases diagnostics) each cantilever should be differently functionalized from the others. As a consequence, the biggest trouble would be the cross contamination among different DNA solutions. This situation would make the device useless, because incapable to detect specific DNA sequences present in an unknown sample. In order to overcome this problem the right distance between deposition points and the volume to be deposited had to be carefully established, as pointed out also in the previous paragraph. In order to make the inspection easier than in case of a saline buffer, a fluorescent dye was spotted: a 80 mM fluorescein solution (in 0.05 M carbonate buffer, pH 9, Sigma-Aldrich). This deposition study was performed by the BioSint group using a contact spotter available in FBK, the Biodyssey Calligrapher Spotter Machine (Biorad). It is smaller than the BioRad VersArray Chip Writer Pro System previously used for the feasibility evaluation of the contact spotting technique, but it has the same functional characteristics (Figure 4.15).

Figure 4.15. (*Left*) Biodyssey Calligrapher Spotter Machine (Biorad) employed for the deposition of fluorescein solution (80 mM).

The plate was cooled (10°C) and the internal humidity of the spotting system was maintained at 60% in order to preserve the fluorescein sample and avoid its rapid evaporation. Two kinds of pins were used, solid and capillary pins. The solid pin employed (MCP 310s, 310 µm diameter) had the best performance. Unlike quill pins, solid pins have the drop ex-

ternally hanged up to the tip and they deposit it also by means of a drop weak contact on the surface. For this reason capillary pins (which require a direct pin contact to release the drop) seem to be more invasive. However, also in case of buffer solution deposition, after a deep procedure study any cantilever damage was observed. Like in the previous deposition test, no washing step was carried out. Figure 4.16 shows the result. Again, the deposition was performed on the whole microcantilevers length, by depositing only one drop. No contamination and crashing of the levers were observed.

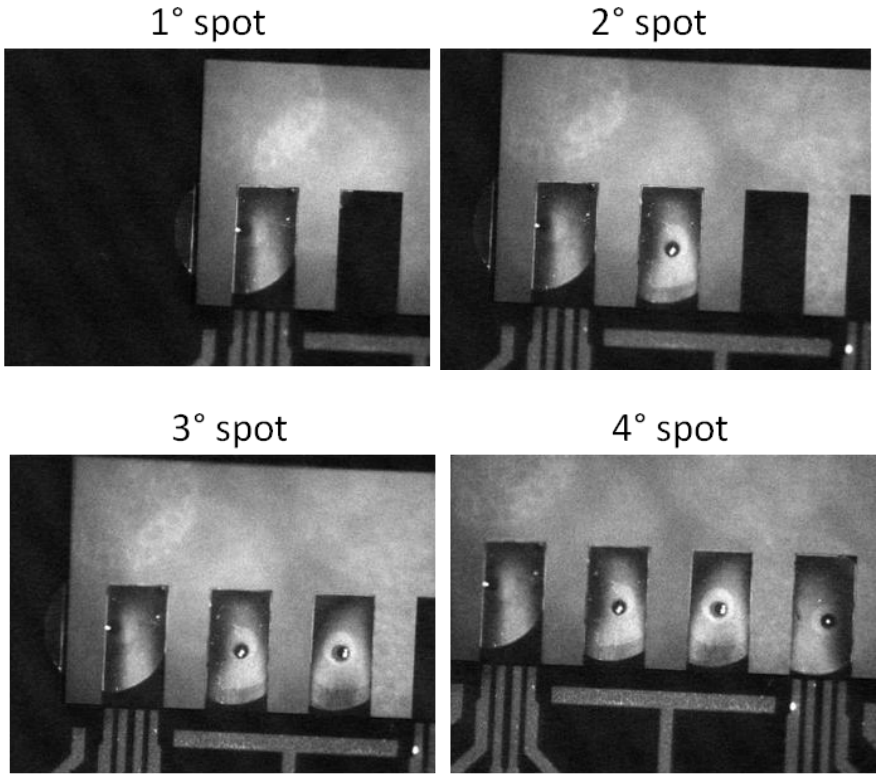

Figure 4.16. Epifluorescence microscopy images of the fluorescein spotting procedure: each picture represents the deposition of one drop on one cantilever at a time until achieving the deposition on the whole array without contaminations and microcantilever breaking (BioSint-FBK).

4.5 Conclusions

Summarizing, this research activity was focused on the detector module of a LOC for early diagnosis of autoimmune diseases such as MS and RA. In particular, the proposed approach consisted of piezoresistive SOI-MEMS cantilever arrays operating in static mode.

Their surface was characterized by a Au immobilization layer deposited in order to allow the future covalent binding of specific thiolated DNA probes. The relative fabrication process was described. Moreover, a deep surface study was performed on macro substrates developed by following the same procedure in order to evaluate the suitability of the top material for the further biological procedure (DNA functionalization). Since the first AFM analysis revealed an evident Au non-uniformity, the substrates were analyzed at different microfabrication steps by XPS. This analysis demonstrated a very low content of Au after the microfabrication treatments (annealing and oxygen plasma) with the presence of O and C contaminations as well as Cr release from the interface. Different technological and cleaning solutions were chosen. More precisely, a Ti interface replaced the original one made of Cr as adhesion layer. Moreover, an Ar plasma treatment (3 min, 15 Watt power, 30% flow) was carried out as cleaning procedure. These two modifications allowed to increase the Au content from 8.6% to 31.7% and to decrease the O and C contamination with respect to the initial samples. However, especially C contamination was still high and the obtained maximum value of Au did not represent a good starting point for further biological functionalization. For this reason, as future perspective, other improvements are required.

Moreover, also the feasibility of the spotting technique was demonstrated for high density microcantilevers array functionalization by employing a typical immobilization buffer used also in microarray technology (KH_2PO_4) and a fluorescent dye (fluorescein). By studying the right spotter parameters (x, y, and z pin directions, pin type, time contact, humidity and temperature) both the microcantilever mechanical resistance and a good surface coverage were assessed. Moreover, no cross contamination among microcantilevers was observed with a 100% deposition yield.

Chapter 5

5 Conclusions

5.1 Lab-on-Cell Results Discussion and Future Perspectives

Starting from the summary reported in *Paragraph 3.7 Conclusions*, the results obtained by using the Lab-on-Cell integrated platform are here discussed and interpreted in order to suggest optimal solutions and evaluate future improvements.

5.1.1 Electroporation Protocol Optimization

During the electroporation tests protocols were optimized by investigating biological and physical factors (*Paragraph 3.5.2 Choice of the Electroporation Protocol*). Regarding the physical parameters, a single rectangular pulse (100 μs width) was always applied, while its intensity was increased from 6 V (enough for LY transfection) to 7 V in order to allow a significant plasmid delivery. This result demonstrated the effect of the applied voltage on pores diameter: higher the pulse amplitude, higher the pores dimension. This conclusion confirms the data reported by Wolf et al.: higher the electric field, higher the electropermeabilization [Wolf 1994]. It follows that the pulse amplitude represents a key parameter to induce permeabilization and to control the cell surface area where electroporation occurs, as demonstrated by the different molecular weight of the biomolecules delivered into cells. Moreover, it must be pointed out that the pulses were applied to the electronic circuit. However, the voltage reaching the cell membrane should be proportional to the applied pulse amplitude, even if lower and strongly dependent on the cell adhesion strength. For this reason, further studies (Electrochemical Impedance Spectroscopy-EIS and voltam-

metry) should be performed in order to assess the real voltage amplitude applied to HeLa cells. Two different conditions should be evaluated: in presence or not of HeLa cells. The same study should be repeated also after the electroporation event providing interesting insights about the adhesion status and general cell culture condition.

Since the 50% electroporation efficiency represents a preliminary result, it is difficult to carry out a real comparison with other systems. However, it can be considered a good achievement with respect to traditional physical methods, especially in terms of good cell condition maintenance after the electroporation event [Mehier-Humbert 2005].

Nevertheless, considering that in case of voltages $\geq$ 8 V cell detachment often occurred (data not shown) other parameters could be changed in order to improve the electroporation experiments and thus the efficiency. As future perspective, other physical and biological factors should be taken into account: other pulse features and buffer composition.

- Width, number and delay between pulses

Higher is the pulse width, lower is the voltage necessary to the pores generation, because the permeabilization increases when the pulse duration increases too. The pulse number improves both electroporation itself until a plateau as well as the electroporation velocity. On the other hand, the delay between pulses should be as short as possible, because the transfection yield decreases when the time delay between pulses increases [Wolf 1994]. In case of macromolecules transfection, pulse duration plays a role even more important. The relative transfection mechanism is more difficult than that involving small molecules. In fact, small compounds can diffuse across the electroporated cells also for a certain time after the pulse application. Differently, when plasmid vectors are involved a DNA-membrane complex is generated whose stability depends on pulse duration. In order to increase the obtained 50% value of electroporation efficiency, the single rectangular pulse applied during the experiments should be followed by a decreasing pulsed ramp of higher duration. The first high pulse contributes to the real membrane electropermeabilization, while the second series of lower and decreasing pulses allows the DNA-membrane stabilization and the maintenance of the pores open for a certain time (sufficient for the uptake) [Rabussay 2003].

- Pulse polarity and shape

DNA transfection significantly increases if it is performed by applying bipolar pulses. Together with bipolar pulses also unipolar negative pulses could positively affect the uptake of DNA or negatively charged molecules [Kotnik 2003]. Unlike pulse amplitude, number and duration, the hypothetic role of the pulse shape has not been yet understood and systematically studied. However, the current research opinion considers a sinusoidal pulse less invasive for the cell population.

- Electroporation buffer composition

Electroporation technique often induces damages on cells: DNA breaking, reactive oxygen species production, calcium level fluctuations are some of the possible consequences which contribute to the cell survival reduction [Meldrum 1999]. By modifying the buffer composition cell viability could be preserved. Trehalose represents an example of stable sugar usually excluded from cell membrane which can increase the number of viable electroporated cells when added to the transfectants solution [Massauer 2001].

5.1.2 Electroporation Platform Improvements: Controlled Transfectants Delivery and Electrodes Functionalization

The improvements of the platform mainly consisting of the channel-based microfluidics and ns-TiO_2 functionalization of the microelectrodes allowed the delivery of different transfectants solutions into desired areas of the same cell population (single-site delivery) and increased the adhesion of cells exactly where the voltage was applied. The first aspect has satisfied the current requirement in electroporation field of having a platform able to perform multiple tests on the same chip representing an added value for high-throughput screening. The second one is a key parameter in electroporation of cells grown in adhesion, as it could improve the overall transfection efficiency. Both these observations deserve to be deepened.

5.1.2.1 Microfluidics Module Optimization

Silica tubes and microchannels were filled with the transfectants solutions by means of a syringe pump. This pressure-driven injection system showed a great dead volume in the inlet channels, consequently increasing the reagents consumption.

This drawback could be reduced by providing (i) a hole for each reaction site/electrode and (ii) a dielectrophoresis (DEP)-based delivery:

(i) A µ-hole in the middle of each circular electrode (instead of one hole per well) could improve the transfectant distribution amongst electroporation sites.

(ii) The physical effect called DEP [Clague 2001, Crews 2007] is the movement of particles (also not charged) in non uniform electric fields. In fact, when an electric field is applied to a system consisting of particles suspended in a liquid, a dipole moment is induced, due to the electrical polarizations at the interface between the particle and the suspending liquid. This phenomenon could reduce the transfectant volumes or more precisely the relative concentrations by moving biomolecules instead of fluids. Moreover, the proposed approach could lead to a less invasive injection system. In order to achieve this purpose a new microfluidic structure should be studied. In this context, another research activity carried out in these years regarding a DEP-based microdevice for microbeads and cell separation demonstrated good performances [Morganti 2010]. The possibility to integrate a similar module, mainly consisting in InterDigitated Electrodes (IDEs) arrays, with the electroporation MEA will be taken into consideration.

5.1.2.2 Ns-TiO_2 Film Effects on the Electroporation Protocol

The bioaffinity studies reported in *Chapter 3* (*Paragraph 3.1.4 Materials Bioaffinity: Cell Viability and Morphology Studies*) not only confirmed the yet well known biocompatibility of Ti [Casaletto 2001, Matsuno 2001, Brunette 2001, Armitage 2003, Carbone 2006], but by considering the only well adherent spread phenotype, showed that ns-TiO_2 film increased the percentage of spread cells. The cell-Ti interaction has been yet studied by

means of gene expression profiling [Carinci 2003] and as reported in literature cluster assembled TiO_2 shows a surface morphology that mimics the extracellular environment [Raspanti 2006]. For this reason, the obtained results find confirmations also in literature and suggest that this ns-material represents an ideal surface for living cells and can promote their adhesion.

The electroporation tests reported in this thesis were performed on integrated platforms with ns-TiO_2 functionalized MEAs. However, preliminary results obtained from a comparative study between functionalized and not MEAs revealed that in presence of the ns-material the electric pulse required to the pores opening was about 1 V lower. The voltage decrease could represent the direct consequence of the cell adhesion increase evinced also from the bioaffinity studies. In general, because of electrode reactions and the electric double layer formation the electrode/solution interface is affected by an important potential loss. Unlike bulk electroporation (characterized by a large amplitude of the total potential, kV), in microsystems the most part of the potential applied drops across the interface (V). For this reason, when the cell is well spread, the contact between cell and electrode is stronger, thus reducing the electrode/solution interface and justifying the necessity of a weaker pulse for the electropermeabilization. Unfortunately, because of a not significant statistics, the obtained data were not reported. For this reason, the influence of nt-TiO_2 film on the electroporation parameters should be deepened (considering also different film thicknesses and the relative degree of cell adhesion -focal contacts- for example by staining with anti-Vinculin antibodies) as well as its potential role on the overall transfection efficiency. Considering the effects of TiO_2 on cell adhesion, an higher transfection efficiency could be expected with respect to simple matrix of electrodes.

In this context, also the DEP-based microdevice relative to the research activity anticipated in the previous paragraph revealed a change in experimental parameters due to the presence of nt-TiO_2 film deposited by PMCS. Impedance measurements were carried out on microdevices with and without TiO_2 coating by using the interdigitated electrodes and employing different buffer conductivities. As expected, the graphs showed a variation in the curves slope at low frequencies. This was due to the presence of the film that changed the interface impedance. In particular, the interface behaviour seemed to be more resistive after the film deposition, as also visible in the phase graph. Tests performed on ns-TiO_2 coated microdevices confirmed the preservation of functional efficiency and DEP capabil-

ity with both beads and cells, but their specific cross-over frequencies were significantly reduced. These variations were probably due to the impedance change seen by the electrodes after film deposition that caused a shift in the Clausius-Mossotti factor curves. Moreover, using microdevices without the ns-film, the formation of particle aggregates was often observed. When this situation occurred, the particle levitation was hampered. Presumably, this was due to electrical interactions between the metal electrode surface and the particles caused by the absence of passivation of the chip. This effect was strongly limited in presence of the ns-TiO_2 film and a better bead detachment was observed [Morganti 2010]. Thus, a correlation between electroporation and DEP results should be investigated and deeply studied improving our understanding about the ns-TiO_2 influence on the experimental procedure in general.

5.1.3 Cell Entrapment and Internal Reference Electrodes

Since DEP represents an efficient method for molecules manipulation as well as separation, it could be integrated on the MEA module in order to provide cells entrapment on the electrodes. The main result would be represented by a substantial increase of the probability to have cells on the electrodes (otherwise randomly seeded on the MEA). In this perspective, a different MEA layout should be designed.

With respect of the employed prototypes, new devices could have a higher number of electrodes (up to 300 electrodes) with improved functionalities. More precisely, with the aim of exploiting the DEP effect a metal line could be included all around the working electrodes. The same metal line may work as internal reference electrode as well. Another possibility in order to replace the external Pt electrode (optimal because of a good electric field distribution) with an inner one is represented by the integration of a large electrode in the electroporation chamber.

Besides the DEP-based cell entrapment, an alternative solution concerns the MEA coating with a repulsive/toxic film except the electrodes active areas. This feature could solve also another issue; that one observed 24 hours after the electroporation (*Paragraph 3.6. Single-Site Electroporation Results: Lucifer Yellow (LY) Uptake and Gene Expression*): cell migration. In perspective of long-term experiments and in order to perform multiple transfec-

tions over time, cells should be blocked on their relative electrodes. Nevertheless, this approach needs to be deeply studied. Since it drastically reduces the total number of cells (able to grow only on the electrodes), the cell culture status in such environment (very far from the *in-vivo* condition) should be evaluated.

5.1.4 Different Cells and New Applications

In order to evaluate the feasibility of the technique a small fluorescent dye (LY) was employed demonstrating the specificity of the transfection. Moreover, gene expression and maintained cell viability after electroporation were assessed by transfecting pEGFP-N1 plasmid and observing cell morphology 24 hours after the electroporation. Nevertheless, thanks to its structure, which can allow multiple *in-vitro* assays, this versatile integrated platform may provide an useful tool for high-throughput screening in general and basic biomedical research. Many other cell lines and primary cultures could be employed and different applications achieved. Moreover, in principle, any transfectant solution could be used.

Here few application examples (from gene analysis related applications to more general ones, for basic research and high-throughput screenings) are listed:

- Functional genomics studies

  At present, plasmidic vectors are frequently used to deliver genes into cells. They have three main features: 1. *Ori* sequence directing plasmid replication in host cells; 2. A selective dominant marker to make transfected cells easy to be distinguished from cells without plasmid; 3. Unique sites for the restriction enzyme cleavage forming the polylinker region or multiple cloning site where genes of interest can be enclosed. The employed GFP encoded plasmid represents a widely used marker to follow expression dynamics and localize proteins. By adding to this reporter gene DNA sequences with unknown function it is possible to obtain easily identifiable chimera proteins [Naylor 1999].

Together with gene transfection, RNA interference could improve the knowledge about gene function by silencing procedures involving short interfering RNAs (si-RNAs) delivered into cells [Hannon 2002].

These two mechanisms are useful also for the identification of regulative sequences involved in gene expression control and considerable protein production.

- Identification of gene expression localization

  Neurons could be cultivated on Lab-on-Cell to identify were the gene expression occurs. The system may have a great potentiality coming from the possibility to electroporate different cell compartments with different electrodes and different transfectant solutions.

- Study of signal transmission pathways

  The communications between neurons, for example, may be stimulated by delivering calcium or other second messengers, or through the expression and silencing of genes involved in the synaptic plasticity.

- Identification of gap-junction among cells

  It can be assessed by observing the delivery of transfected molecules from a cell to another one.

- New particles transfection and high-throughput screenings in general:

  Study of nanoparticle delivery such as Quantum Dots (QDs) and relative toxicity in cells;

High-throughput drug screening for pharmacological analysis and preclinical assessments. In this context, multiple transfections over time could give indication about the possible toxicity of the drug after more than one dose.

5.2 Cantilever-based Sensors Results: Discussion and Future Perspectives

Starting from the summary reported in *Chapter 4* (*Paragraph 4.5 Conclusions*), the results obtained by analyzing the immobilization layer surface and by spotting on microcantilevers are here discussed in order to suggest further solutions and biological protocols for the real POC application of the proposed detection module.

5.2.1 Further Improvements of the Au Immobilization Layer: Cantilevers Cleaning

As previously described in *Paragraph 4.3 Microcantilever Material Characterization: Gold Layer Analysis* the quality of the immobilization layer which covers the top surface of the microcantilevers was assessed. In order to solve the problem of Au non-uniformity and low content (8.6 %) together with O and C contaminations, technical changes and cleaning procedure were performed. In detail, the Cr interface was replaced with a Ti adhesion layer. Moreover, an Ar plasma treatment (3 min, 15 Watt power, 30 % flow) was carried out as cleaning step. These two modifications allowed to increase the Au percentage from 8.6 % to 31.7% and to decrease the O and C contaminations with respect to the initial samples. However, especially C contamination was still high and the obtained maximum value of Au did not represent a good starting point for further biofunctionalization. Other steps should be evaluated, for instance the coverage and protection of the Al read-out contacts followed by wet-cleaning with piranha solution (10 min) and a rinse with deionized water. This cleaning step was adopted also by [Steel 2000, Alvarez 2004]. Nevertheless, also the contacts “passivation” by means of epoxy resin would not be sufficient. In fact, resin is etched by piranha too. In general, oxides are piranha-resistant materials. However,

their deposition is not completely compatible with the necessity to create the read-out connections. Thus, the microfabrication process should be better controlled. Other cleaning procedure described in literature consist of a rinse with isopropanol, acetone, ethanol and deionised water (DI water) [Calleja 2005], or UV-ozone treatment for 20 min by using an UV tip cleaner (Bioforce Laboratories) [Mukhopadhyay 2005]. In any case, the XPS surface analysis should be carried out immediately after the microfabrication in order to not leave the systems exposed to air which represents the main cause of C contamination. Moreover, the right procedure for the array immersion in liquid will be evaluated in order to avoid the cantilever sticking and damage.

5.2.2 Real Usage of Microcantilever Arrays for Autoimmune Diseases Diagnostics: Biological Protocols and Procedures

The research activity relative to Chapter *4. Cantilever-based Sensors for Gene Analysis* was focused on the detection module of a LOC for early diagnosis of autoimmune diseases such as MS and RA. In particular, the proposed approach consisted of piezoresistive SOI-MEMS cantilever arrays operating in static mode. The suitability of the spotting technique on simple mechanical structures (with no integrated read-out) was demonstrated (*Section 4.4 Cantilever Functionalization).* Thus, after further improvements of the Au immobilization layer discussed in the previous paragraph, the proposed system could be employed for the application in exam. In particular, this section describes all the steps involved in the process, from the sensitive layer generation with high HLA detection ability to the DNA target hybridization and relative device sensitivity and response evaluation.

5.2.2.1 DNA Probes Synthesis

The DNA sequences, specific for MS and RA diagnosis, identified by a genotyping through Illumina technique [Steemers 2007] on healthy individuals and patients, will be produced using an automated DNA synthesizer (external service, for example from M-Medical S.r.l).

One of their terminal ends (either 3' or 5') will be modified during the synthesis by adding a linker moiety for surface immobilization. More precisely, a hexyl spacer $(CH_2)_6$ linked to a thiol functional group (-SH) will be added to one end of the HLA sequences. The thiol group will be necessary to enable the covalent linkage between DNA probes and gold surface of the microcantilevers. The choice of this modification depends on the high specificity of the sulphur-gold linkage. Its free energy is so low that the desorption will occur with very low probability. The hexyl spacer will increase the spacing between the DNA chain and the sensor surface improving the accessibility of probes to the DNA target.

5.2.2.2 DNA Grafting Density and Hybridization Efficiency

Before performing the real microcantilever functionalization with the synthesized DNA probes, some parameters could be evaluated also on macro substrates (like those used for the Au layer surface analysis, *Section 4.3 Microcantilever Material Characterization: Gold Layer Analysis*) to find out the best experimental condition:

- Length of the probes chain

  It will be evaluated in order to be long enough to include the specific SNP relevant for the disease, but not too much in order to avoid unwanted flattened configuration during the following step of immobilization [Steel 2000]. Although the best length from the detector point of view is in general < 24-mer, the best value will need to be experimentally tested. As reported by Castelino et al. the grafting density (number of immobilized DNA probes/surface) strictly depends on the chain length: smaller is the length, higher will be the immobilized probes density [Castelino 2005].

- SNP position along the DNA chain

  The DNA probe sequence will be chosen paying attention also to the SNP position along the chain. In fact, it has been demonstrated that with respect to perfectly

complementary sequences the DNA target hybridization density (number of hybridized DNA target strands/surface) gradually lower for the following cases: a single SNP near the anchorage point of the DNA probe, a single SNP in the middle of the chain, multiple SNPs [Castelino 2005].

- Probes and DNA target concentration

The final concentration of synthesized DNA solution will be in the order of 10^{-6} M that is the typical desired concentration for immobilization purposes. Steel et al. demonstrated that DNA concentrations in the range of 1-10 μM are sufficient to saturate the active gold area [Steel 2000]. In general, the same DNA target concentration could be employed for the hybridization experiments in order to have 1:1 DNA probes/targets ratio. Higher DNA target concentration could increase the DNA probes probability to be "seen" by the targets as well as the hybridization kinetics. Castelino et al. used 2 μM DNA target [Castelino 2005]. However, in case of real microcantilever measurements and not only studies of hybridization density on planar substrates, lower concentrations could be enough to generate a good stress with high response. For instance, the detection limit was identified even at 10 nM concentration [Fritz 2000].

- Ionic strength of the immobilization and hybridization buffer

Higher is the ionic strength of the immobilization buffer, higher is the grafting density until 200 mM. In fact, below the 200 mM osmotic forces are dominant, whereas above this value hydration forces become important. On the other hand, the hybridization density increases at high salt concentration. However, large probe densities give rise to steric and electrostatic hindrances which limit the hybridization event. Thus, lower is the grafting density, higher is the hybridization efficiency (fraction of surface-grafted probe ss-DNA that is hybridized by target ss-DNA or hybridization density/surface grafting density) [Castelino 2005]. For this reason, the right compromise must be defined.

In order to select the best protocol a deep characterization should be performed by changing one of the above parameters at a time. At the beginning, a selective etching followed by SEM inspection could be performed in order to rapidly assess the presence of a SAM or not on a Au substrate [Bietsch 2004]. However, in order to qualitatively verify and characterize both the DNA SAM deposition and the hybridization event, a microscope inspection or fluorescence scanning could be performed by using fluorescently labelled DNA probes/targets (Cy3 and Cy5 are often employed to label DNA strands), intercalating agents, or radiolabelling technique. For example, acridine orange is a fluorescent dye which permits to distinguish single-stranded DNA (ss-DNA) from double-stranded DNA (ds-DNA) thanks to different Stokes shifts (the emitted fluorescence is orange-red and green, respectively).

On the other hand, a quantitative study of the grafting and hybridization densities will be necessary in order to optimize the experimental conditions resulting in high hybridization efficiency. As described by Casero et al. XPS and AFM analysis could provide semiquantitative information about the amount of deposited sample, its morphology, coverage information [Casero 2003, Petrovykh 2004]. Others employed XPS and fluorescence intensity in order to characterize mixed DNA/Alkylthiol Monolayers on Au [Lee 2006]. However, the best analysis for quantitative measurement of DNA sample could be obtained by displacing immobilized ss-DNA probes and hybridized ds-DNA by means of 12 mM β-mercaptoethanol treatment for 24 hours [Castelino 2005]. The obtained sample should be then analyzed by means of:

- Spectroscopy in UV-visible (UV/vis) light: the quantitative analysis can be performed by exploiting the characteristic nucleic acids absorption at the specific wavelength of 260 nm.

- Spectrofluorimetry: by using fluorescently labelled DNA probes/targets the quantitative analysis can be performed by measuring the emitted radiation (instead of absorbed light) after excitation at the specific wavelength for the adopted fluorophore.

5.2.2.3 DNA Probes Accessibility Enhancement: MCH Incubation

DNA probes can not only bind to Au through a covalent linkage by means of their sulphur group, but also by weak chemisorptions via multiple amine moieties [Xu 1993, Leff 1996]. Such adsorption could interfere with the next step of DNA target hybridization. For this reason, it will be necessary to displace the weakly adsorbed DNA probes (linked trough amine-gold and not sulphur-gold interactions) and extend the properly bound chains in order to enhance their accessibility. This aspect is crucial. According to the literature that describes the preparation of SAM on Au substrate, the treatment with 6-mercapto-1-hexanol (MCH) [Steel 2000, Wang 2002] will be taken into account. This 6-carbon chain molecule terminates with a thiol group (-SH) on one end and with an hydroxyl group (-OH) on the other end. Through its -SH group it displaces the weakly adsorbed molecules, while through its -OH group, which does not interact with the oligonucleotide probes, it acts as a spacer between them, increasing their accessibility [Levicky 1998]. A mixed DNA probes/MCH monolayer will be generated. As described in some works about DNA detection by means of cantilevers [Alvarez 2004, Calleja 2005] the treatment could consist in 1 hour incubation with 1mM MCH, introduced into the liquid cell after oligonucleotides immobilization. Thus, the MCH treatment represents another step to be included for the optimization of the process. The target hybridization will be performed on macro substrates both with and without MCH to compare the hybridization efficiency.

5.2.2.4 Cantilever Biofunctionalization

Once carried out the cleaning procedure (*Paragraph 5.2.1 Further Improvements of the Au Immobilization Layer: Cantilevers Cleaning***)**, each cantilever should be coated by the previously synthesized DNA probes in order to create the biologically active surface. The spotting technique described in *Chapter 4* (*Paragraph 4.4 Cantilever functionalization*) will be employed. However, also reference cantilevers, without any immobilized DNA probe, will be taken into account. The optimal concentration of DNA probes with specific chain length, SNP position and phosphate buffer (PB) ionic strength will be employed paying attention also to incubation time and temperature suitable for the deposition. Once

functionalized, the cantilevers array should be rinsed in order to displace aspecific bindings and could be maintained in vacuum until the hybridization procedure.

5.2.2.5 Sensitivity and Response Estimation: DNA Target Hybridization

As described in *Chapter 2.* (*Paragraph 2.2.1 Micro-ElectroMechanical Systems (MEMSs) for DNA Hybridization Detection: Cantilever-based Arrays*), the hybridization event makes the cantilever to bend due to mechanical deformation. This bending will be detected through the piezoresisitive electric system based on the Wheatstone bridge circuit made of four resistors. Since under mechanical stress doped monocrystalline silicon changes its electric resistance, it will be sufficient to measure the resistance changes during the reactions. The tentative specifications for the response estimation are inserted in Table 5.1. These specifications are based on studies performed by M. Decarli et al. using MEMS-based silicon cantilevers arrays for another application (combinatorial analysis of thin-film materials [Decarli 2006]) and will be tested for DNA hybridization detection purpose.

Table 5.1. Bias and signal: tentative specifications

Target resistance	15 kΩ per resistors
Bias	2-5 V
Output signal	3-20 μV
Response time (detector)	0.5-1 h
Configuration	Weathstone bridge

In order to evaluate the capability of the sensor to detect hybridization events, different types of experiments could be performed: in presence of sample containing only full complementary or completely aspecific (non-complementary) ss-DNAs. Tests will be carried out also using mixed DNA target sample (complementary and non-complementary ss-DNAs together) in order to evaluate the noise and the interference caused by the presence of aspecific DNA. Another important step will be to check the ability of the cantilever-

based device to distinguish between closely related sequences different only for single nucleotides (SNPs detection) by comparing the output signals coming from the two tests (in presence or not of SNPs). It could be interesting also evaluate the sensor response lowering the homology (increasing the number of mismatches). The signal will be measured varying the concentration of DNA target; more precisely serial dilutions will be performed in order to establish the sensitivity of the sensor (detection limit). A strong correlation between signal intensity and DNA concentration is expected: higher the concentration, higher should be the signal until a saturation point. Very interesting would be also to observe if the absorption of the complementary and mismatched strands causes a tensile or compressive stress as a function of the hybridization buffer pH. Moreover, the position of a single or multiple SNPs along the DNA chain could be considered in order to evaluate the best configuration ensuring the highest surface stress and, consequently, the highest cantilever deflection. Since the literature works cited in *5.2.2.3 DNA Probes Accessibility Enhancement: MCH Incubation* don't give any information about an improvement of the cantilever sensitivity after MCH treatment, but emphasize only the increased quality of the DNA monolayer, the target hybridization with both MCH treated and not treated cantilevers should be evaluated in terms of detection accuracy and sensitivity.

It must be pointed out that, at the beginning, the hybridization experiments will be easily performed distributing the sample (only DNA targets suspended in hybridization PB) directly on the array by means of a pipette, or by immersion of the cantilever array in a liquid cell containing the sample. After preliminary tests, it will be taken into consideration also the microfluidic part to perform the sample delivering from the DNA amplification module of the LOC to the cantilever array, studying the volumes involved: that one coming from the µ-PCR module (~9µl) and that one needed to cover the whole cantilever array (~90µl capacity). The possibility to add PB or Saline-Sodium Citrate (SSC) buffer (as in microarray technology) will be also considered, by previously filling the hybridization chamber ensuring a complete coverage of the array. Moreover, it must be noticed that the PCR sample is more complex than short ss-DNAs in PB usually employed for preliminary sensitivity and response evaluation. Firstly, PCR products are in general ~ 60-mer long, whereas DNA probes are shorter (~ 12-14-mer). This complication could be solved for example by choosing the PCR primers in such a way to generate DNA targets with a free end (more precisely, the opposite end with respect to the anchorage point of the DNA probes). In this

manner a hybrid with a free ss-DNA (~46-mer) will be produced without interfering with the DNA probes and allowing an efficient hybridization. Secondly, the hybridization tests will be performed in presence of the solution coming from the PCR module which contains milliQ H_2O, PCR buffer (Tris-HCl, KCl) and besides the DNA strands, $MgCl_2$, Taq polymerase, dNTPs and primers. The signals obtained with short ss-DNAs in PB and PCR products in the complex sample will be compared. The necessity to perform a washing step after hybridization will be evaluated. If the cantilever bending exclusively depends on the surface stress generated due to hybridization reaction, the washing step will be not required. A comparative study (in case of washing or not) will be carried out.

At the end it will be also evaluated how many times the same cantilever array could be reused. This analysis will be performed by removing the bound targets and repeating the hybridization comparing each time the hybridization signals. For this purpose, after each assay, the regeneration of the ss-DNA surface will be carried out by applying thermal or chemical protocols: high temperature (95°C) can denature the double-stranded DNA (ds-DNA) in two ss-DNAs and 30% urea in H_2O breaks the hydrogen bonds between complementary bases. This last method could enable the same cantilever to be reused for at least 10 times [Fritz 2000].

5.2.3 Cantilever-based Sensors Future Applications

Once overcome cleaning difficulties and optimized the experimental conditions, the proposed cantilever array would become of real importance in the field of autoimmune diseases diagnostics. Its new application (HLA detection) and the effort to achieve a density up to, at least, one hundred of cantilevers represent ambitious challenges in biomedical field. The approach would permit *in-situ* and fast measurements (few minutes instead of days) starting from a low amount of sample. The expected ultra-high sensitivity of the device (which can reduce or even avoid the need of DNA amplification, simplifying the structure of a LOC device), and the label-free detection mechanism could give a high added value to this project. Additionally, once proved the reliability of the system, the same technique could be extended to the diagnostics of any other disease based on genetic mutations, by changing the ss-DNA probes of the functional layer. In general, the proposed

system could be used by the family doctor in its office, as diagnosis test before a specialized visit in a hospital.

Acknowledgments

This work has been developed at the Fondazione Bruno Kessler (FBK) in Trento, in collaboration with the BioMEMS Research Unit, headed by Dr. Leandro Lorenzelli. All the devices presented in this work have been fabricated by the BioMEMS group, in particular by Cristian Collini and Massimiliano Decarli, using the FBK's clean room facilities. I would thank also C. Ress, C. Collini, E. Morganti, S. Pedrotti and A. Adami for their contribution during different phases of the research activity.

This work has been supported by CARITRO Foundation under the project CELTIC (Development of an integrated system based on innovative nano-microfabrication technologies for in vitro diagnostic assays) and partially funded by the European project POCEMON (Point-Of-Care MONitoring and Diagnostics for Autoimmune Diseases, FP7-ICT-2007-216088).

I would thank S. Vassanelli (Department of Human Anatomy and Physiology, University of Padova), P. Macchi (CIBIO Centre for Integrative Biology, University of Trento), S. Iannotta **(**IFN-CNR, Institute of Photonics and Nanotechnology, Trento) and C. Pederzolli (BioSint Unit-FBK) and their research groups for the collaboration and useful discussions.

Unfortunately, due to lack of time and project bureaucratic problems it was not possible to carry out the tests suggested in conclusions. However, I hope that in future they could be performed in order to deepen many of the innovative aspects of this research field.

Bibliography

[Abdulhaim 2008] I. Abdulhaim, M. Zourob, A. Lakhtakia, Surface Plasmon Resonance for Biosensing: A Mini-review, *Electromagnetics* 28 (2008), 214-242.

[Adami 2010] A. Adami, Mems Piezoresistive Micro-Cantilever Arrays For Sensing Applications (2010).

[Agarwal 2009] A. Agarwal, M. Wang, J. Olofsson, O. Orwar, S.G. Weber, Control of the Release of Freely Diffusing Molecules in Single-Cell Electroporation, *Anal. Chem.* 81 (2009) 8001–8008.

[Alberg 2001] M.A.I. Aberg, F. Ryttsén, G. Hellgren, K. Lindell, L.E. Rosengren, A.J. MacLennan, B. Carlsson, O. Orwar, P.S. Eriksson, Selective introduction of antisense oligonucleotides into single adult CNS progenitor cells using electroporation demonstrates the requirement of STAT3 activation for cntf-induced gliogenesis, *Mol. Cell Neurosci.* 17 (3) (2001) 426–443.

[Alberts 2000] B. Alberts, D. Bray, J. Lewis, M. Raff, K. Roberts, J.D. Watson, Molecular Biology of Cell (2000) *3rd edition Zanichelli*.

[Alvarez 2004] M. Alvarez, L. Carrascosa, M. Moreno, A. Calle, A. Zaballos, L.M. Lechuga, C. Martinez-A, J. Tamayo, Nanomechanics of the Formation of DNA Self-Assembled Monolayers and Hybridization on Microcantilevers, *Langmuir* 20 (2004) 9663-9668.

[Anderson 2000] R.C. Anderson, X. Su, G.J. Bogdan, J. Frenton, A miniature integrated device for automated multistep genetic assays, *Nucleic Acids Res.* 28 (12) e60.

[Andresen 2010] K.Ø. Andresen, M. Hansen, M. Matschuk, S.T. Jepsen, H.S. Sørensen, P. Utko, D. Selmeczi, T.S. Hansen, N.B. Larsen, N. Rozlosnik, R. Taboryski, Injection molded chips with integrated conducting polymer electrodes for electroporation of cells, *J. Micromech. Microeng.* 20 (2010) 055010 (9pp).

[Anson 2004] D.S. Anson, The use of retroviral vectors for gene therapy-what are the risks? A review of retroviral pathogenesis and its relevance to retroviral vector-mediated gene delivery, *Genet. Vaccines Ther.* 2 (9) (2004).

[Armitage 2003] D.A. Armitage, T.L. Parker, D.M. Grant, Biocompatibility and hemocompatibility of surface-modified NiTi alloys, *J. Biomed. Mater. Res. A* 66 (2003) 129–137.

[Bajaj 2007] P. Bajaj, D. Akin, A. Gupta, D. Sherman, B. Shi, O. Auciello, R. Bashir, Ultrananocrystalline diamond film as an optimal cell interface for biomedical applications, *Biomed. Microdevices* 9 (2007) 787–794.

[Balachandran 1982] U. Balachandran, N.G. Eror, Raman spectra of titanium dioxide, *J. Solid State Chem.* 42 (3) (1982) 276-282.

[Baller 2000] M.K. Baller, H.P. Lang, J. Fritz, Ch. Gerber, J.K. Gimzewski, U. Drechsler, H. Rothuizen, M. Despont, P. Vettiger, F.M. Battiston, J.P. Ramseyer, P. Fornaro, E. Meyer, H.J. Güntherodt, A cantilever array-based artificial nose, *Ultramicroscopy* 82 (2000) 1-9.

[Barker 2009] M. Barker, B. Billups, M. Hamann, Focal macromolecule delivery in neuronal tissue using simultaneous pressure ejection and local electroporation, *J. Neurosci. Methods* 177 (2009) 273–284.

[Barr 1994] T.L. Barr, Modern ESCA: the principles and practice of x-ray photoelectron spectroscopy, *CRC Press* (1994).

[Bashir 2004] R. Bashir, BioMEMS: state-of-the-art in detection, opportunities and prospects, *Adv. Drug Deliv. Rev.* 56 (2004) 1565-1586.

[Beebe 2003] S.J. Beebe, J. White, P.F. Blackmore, Y. Deng, K. Somers, K.H. Schoenbach, Diverse effects of nanosecond pulsed electric fields on cells and tissues**,** *DNA Cell Biol.* 22 (12) (2003) 785–796.

[Beeby 2004] S. Beeby, G. Ensell, M. Kraft, N. White, MEMS Mechanical Sensors, Chapter 2: Materials and Fabrication Techniques, 7-38 (2004), *Artech House MEMS library*.

[Berry 2004] C.C. Berry, G. Campbell, A. Spadiccino, M. Robertson, A.S.G. Curtis, The influence of microscale topography on fibroblast attachment and motility, *Biomaterials* 25 (2004) 5781–5788.

[Bestman 2006] J.E. Bestman, R.C. Ewald, S.L. Chiu, H.T. Cline, In vivo single-cell electroporation for transfer of DNA and macromolecules, *Nat. Protoc.* 1 (3) (2006) 1267-1272.

[Bhadriraju 2002] K. Bhadriraju, C.S. Chen, Engineering cellular microenvironments to improve cell-based drug testing, *Drug Discov. Today* 7 (11) (2002) 612-620.

[Bietsch 2004] A. Bietsch, J. Zhang, M. Hegner, H.P. Lang, C. Gerber, Rapid functionalization of cantilever array sensors by inkjet printing, *Nanotechnology* 15 (2004) 873–880.

[Bliss 2007] C.L. Bliss, J.N. McMullin, C.J. Backhouse, Rapid fabrication of a microfluidic device with integrated optical waveguides for DNA fragment analysis, *Lab Chip* 7 (2007) 1280–1287.

[Boozer 2006] C. Boozer, G. Kim, S. Cong, H.W. Guan, T. Londergan, Looking towards label-free biomolecular interaction analysis in a high-throughput format: a review of new surface plasmon resonance technologies, *Curr. Opin. Biotechnol.* 17 (2006) 400-405.

[Braeken 2009] D. Braeken, R. Huys, D. Jans, J. Loo, S. Severi, F. Vleugels, G. Borghs, G. Callewaert, C. Bartic, Local electrical stimulation of single adherent cells using threedimensional electrode arrays with small interelectrode distances, 31st Annual International Conference of the IEEE EMBS, Minneapolis, Minnesota, USA, September 2-6 (2009) 2756-2759.

[Braeken 2010] D. Braeken, R. Huys, J. Loo, C. Bartic, G. Borghs, G. Callewaert, W. Eberle, Localized electricalstimulation of in vitro neurons using an array of sub-cellular sized electrodes, *Biosens. Bioelectron.* 26 (2010) 1474–1477.

[Brunette 2001] D.M. Brunette, P. Tengvall, M. Textor, P. Thomsen, editors, Titanium in medicine: material science, surface science, engineering, biological responses and medical applications, Berlin: Springer (2001).

[Butt 1995] H.J. Butt, M. Jashke, Calculation of thermal noise in atomic force microscopy, *Nanotechnology* 6 (1995) 1-7.

[Calleja 2005] M. Calleja, M. Nordstr, M. Alvarez, J. Tamayo, L.M. Lechuga, A. Boisen, Highly sensitive polymer-based cantilever-sensors for DNA detection, *Ultramicroscopy* 105 (2005) 215–222.

[Campas 2004] M. Campas, I. Katakis, DNA biochip arraying, detection and amplification strategies, *Trends Analyt. Chem.* 23 (1) (2004) 49-62.

[Canatella 2001] P.J. Cannatella, J.F. Karr, J.A. Petros, M.R. Praunitz, Quantitative study of electroporation mediated uptake and cell viability, *Biophys. J.* 80 (2001) 755-764.

[Cantion] www.cantion.com

[Carbone 2006] R.Carbone, I. Marangi, A. Zanardi, L. Giorgetti, E. Chierici, G. Berlanda, A. Podesta`, F. Fiorentini, G. Bongiorno, P. Piseri, P.G. Pelicci, P. Milani, Biocompatibility of cluster-assembled nanostructured TiO_2 with primary and cancer cells, *Biomaterials* 27 (2006) 3221–3229.

[Carinci 2003] F. Carinci, S. Volinia, F. Pezzetti,F. Francioso, L. Tosi, A. Piattelli, Titanium–cell interaction: analysis of gene expression profiling, *J. Biomed. Mater. Res. B Appl. Biomater.* 66 (2003) 341–346.

[Carrascosa 2006] L.G. Carrascosa, M. Moreno, M. Alvarez, L.M. Lechuga, Nanomechanical biosensors: a new sensing tool, *Trends Analyt. Chem.* 25 (2006) 196-206.

[Casaletto 2001] M.P. Casaletto, G.M. Ingo, S. Kaciulis, G. Mattogno, L. Pandolfi, G. Scavia, Surface studies of in vitro biocompatibilities of titanium oxide coatings, *Appl. Surf. Sci.* 172 (2001) 167–177.

[Casero 2003] E. Casero, M. Darder, D.J. Díaz, F. Pariente, J.A. Martín-Gago, H. Abruña, E. Lorenzo, XPS and AFM Characterization of Oligonucleotides Immobilized on Gold Substrates, *Langmuir* 19 (15) (2003) 6230–6235.

[Castelino 2005] K. Castelino, B. Kannan, A. Majumdar, Characterization of Grafting Density and Binding Efficiency of DNA and Proteins on Gold Surfaces. *Langmuir* 21 (2005) 1956-1961.

[Chang 2009] W.C. Chang, D.W. Sretavan, Single cell and neural process experimentation using laterally applied electrical fields between pairs of closely apposed microelectrodes with vertical sidewalls, *Biosens. Bioelectron.* 24 (2009) 3600–3607.

[Chao 2008] T.C. Chao, A. Ros, Microfluidic single-cell analysis of intracellular compounds, *J. R. Soc. Interface* 5 (2008) S139–S150.

[Choundhury 2007] A. Choundhury, P.J. Hesketh, T. Thundat, Z. Hu, A piezoresistive microcantilever array for surface stress measurement: curvature model and fabrication, *J. Micromech. Microeng.* 17 (2007) 2065-2076.

[Chuah 2003] M.K. Chuah, D. Collen, T. VandenDriessche, Biosafety of adenoviral vectors, *Curr. Gene Ther.* 3 (6) (2003) 527– 543.

[Clague 2001] D.S. Clague, E.K. Wheeler, Dielectrophoretic manipulation of macromolecules: the electric field, *Phys. Rev. E* 64 (2) (2001) 026605-1.

[Creemer 2001] J.F. Creemer, F. Fruett, G.C.M. Mejer, P.J. French, The Piezojunction Effect in Silicon Sensors and Circuits and its Relation to Piezoresistance, *IEEE Sens. J.* 1 (2) (2001) 98-108.

[Crews 2007] N. Crews, J. Darabi, P. Voglevede, F. Guo, A. Bayoumi, An analysis of interdigitated electrode geometry for dielectrophoretic particle transport in micro-fluidics, *Sens. Actuators B Chem.* 125 (2007) 672-679.

[Datskos 2004] P.G. Datskos, T. Thundat, N.V. Lavrik, Micro and Nanocantilever Sensors, *Encyclopedia of Nanoscience and Nanotechnology* X (2004) 1-10 edited by H. S. Nalwa, American Scientific Publishers.

[Decarli 2006] M. Decarli, A. Adami, L. Lorenzelli, N. Laidani, MEMS-based Silicon Cantilevers Arrays for combinatorial analysis of thin-film materials, *Proceeding Eurosensors XX* (2006).

[Desikan 2006] R. Desikan, I. Lee, T. Thundat, Effect of nanometer surface morphology on surface stress and adsorption kinetics of alkanethiol self-assembled monolayers, *Ultramicroscopy* 106 (2006) 795-799.

[Dewez 1999] J-L. Dewez, A. Doren, Y-J. Schneider, P.G. Rouxhet, Competitive adsorption of proteins: key of the relationship between substratum surface properties and adhesion of epithelial cells, *Biomaterials* 20 (1999) 547–559.

[Digabel 2010] J. le Digabel, M. Ghibaudo, L. Trichet, A. Richert, B. Ladoux, Microfabricated substrates as a tool to study cell mechanotransduction, *Med. Biol. Eng. Comput.* 48 (2010) 965–976.

[Dobson 2007] M.G. Dobson, P. Galvin, D.E. Barton, Emerging technologies for point-of-care genetic testing, *Expert Rev. Mol. Diagn.* 7 (4) (2007) 359-370.

[Drummond 2003] T.G. Drummond, M.G. Hill, J.K. Barton, Electrochemical DNA sensors, *Nat. Biotechnol.* 21 (10) (2003) 1192-1199.

[Easley 2006] C.J. Easley, J.M. Karlinsey, J.M. Bienvenue, L.A. Legendre, M.G. Roper, S.H. Feldman, M.A. Hughes, E.L. Hewlett, T.J. Merkel, J.P. Ferrance, J.P. Landers, A fully integrated microfluidic genetic analysis system, *PNAS* 103 (51) (2006) 19272-19277.

[Edwards 1994] M.C. Edwards, R.A. Gibbs, Multiplex PCR: advantages, development and applications, *Genome Res.* 3 (1994) S65-S75.

[Eisenbarth 2002] E. Eisenbarth, P. Linez, V. Biehl, D. Velten, J. Breme, H. F. Hildebrand, Cell orientation and cytoskeleton organisation on ground titanium surfaces, *Biomol. Eng.* 19 (2002) 233-237.

[Felgner 1987] P.L. Felgner, T.R. Gadek, M. Holm, R. Roman, H.W. Chan, M. Wenz, J.P. Northrop, G.M. Ringold, M. Danielsen, Lipofection: A highly efficient, lipid-mediated DNA-transfection procedure, *Proc. Natl. Acad. Sci. USA* 84 (1987) 7413–7417.

[Ferraro 2003] J.R. Ferraro, K. Nakamoto, C.W. Brown, Introductory Raman spectroscopy, Academic Press (2003).

[Fox 2006] M.B. Fox, D.C. Esveld, A. Valero, R. Luttge, H.C. Mastwijk, P.V. Bartels, A. van den Berg, R.M. Boom, Electroporation of cells in microfluidic devices: a review, *Anal. Bioanal. Chem.* 385 (2006) 474–485.

[Fritz 2000] J. Fritz, M.K. Baller, H.P. Lang, H. Rothuizen, P. Vettiger, E. Meyer, H-J. Guntherodt, Ch. Gerber, and J. K. Gimzewski, Translating Biomolecular Recognition into Nanomechanics, *Science* 288 (2000) 316-318.

[Fritz 2002] J. Fritz, E.B. Cooper, S. Gaudet, P.K. Sorger, S.R. Manalis, Electronic detection of DNA by its intrinsic molecular charge, *PNAS* 99 (22) (2002) 14142-14146.

[Gabriel 1997] B. Gabriel, J. Teissie, Direct observation in the millisecond time range of fluorescent molecule asymmetrical interaction with the electropermeabilized cell membrane, *Biophys. J.* 73 (1997) 2630–2637.

[Gallagher 2006] W.M. Gallagher, I. Lynch, L.T. Allen, I. Miller, S.C. Penney, D.P. O'Connor, S. Pennington, A.K. Keenan, K.A. Dawson, Molecular basis of cell–biomaterial interaction: Insights gained from transcriptomic and proteomic studies, *Biomaterials* 27 (2006) 5871-5882.

[Geng 2010] T. Geng, Y. Zhan, H-Y Wang, S.R. Witting, K.G. Cornetta, C. Lu, Flow-through electroporation based on constant voltage for large-volume transfection of cells, *J. Control Release* 144 (2010) 91–100.

[Giarola 2010] M.Giarola, A. Sanson, F. Monti, G. Mariotto, M. Bettinelli, A. Speghini, G. Salviulo, Vibrational dynamics of anatase TiO_2: Polarized Raman spectroscopy and *ab initio* calculations, *Phys. Rev. B* 81(2010) 174305.

[Gleixner 2006] R. Gleixner, P. Fromherz, The Extracellular Electrical Resistivity in Cell Adhesion, *Biophys. J.* 90 (2006) 2600–2611.

[Goldstein 2003] J. Goldstein, D.E. Newbury, D.C. Joy, C.E. Lyman, P. Echlin, E. Lifshin, L. Sawyer, J.R. Michael, Scanning electron microscopy and x-ray microanalysis, 3rd edition (2003).

[Grahm 1973] F.L. Graham, A.J. van der Eb, A new technique for the assay of infectivity of human adenovirus 5 DNA, *Virology* 52 (1973) 456–67.

[Gumbiner 1996] B.M. Gumbiner, Cell Adhesion: The Molecular Basis of Tissue Architecture and Morphogenesis, *Cell* 84 (1996) 345–357.

[Haas 2001] K. Haas, W-C Sin, A. Javaherian, Z. Li, H.T. Cline, Single-Cell Electroporation for Gene Transfer In Vivo, *Neuron* 29 (2001) 583–591.

[Hannon 2002] G.J. Hannon, RNA interference, *Nature* 418 (2002) 244-251.

[Hansen 2001] K.M. Hansen, H.F. Ji, G. Wu, R. Datar, R. Cote, A. Majumdar, T. Thundat, Cantilever-Based Optical Deflection Assay for Discrimination of DNA Single-Nucleotide Mismatches, *Anal. Chem.* 73 (7) (2001) 1567-1571.

[Haque 2009] A. ul Haque, M. Zuberi, R.E. Diaz-Rivera, D.M. Porterfield, Electrical characterization of a single cell electroporation biochip with the 2-D scanning vibrating electrode technology, *Biomed. Microdevices* 11 (2009) 1239–1250.

[He 2007] H. He, D.C. Chang, Y-K Lee, Using a micro electroporation chip to determine the optimal physical parameters in the uptake of biomolecules in HeLa cells, *Bioelectrochemistry* 70 (2) (2007) 363–368.

[Healy 1999] K.E. Healy, Molecular engineering of materials for bioreactivity, *Current Opinion in Solid State and Materials Science* 4 (1999) 381-387.

[Hewapathirane 2008] D.S. Hewapathirane, K. Haas, Single cell electroporation in vivo within the intact developing brain, *J. Vis. Exp.* 2008 (17). pii: 705. doi: 10.3791/705.

[Ho 1996] S.Y. Ho, G.S. Mittal, Electroporation of cell membranes: A review, *Crit. Rev. Biotechnol.* 16 (4) (1996) 349-362.

[Huang 2001] Y. Huang, B. Rubinsky, Microfabricated electroporation chip for single cell membrane permeabilization, *Sens. Actuators A Phys.* 89 (2001) 242-249.

[Huang 2003] Y. Huang, B. Rubinsky, Flow-through micro-electroporation chip for high efficiency single-cell genetic manipulation, *Sens. Actuators A Phys.* 104 (2003) 205–212.

[Ingebrandt 2007] S. Ingebrandt, Y. Han, F. Nakamura, A. Poghossian, M.J. Schoning, A. Offenhausser, Label-free detection of single nucleotide polymorphisms utilizing the differential transfer function of field-effect transistors, *Biosens. Bioelectron.* 22 (2007) 2834-2840.

[Ionescu-Zanetti 2008] C. Ionescu-Zanetti, A. Blatz, M. Khine, Electrophoresis-assisted single-cell electroporation for efficient intracellular delivery, *Biomed. Microdevices* 10 (2008) 113–116.

[Ishibashi 2007] T. Ishibashi, K. Takoh, H. Kaji, T. Abe, M. Nishizawa, A porous membrane-based culture substrate for localized in situ electroporation of adherent mammalian cells, *Sens. Actuators B* 128 (2007) 5–11.

[Ito 1999] Y. Ito, Surface micropatterning to regulate cell functions, *Biomaterials* 20 (1999) 2333–2342.

[Jen 2004] C-P Jen, W-M Wu, M. Li, Y-C Lin, Site-Specific Enhancement of Gene Transfection Utilizing an Attracting Electric Field for DNA Plasmids on the Electroporation Microchip, *J. Microelectromech. Syst.* 13 (6) (2004) 947-955.

[Jiang 2006] Jiang, B., Li, Y, Wu, H., He, X., Li, C., Li, L., Tang, R., Xie, Yi, and Mao,Y : Application of HLA-DRB1 genotyping by oligonucleotide micro-array technology in forensic medicine. *Forensic Sci. Int.* 162 (2006) 66-73.

[Johansson 2005] A. Johansson, M. Calleja, P.A. Rasmussen, A. Boisen, SU-8 cantilever sensor system with integrated readout, *Sens. Actuators A* 123–124 (2005) 111–115.

[Kaminska 2005] K. Kaminska, A. Amassian, L. Martinu, K. Robbie, Growth of vacuum evaporated ultraporous silicon studied with spectroscopic ellipsometry and scanning electron microscopy, *J. Appl. Phys.* 97 (2005) 013511.

[Karlsson 2000] M. Karlsson**,** K. Nolkrantz, M.J. Davidson, A. Strömberg, F. Ryttsén, B. Åkerman, O. Orwar, Electroinjection of colloid particles and biopolymers into single unilamellar liposomes and cells for bioanalytical applications, *Anal. Chem.* 72 (2000) 5857–5862.

[Khine 2005] M. Khine, A. Lau, C. Ionescu-Zanetti, J. Seo, L.P. Lee, A single cell electroporation chip, *Lab Chip* 5 (2005) 38–43.

[Khine 2007] M. Khine, C. Ionescu-Zanetti, A. Blatz, L-P Wang, L.P. Lee, Single-cell electroporation arrays with real-time monitoring and feedback control, *Lab Chip* 7 (2007) 457–462.

[Kim 2004] D-S Kim, Y-T Jeong, H-J Park, J-K Shin, P. Choi, J-H Lee, G. Lim, An FET-type charge sensor for highly sensitive detection of DNA sequence, *Biosens. Bioelectron.* 20 (1) (2004) 69-74.

[Kim 2007] J.A. Kim, K. Cho, Y.S. Shin, N. Jung, C. Chung, J.K. Chang, A multi-channel electroporation microchip for gene transfection in mammalian cells, *Biosens. Bioelectron.* 22 (2007) 3273–3277.

[Koester 2010] P.J. Koester, C. Tautorat, H. Beikirch, J. Gimsa, W. Baumann, Recording electric potentials from single adherent cells with 3D microelectrode arrays after local electroporation, *Biosens. Bioelectron.* 26 (2010) 1731–1735.

[Kotnik 2003] T. Kotnik, G. Pucihar, M. Rebersek, D. Miklavcic, L.M. Mir, Role of pulse shape in cell membrane electropermeabilization, *Biochim. Biophys. Acta* 1614 (2003) 193-200.

[Kurosawa 2006] O. Kurosawa, H. Oana, S.Matsuoka, A. Noma, H. Kotera, M. Washizu, Electroporation through a micro-fabricated orifice and its application to the measurement of cell response to external stimuli, *Meas. Sci. Technol.* 17 (2006) 3127–3133.

[Lampin 1997] M. Lampin, C. Warocquier, C. Legris, M. Degrange, M.F. Sigot-Luizard, Correlation between substratum roughness and wettability, cell adhesion, and cell migration, *J. Biomed. Mater. Res.* 36 (1997) 99–108.

[Lan 2005] S. Lan, M. Veiseh, M. Zhang, Surface modification of silicon and gold-patterned silicon surfaces for improved biocompatibility and cell patterning selectivity, *Biosens. Bioelectron.* 20 (2005) 1697–1708.

[Lang 2005] H.P. Lang, M. Hegner, C. Gerber, Cantilever array sensors, *Mater. Today* 8 (4) (2005) 30–36.

[Lee 2004] S.J. Lee, S.Y. Lee, Micro total analysis system (μ-TAS) in biotechnology, *Appl. Microbiol. Biotechnol.* 64 (2004) 289–299.

[Lee 2006] C-Y Lee, P. Gong, G.M. Harbers, D. W. Grainger, D. G. Castner, L. J. Gamble, Surface Coverage and Structure of Mixed DNA/Alkylthiol Monolayers on Gold: Characterization by XPS, NEXAFS, and Fluorescence Intensity Measurements, *Anal. Chem.* 78 (10) (2006) 3316–3325.

[Leff 1996] D.V. Leff, L. Brandt, J. R. Heath, Synthesis and characterization of hydrophobic, organically-soluble gold nanocrystals functionalized with primary amines, *Langmuir* 12 (1996) 4723– 4730.

[Levicky 1998] R. Levicky, T.M. Herne, M.J. Tarlov, S.K. Satija, Using self-assembly to control the structure of DNA monolayers on gold: A neutron reflectivity study, *J. Am. Chem. Soc.* 120 (1998) 9787–9792.

[Levinson 2005] H.J. Levinson, Principles of lithography, SPIE Press (2005).

[Lin 2001] Y-C Lin, M-Y Huang, Electroporation microchips for *in vitro* gene transfection, *J. Micromech. Microeng.* 11 (2001) 542–547.

[Lin 2003] Y-C Lin, M. Li, C-S Fan, L-W Wu, A microchip for electroporation of primary endothelial cells, *Sens. Actuators A Phys.* 108 (2003) 12–19.

[Losurdo 2002] M. Losurdo, D. Barreca, P. Capezzuto, G. Bruno, E. Tondello, Interrelation between nanostructure and optical properties of oxide thin films by spectroscopic ellipsometry, *Surface and Coatings Technology* 151 –152 (2002) 2–8.

[Lu 2006] K-Y. Lu, A.M. Wo, Y-J. Lo, K-C. Chen, C-M. Lin, C-R. Yang, Three dimensional electrode array for cell lysis via electroporation, *Biosens. Bioelectron.* 22 (2006) 568–574.

[Lundqvist 1998] J.A. Lundqvist, F. Sahlin, M.A.I. Åberg, A. Stromberg, P.S. Eriksson, O. Orwar, Altering the biochemical state of individual cultured cells and organelles with ultramicroelectrodes, *Proc. Natl. Acad. Sci. U S A* 95 (1998) 10356–10360.

[Lynch 2007] I. Lynch, K.A. Dawson, Are there generic mechanisms governing interactions between nanoparticles and cells? Random epitope mapping for the outer layer of the protein–material interface, *Physica A* 373 (2007) 511–520.

[MacQueen 2008] L.A. MacQueen, M.D. Buschmann, M.R. Wertheimer, Gene delivery by electroporation after dielectrophoretic positioning of cells in a non-uniform electric field, *Bioelectrochemistry* 72 (2008) 141–148.

[Malic 2007] L. Malic, M. Herrmann, X.D. Hoa, M. Tabrizian, Current state of intellectual property in microfluidic nucleic acid analysis, *Rec. Pat. on Eng.* 1 (1) (2007) 71-88.

[Maluf 2004 a] N. Maluf, K. Williams, An introduction to Microelectromechanical Systems Engineering, Chapter 2: Materials for MEMS, 13-32, Second Edition (2004), *Artech House MEMS library*.

[Maluf 2004 b] N. Maluf, K. Williams, An introduction to Microelectromechanical Systems Engineering, Chapter 3: Processes for Micromachining, 33-77, Second Edition (2004), *Artech House microelectromechanical library*.

[Massauer 2001] H. Massauer, V.L. Sukorov, U. Zimmermann, Trehalose Improves Survival of Electrotransfected Mammalian Cells, *Cytometry* 45 (2001) 161-169.

[Matsuno 2001] H. Matsuno, A.Yokoyama, F. Watari, M. Uo, T. Kawasaki, Biocompatibility and osteogenesis of refractory metal implants, titanium, hafnium, niobium, tantalum and rhenium, *Biomaterials* 22 (2001) 1253–1262.

[McCutchan 1968] J.H. McCutchan, J.S. Pagano, Enhancement of the infectivity of simian virus 40 deoxyribonucleic acid with diethylaminoethyl-dextran, *J. Natl. Cancer Inst.* 41 (1968) 351–357.

[McKendry 2002] R. McKendry, J. Zhang, Y. Arntz, T. Strunz, M. Hegner, H.P. Lang, M.K. Baller, U. Certa, E. Meyer, H-J. Güntherodt, C. Gerber, Multiple label-free biodetection and quantitative DNA-binding assays on a nanomechanical cantilever array. *PNAS* 99 (2002) 9783-9788.

[Mehier-Humbert 2005] S. Mehier-Humbert, R.H. Guy, Physical methods for gene transfer: Improving the kinetics of gene delivery into cells, *Adv. Drug Deliv. Rev.* 57 (2005) 733-753.

[Meldrum 1999] R.A. Meldrum, M. Bowl, S.B. Ong, S. Richardson, Optimisation of Electroporation for Biochemical Experiments in Live Cells. *Biochem. Biophys. Res. Commun.* 256 (1999) 235-239.

[Morganti 2010] E. Morganti, C. Collini, R. Cunaccia, A. Gianfelice, L. Odorizzi, A. Adami, L. Lorenzelli, E. Jacchetti, A. Podestà, C. Lenardi, P. Milani. A dielectrophoresis-based microdevice coated with nanostructured TiO_2 for separation of particles and cells. *Microfluid. Nanofluid.* (Springer), DOI 10.1007/s10404-010-0751-8, published online 18 december (2010).

[Mottet 2010] G. Mottet, J. Villemejane, L.M. Mir, B. Le Pioufle, A technique to design complex 3D lab on a chip involving multilayered fluidics, embedded thick electrodes and hard packaging-application to dielectrophoresis and electroporation of cells, *J. Micromech. Microeng.* 20 (2010) 047001 (8pp).

[Mukhopadhyay 2005] R. Mukhopadhyay, M. Lorentzen, J. Kjems, F. Besenbacher, Nanomechanical Sensing of DNA Sequences Using Piezoresistive Cantilevers, *Langmuir* 21 (2005) 8400-8408.

[Myszka 2004] D.G. Myszka, Analysis of small-molecule interactions using Biacore S51 technology, *Anal. Biochem.* 329 (2) (2004) 316-323.

[Nawarathna 2008] D. Nawarathna, K. Unal, H.K. Wickramasinghe, Localized electroporation and molecular delivery into single living cells by atomic force microscopy, *Appl. Phys. Lett.* 93 (2008) 153111.

[Naylor 1999] L.H. Naylor, Reporter gene technology: the future looks bright, *Biochem. Pharmacol.* 58 (1999) 749-757.

[Neumann 1972] E. Neumann, K. Rosenheck, Permeability changes induced by electric impulses in vesicular membranes, *J. Membr. Biol.* 10 (1972) 279-290.

[Neumann 1999] E. Neumann, S. Kakorin, K. Toensing, Fundamentals of electroporative delivery of drugs and genes, *Bioelectrochem. Bioenerg.* 48 (1999) 3-16.

[Nolkrantz 2001] K. Nolkrantz, C. Farre, A. Brederlau, R.I. Karlsson, C. Brennan, P.S. Eriksson, S.G. Weber, M. Sandberg, O. Orwar, Electroporation of single cells and tissues with an electrolyte-filled capillary, *Anal. Chem.* 73 (2001) 4469–4477.

[Numnuam 2008] A. Numnuam, K.Y. Chumbimuni-Torres, Y. Xiang, R. Bash, P. Thavarungkul, P. Kanatharana, E. Pretsch, J. Wang, E. Bakker, Potentiometric Detection of DNA Hybridization, *J. Am. Chem. Soc.* 130 (2) (2008) 410–411.

[Olofsson 2003] J. Olofsson, K. Nolkrantz, F. Rittsen, B.A. Lambie, S.G. Weber, O. Orwar, Single-cell electroporation, *Curr. Opin. Biotechnol.* 14 (2003) 29–34.

[Pakhomov 2007] A.G. Pakhomov, J.F. Kolb, J.A. White, R.P. Joshi, S. Xiao, K.H. Schoenbach, Long-lasting plasma membrane permeabilization in mammalian cells by nanosecond pulsed electric field (NSPEF), *Bioelectromagnetics* 28 (2007) 655–663.

[Park 2003] T.H. Park, M.L. Shuler, Integration of Cell Culture and Microfabrication Technology, *Biotechnol. Prog.* 19 (2003) 243-253.

[Petronis 2003] S. Petronis, J. Gold, B. Kasemo, Microfabricated force-sensitive elastic substrates for investigation of mechanical cell–substrate interactions, *J. Micromech. Microeng.* 13 (2003) 900–913.

[Petrovykh 2004] D.Y. Petrovykh, H. Kimura-Suda, M.J. Tarlov, L.J. Whitman, Quantitative Characterization of DNA Films by X-ray Photoelectron Spectroscopy, *Langmuir* 20 (2) (2004) 429–440.

[Polizu 2006] S. Polizu, M. Maugey , S. Poulin, P. Poulin, L'H. Yahia, Nanoscale surface of carbon nanotube fibers for medical applications: Structure and chemistry revealed by TOF-SIMS analysis, *Appl. Surf. Sci.* 252 (2006) 6750–6753.

[Pritchard 2008] C. Pritchard, P. Underhill, A. Greenfield, Using DNA microarrays. *Methods Mol. Biol.* 461 (2008) 605-629.

[Rabussay 2003] D. Rabussay, N.B. Dev, J. Fewell, L.C. Smith, G. Widera, L. Zhang, Enhancement of therapeutic drug and DNA delivery into cells by electroporation, *J. Phys. D: Appl. Phys.* 36 (2003) 348–363.

[Rae 2002] J.L. Rae, R.A. Levis, Single-cell electroporation, *Pflugers Arch.* 443 (2002) 664–670.

[Raiteri 2001] R. Raiteri, M. Grattarola, H.-J. Butt, P. Skládal, Micromechanical cantilever-based biosensors, *Sens. Actuators B* 79 (2001) 115-126.

[Ramadan 2006] Q. Ramadan, V. Samper, D. Poenar, Z. Liang, C. Yu, T.M. Lim, Simultaneous cell lysis and bead trapping in a continuous flow microfluidic device, *Sens. Actuators B Chem.* 113 (2006) 944–955.

[Rasmussen 2003] P.A. Rasmussen, J. Thaysen, O. Hansen, S.C. Eriksen, A. Boisen, Optimized cantilever biosensors with piezoresistive read-out, *Ultramicroscopy* 97 (2003) 371 – 376.

[Raspanti 2006] M. Raspanti, M. Protasoni, A. Manelli, S. Guizzardi, V. Mantovani, A. Sala, The extracellular matrix of the human aortic wall: ultrastructural observations by FEG-SEM and tapping-mode AFM, *Micron.* 37 (2006) 81–86.

[Rathenberg 2003] J. Rathenberg, T. Nevian, V. Witzemann, High-efficiency transfection of individual neurons using modified electrophysiology techniques, *J. Neurosci. Methods* 126 (2003) 91–98.

[Rogers 2003] B. Rogers, L. Manning, M. Jones, T. Sulchek, K. Murray, B. Beneschott, J. D. Adams, Z. Hu, T. Thundat, H. Cavazos, S. C. Minne, Mercury vapor detection with a self-sensing, resonating piezoelectric cantilever, *Review of Sci. Instrum.* 74 (2003) 4899-4901.

[Rols 2006] M.P. Rols, Electropermeabilization, a physical method for the delivery of therapeutic molecules into cells, *Biochim. Biophys. Acta Biomembr.* 1758 (2006) 423–428.

[Ryttsen 2000] F. Ryttsen, C. Farre, C. Brennan, S.G. Weber, K. Nolkrantz, K. Jardemark, D.T. Chiu, O. Orwar, Characterization of Single-Cell Electroporation by Using Patch-Clamp and Fluorescence Microscopy, *Biophys. J.* 79 (2000) 1993–2001.

[Sepaniak 2002] M. Sepaniak, P. Datskos, N. Lavrik, C. Tipple, Microcantilever Transducers: A New Approach in Sensor Technology, *Anal. Chem.* 1 (2002) 568-575.

[Sepúlveda 2006] B. Sepúlveda, J. Sánchez del Río, M. Moreno, F.J. Blanco, K. Mayora, C. Domínguez, L.M. Lechuga, Optical biosensor microsystems based on the integration of highly sensitive Mach–Zehnder interferometer devices, *J. Opt. A: Pure Appl. Opt.* 8 (2006) S561–S566.

[Sniadecki 2006] N.J. Sniadecki, R.A. Desai, S.A. Ruiz, C.S. Chen, Nanotechnology for Cell–Substrate Interactions, *Ann. Biomed. Eng.* 34 (1) (2006) 59-74.

[Stachoviak 2006] J.C. Stachoviak, M. Yue, K. Castelino, A. Chakraborty, A. Majumdar, Chemomechanics of Surface Stresses Induced by DNA Hybridization, *Langmuir* 22 (2006) 263-268.

[Steel 2000] B. Steel, R.L Levicky, T.M. Herne, M.J. Tarlov, Immobilization of Nucleic Acids at Solid Surfaces: Effect of Oligonucleotide Length on Layer Assembly, *Biophys. J.* 79 (2000) 975–981.

[Steemers 2007] F.J. Steemers, K.L. Gunderson, Whole genome genotyping technologies on the BeadArray™ platform, *Biotechnol. J.* 2 (2007) 41–49.

[Szita 2010] N. Szita, K. Polizzi, N. Jaccard, F. Baganz, Microfluidic approaches for systems and synthetic biology, *Curr. Opin. Biotechnol.* 21 (2010) 517–523.

[Tabard-Cossa 2007] V. Tabard-Cossa, M. Godin, I.J. Burgess, T. Monga, R. B. Lennox, P. Grütter, Microcantilever-based sensors: effect of morphology, adhesion, and cleanliness of the sensing surface on surface stress, *Anal. Chem.* 79 (21) (2007) 8136–8143.

[Tanaka 2009] M. Tanaka, Y. Yanagawa, N. Hirashima, Transfer of small interfering RNA by single-cell electroporation in cerebellar cell cultures, *J. Neurosci. Methods* 178 (2009) 80–86.

[Teissie 1993] J. Teissie, M.P. Rols, An experimental evaluation of the critical potential difference inducing cell membrane electropermeabilization, *Biophys J.* 65 (1993) 409–413.

[Thaysen 2002] J. Thaysen, A.D. Yalcinkaya, P. Vettiger, A. Menon, Polymer-based stress sensor with integrated readout, *J. Phys. D Appl. Phys.* 35 (2002) 2698–2703.

[Toccoli 2003] T. Toccoli, S. Capone, L. Guerini, M. Anderle, A. Boschetti, E. Iacob E, Micheli, P. Siciliano, S. Iannotta, Growth of Titanium Dioxide Films by Cluster Supersonic Beams for VOC Sensing Applications, *IEEE Sens. J.* 3 (2) (2003) 199-205.

[Uesaka 2008] N. Uesaka, M. Nishiwaki, N. Yamamoto, Single cell electroporation method for axon tracing in cultured slices, *Develop. Growth Differ.* 50 (2008) 475–477.

[Valero 2008] A. Valero, J.N. Post, J.W. van Nieuwkasteele, P.M. ter Braak, W. Kruijerb, A. van den Berg, Gene transfer and protein dynamics in stem cells using single cell electroporation in a microfluidic device, *Lab Chip* 8 (2008) 62–67.

[Vassanelli 2008] S. Vassanelli, L. Bandiera, M. Borgo, G. Cellere, L. Santoni, C. Bersani, M. Salamon, M. Zaccolo, L. Lorenzelli, S. Girardi, M. Maschietto, M. Dal Maschio, A. Paccagnella, Space and time resolved gene expression experiments on cultured mammalian cells by a single-cell electroporation microarray, *N. Biotechnol.* 25 (1) (2008) 55-67.

[Vedam 1998] K. Vedam, Spectroscopic ellipsometry: a historical overview, *Thin Solid Films* 313-314 (1998) 1-9.

[Verd 2005] J.Verd, G. Abadal, J. Teva, M.V. Gaudó, A. Uranga, X. Borrisé, F. Campabadal, J. Esteve, E.F. Costa, F. Pérez-Murano, Z.J. Davis, E. Forsén, A. Boisen, N. Barniol, Design, Fabrication, and Characterization of a submicro-electromechanical Resonator With Monolithically Integrated CMOS Readout Circuit, *J. Microelectromech. Syst.* 14 (2005) 508-519.

[Vernier 2006] P.T. Vernier, Y. Sun, M.A. Gundersen, Nanoelectropulse-driven membrane perturbation and small molecule permeabilization, *BMC Cell Biol.* 7 (2006).

[Vidic 2003] A. Vidic, D. Then, Ch. Ziegler, A new cantilever system for gas and liquid sensing, *Ultramicroscopy* 97 (2003) 407 – 416.

[Wang 1997] J. Wang, P.E. Nielsen, M. Jiang, X. Cai, J.R. Fernandes, D.H. Grant, M. Ozsoz, A. Beglieter, M. Mowat, Mismatch-Sensitive Hybridization Detection by Peptide Nucleic Acids Immobilized on a Quartz Crystal Microbalance, *Anal. Chem.* 69 (24) (1997) 5200–5202.

[Wang 2002] J. Wang, Electrochemical nucleic acid biosensors, *Anal. Chim. Acta* 469 (2002) 63–71.

[Wang 2006] H-Y. Wang, A.K. Bhunia, C. Lu, A microfluidic flow-through device for high throughput electrical lysis of bacterial cells based on continuous dc voltage, *Biosens. Bioelectron.* 22 (2006) 582–588.

[Wang 2008] H-Y. Wang, C. Lu, Microfluidic Electroporation for Delivery of Small Molecules and Genes Into Cells Using a Common DC Power Supply, *Biotechnol. Bioeng.* 100 (2008) 579–586.

[Wang 2009] M. Wang, O. Orwar, S.G. Weber, Single-Cell Transfection by Electroporation Using an Electrolyte/Plasmid-Filled Capillary, *Anal. Chem.* 81 (2009) 4060–4067.

[Wang 2010] M. Wang, O. Orwar, J. Olofsson, S.G. Weber, Single-cell electroporation, *Anal. Bioanal. Chem.* 397 (2010) 3235–3248.

[Weaver 1993] J.C. Weaver, Electroporation: A General Phenomenon for Manipulating Cells and Tissue, *J. Cell. Biochem.* 51 (1993) 426-435.

[Weaver 1996] J.C. Weaver, Y.A. Chizmadzhev, Theory of electroporation: A review, *Bioelectrochem. Bioenerg.* 41 (1996) 135-160.

[Wegner 2006] K. Wegner, P. Piseri, H.V. Tafreshi, P. Milani, Cluster beam deposition: a tool for nanoscale science and technology, *J. Phys. D Appl. Phys.* 39 (2006) R439–R459

[West 2008] J. West, M. Becker, S. Tombrink, A. Manz, Micro Total Analysis Systems: Latest Achievements, *Anal. Chem.* 80 (12) (2008) 4403-4419.

[Wolf 1994] H. Wolf, M.P. Rols, E. Boldt, E. Neumann, J. Teissié, Control by Pulse Parameters of Electric Field-Mediated Gene Transfer in Mammalian Cells, *Biophys. J.* 66 (1994) 524-531.

[Xu 1993] C. Xu, L. Sun, L.J. Kepley, R.M. Crooks, Molecular Interactions between Organized, Surface-Confined Monolayers and Vapor-Phase Probe Molecules. 6. In-situ FTIR External Reflectance Spectroscopy of Monolayer Adsorption and Reaction Chemistry, *Anal. Chem.* 65 (1993) 2102–2107.

[Yang 2008] S.M. Yang, C. Chang, T.I. Yin, P.L. Kuo, DNA hybridization measurement by self-sensing piezoresistive microcantilevers in CMOS biosensor, *Sens. Actuators B* 130 (2008) 674-681.

[Yi 2006] C. Yi, C.W. Li, S. Ji, M. Yang, Microfluidics technology for manipulation and analysis of biological cells, *Anal. Chim. Acta* 560 (2006) 1–23.

[Yim 2005] E.K.F. Yim, R.M. Reano, S.W. Pang, A.F. Yee, C.S. Chen, K.W. Leong, Nanopattern-induced changes in morphology and motility of smooth muscle cells, *Biomaterials* 26 (2005) 5405–5413.

[Yu 2005] A.A. Yu, T.A. Savas, G.S. Taylor, A. Guiseppe-Elie, H.I. Smith, F. Stellacci, Supramolecular Nanostamping: Using DNA as Movable Type, *Nano Lett. 5* (6) (2005) 1061–1064.

[Yu 2007] X. Yu, Y. Tang, H. Zhang, T. Li, W. Wang, Design of High-Sensitivity Cantilever and Its Monolithic Integration With CMOS Circuits, *IEEE Sens. J.* 7 (2007) 489-495.

[Yu 2008] X. Yu, Y. Tang and H. Zhang, Monolithic integration of micromachined sensors and CMOS circuits based on SOI technologies, *J. Micromech. Microeng.* 18 (2008) 037002 7pp.

[Zhan 2009] Y. Zhan, J. Wang, N. Bao, C. Lu, Electroporation of cells in microfluidic droplets, *Anal. Chem.* 81 (5) (2009) 2027–2031.

[Zhang 2007] C. Zhang, D. Xing, Miniaturized PCR chips for nucleic acid amplification and analysis: latest advances and future trends, *Nucleic Acids Res.* 35 (13) (2007) 4223–4237.

[Ziegler 2004] C. Ziegler, Cantilever-based biosensors, *Anal. Bioanal. Chem.* 379 (2004) 946-959.

[Zimmermann 1974] U. Zimmermann, G. Pilwat, F. Riemann, Dielectric breakdown of cell membranes, *Biophys. J*. 14 (11) (1974) 881-899.

Appendix A

1. Biological Protocols for SKOV-3 Cell Line Maintenance and Culture on Substrates

1.1. Cell culture solutions and reagents for cell viability assays:

- Complete RPMI medium: RPMI (Sigma-Aldrich, St. Louis, MO, U.S.A.) supplemented with 10% heat-inactivated of Fetal Bovine Serum (FBS) (Euroclone) and L-glutamine (200 mM) (Sigma-Aldrich, St. Louis, MO, U.S.A.).
  Since antibiotics act on cell membrane, penicillin and streptomycin were not added in order to maintain cell culture as similar as possible to the *in-vivo* condition, necessary requirement in bioaffinity studies.

- Trypsin-EDTA Solution (1:10, Sigma-Aldrich, St. Louis, MO, U.S.A.) for the dissociation of adherent cells from the culture substrates.

- Phosphate Buffered Saline (PBS): NaCl 137 mM, KCl 2.7 mM, Na_2HPO_4 10 mM, $KH_2\ PO_4$ 2 mM (Sigma-Aldrich, St. Louis, MO, U.S.A.) in milliQ H_2O; pH 7.4.

- Dulbecco Phosphate Buffer Saline (DPBS) (Sigma-Aldrich, St. Louis, MO, U.S.A.): PBS with added ions. It was supplemented with EDTA 1mM (MERK), the most commonly used ion chelating agent.

- Calcein AM (Molecular Probes): stock solution 1 mM in DMSO, then diluted in PBS (final concentration 0.5 μM).

1.2. SKOV-3 cells maintenance

SKOV-3 human ovarian carcinoma cells (American Type Culture Collection, ATCC) were routinely maintained in complete RPMI medium (pH 7.2-7.4) in 75 cm^3 Tissue Culture (TC) flasks (Corning, Inc) and incubated at 37°C in a 5% CO_2 environment. The exhausted medium was renewed two-three times a week with fresh complete RPMI medium.
When the cell culture reached the confluence, the medium was removed, the cell monolayer rinsed with PBS and detached by incubation with Trypsin-EDTA (5 min, 37°C). The enzyme was inactivated by adding fresh medium and the cell suspension centrifuged for 5 min at 1300 rpm and room temperature. Pellet was resuspended in fresh medium and transferred in new TC flasks (1:3).

1.3. Culture conditions for bioaffinity evaluation

Before seeding the cells on the different substrates, the monolayer was incubated with DPBS supplemented with EDTA (1h, 37°C). This detachment procedure is slower than the trypsin enzymatic activity, but it was preferred in order to preserve the membrane receptors, desirable requirement especially in case of bioaffinity studies. Cell suspension was centrifuged (5 min, 1300 rpm, room temperature) and the pellet was suspended in DPBS. Then cells were directly counted by Bürker camera and finally seeded on substrates ($5x10^3$ cells/cm^2). Samples were maintained in complete RPMI medium and incubated at 37°C in a 5% CO_2 environment.

2. Biological Protocols for Hela Cell Line Maintenance and Culture on Lab-on-Cell Integrated Microsystem

2.1 Cell culture solutions:

- Complete DMEM medium: high glucose DMEM (Sigma-Aldrich, St. Louis, MO, U.S.A.) supplemented with 10% heat-inactivated of Fetal Bovine Serum (FBS), 2

mM L-glutamine and 100 U/mL penicillin-streptomycin (Lonza, Basel, Switzerland).

- Trypsin-EDTA Solution (1:10, Sigma-Aldrich, St. Louis, MO, U.S.A.) for the dissociation of adherent cells from the culture substrates.

- Phosphate Buffered Saline (PBS): NaCl 137 mM, KCl 2.7 mM, Na_2HPO_4 10 mM, $KH_2\ PO_4$ 2 mM (Sigma-Aldrich, St. Louis, MO, U.S.A.) in milliQ H_2O; pH 7.4.

2.2. HeLa cells maintenance and culture on chips

HeLa cells (American Type Culture Collection, ATCC) were routinely maintained in complete DMEM medium (pH 7.2-7.4) in 75 cm^3 Tissue Culture (TC) flasks (Corning, Inc) and incubated at 37°C in a 5% CO_2 environment. The exhausted medium was renewed two-three times a week with fresh complete DMEM medium. When the cell culture reached the confluence, the medium was removed, the cell monolayer rinsed with PBS and detached by incubation with Trypsin-EDTA (5 min, 37°C). The enzyme was inactivated by adding fresh medium and the cell suspension centrifuged for 5 min at 1300 rpm. Pellet was resuspended in fresh medium and transferred in new TC flask (1:3).
Before seeding the cells on sterilized integrated platforms, the same procedure was carried out, but also direct counting on Bürker camera was performed. Cells were suspended in fresh complete RPMI medium, directly plated on chips ($5x10^4$ cells/cm^2) and incubated at 37°C in a 5% CO_2 environment.

Appendix B

List of Related Publications:

- C. Collini, E. Morganti, R. Cunaccia, L. Odorizzi, C. Ress, and L. Lorenzelli, A. De Toni, G. Marinaro, M. Borgo, M. Maschietto. Fabrication and characterization of a fully integrated microdevice for in-vitro single cell assays. In *The Online Journal of Scientific Posters* (2009) ISSN:1754-1417, http://www.eposters.net/index.aspx?ID=2493.

- H Schicho, H. Grussinger, L. Lorenzelli, M. Decarli, A. Adami, L. Odorizzi, F. Macciardi, F. Kalatzis. Lab-on-chip: Innovative approach towards telemedicine in primary care. 19: 66-67 (2009). Asian Hospital and Healthcare Management.

- A. Adami, M. Decarli, L. Odorizzi, L. Lorenzelli, K. Fincati, K., H. Gruessinger, K. Schicho, F. Macciardi, F.Kalatzis. Development of MEMS microcantilever arrays for DNA single nucleotide polymorphism detection in autoimmune diseases diagnostic. *Sensors and Microsystems: AISEM 2009 Proceedings*, Lecture Notes in Electrical Engineering 54: 335-338 (2010) - Springer.

- L. Odorizzi, C. Ress, R. Cunaccia, C. Collini, E. Morganti, L. Lorenzelli. A fully integrated system for single-site electroporation and addressed cell drug delivery. *Sensors and Microsystems: AISEM 2009 Proceedings*, Lecture Notes in Electrical Engineering 54: 319-322 (2010) - Springer.

- C. Ress, L. Odorizzi, C. Collini, L. Lorenzelli, S. Forti, C. Pederzolli, L. Lunelli, L. Vanzetti, N. Coppede', T. Toccoli, G. Tarabella, S. Iannotta. Comparative bioaffinity studies for *in-vitro* cell assays on MEMS-based devices. *Sensors and Microsystems: AISEM 2009 Proceedings*, Lecture Notes in Electrical Engineering 54: 83-87 (2010) - Springer.

- L. Odorizzi, C. Ress, C. Collini, E. Morganti, L. Lorenzelli, N. Coppede', A.B. A-labi, S. Iannotta, L. Vidalino, P. Macchi. An Enhanced Platform for Cell Electro-poration: Controlled Delivery and Electrodes Functionalization. *Eurosensors 2010 Proceedings*. Procedia Engineering 5: 45-48 (2010)

List of Related Conferences:

- C. Collini, E. Morganti, R. Cunaccia, L. Odorizzi, L. Lorenzelli. Integrated modules for single cell transfection and controlled delivery and nanoparticles. NNC National Nanomedicine Congress 2008, 28-29 November 2008, Genova.

- M. Decarli, A. Adami, L. Odorizzi, L. Lorenzelli and K. Fincati. Development of a microfabrication technology for microcantilever-based detection modules in Lab-On-a-Chip application. NNC National Nanomedicine Congress 2008, 28-29 November 2008, Genova.

- A. Adami, M. Decarli, L. Odorizzi, L. Lorenzelli, K. Fincati, K., H. Gruessinger, K. Schicho, F. Macciardi, F.Kalatzis. Development of MEMS microcantilever arrays for DNA single nucleotide polymorphism detection in autoimmune diseases diagnostic. AISEM 2009, 14th National Conference on Sensors and Microsystems, 24-26 February 2009, Pavia.

- L. Odorizzi, C. Ress, R. Cunaccia, C. Collini, E. Morganti, L. Lorenzelli. A fully integrated system for single-site electroporation and addressed cell drug delivery. AISEM 2009, 14th National Conference on Sensors and Microsystems, 24-26 February 2009, Pavia.

- C. Ress, L. Odorizzi, C. Collini, L. Lorenzelli, S. Forti, C. Pederzolli, L. Lunelli, L. Vanzetti, N. Coppede', T. Toccoli, G. Tarabella, S. Iannotta. Comparative bioaffinity studies for *in-vitro* cell assays on MEMS-based devices. AISEM 2009, 14th National Conference on Sensors and Microsystems, 24-26 February 2009, Pavia.

- C. Collini, E. Morganti, R. Cunaccia, L. Odorizzi, C. Ress, and L. Lorenzelli, A. De Toni, G. Marinaro, M. Borgo, M. Maschietto. Fabrication and characterization of a fully integrated microdevice for in-vitro single cell assays. LAB ON CHIP EUROPEAN CONGRESS, 19-20 May 2009, Stoccolma.

- A. Ferrario, M. Scaramuzza, A. De Toni, L. Odorizzi, C. Ress, C. Collini, E. Morganti, L. Lorenzelli. Advanced electrical characterization of an innovative microelectronic/microfluidic device. Biosensors 2010. 26-28 May 2010, Glasgow, UK.

- L. Odorizzi, C. Ress, C. Collini, E. Morganti, L. Lorenzelli, N. Coppedè, A.B. Alabi, S. Iannotta. L. Vidalino, P. Macchi. An integrated platform for single-site cell electroporation. Congresso nazionale biomateriali. 24-26 May, 2010, Camogli (GE).

- L. Odorizzi, C. Ress, C. Collini, E. Morganti, R. Cunaccia, L. Lorenzelli, N. Coppedè, A.B. Alabi, S. Iannotta, L. Vidalino, P. Macchi, A. De Toni, G. Marinaro, S. Vassanelli. A new mea for single-site multiple transfections: surface functionalization and microfluidics integration. MEMS in Italy 2010, 28 June-1 July 2010, Otranto.

- C. Collini, E. Morganti, L. Odorizzi, C. Ress, L. Lorenzelli, N. Coppede', A.B. Alabi, S. Iannotta, L. Vidalino, P. Macchi. Functionalized microelectrodes array with integrated microfluidic channels for single-site multiple transfections. GNB 2010, 8-11 July, Torino.

- L. Odorizzi, C. Ress, C. Collini, E. Morganti, L. Lorenzelli, N. Coppede', A.B. Alabi, S. Iannotta, L. Vidalino, P. Macchi. An Enhanced Platform for Cell Electroporation: Controlled Delivery and Electrodes Functionalization. Eurosensors 2010, 5-8 September 2010, Linz, Austria. **2nd Prize – Best Paper Award (Lecture).**

Appendix C

Other Relevant Publications:

- E. Morganti, C. Collini, R. Cunaccia, L. Odorizzi, L. Lorenzelli. Development of Bio-MEMS Based Technological Platforms for cancer cell separation and detection. In proceedings of the 8th Workshop on biosensors and bioanalytical micro-techniques in environmental and clinical analysis. 3-6 October 2007, Goa, India.

- R. Cunaccia, L. Odorizzi, E. Morganti, C. Collini , L. Lorenzelli, F. Guizzardi, E. Jacchetti, C. Lenardi, P. Milani. A nano-on-micro device for dielectrophoretic cancer cell separation and detection. *Sensors and Microsystems: AISEM 2008 Proceedings*, 238-242 (2009) – World Scientific.

- E. Morganti, C. Collini, R. Cunaccia, A. Gianfelice, L. Odorizzi, A. Adami, L. Lorenzelli, E. Jacchetti, A. Podestà, C. Lenardi, P. Milani. A dielectrophoresis-based microdevice coated with nanostructured TiO_2 for separation of particles and cells. *Microfluid. Nanofluid.* (Springer), DOI 10.1007/s10404-010-0751-8, published online 18 december (2010).

Other Relevant Conferences:

- E. Morganti, C. Collini, R. Cunaccia, L. Odorizzi, L. Lorenzelli. Development of Bio-MEMS Based Technological Platforms for cancer cell separation and detection. 8th Workshop on biosensors and bioanalytical micro-techniques in environmental and clinical analysis. 3-6 October 2007, Goa, India.

- R. Cunaccia, L. Odorizzi, E. Morganti, C. Collini , L. Lorenzelli, F. Guizzardi, E. Jacchetti, C. Lenardi, P. Milani. A nano-on-micro device for dielectrophoretic cancer cell separation and detection. AISEM 2008, 13th National Conference on Sensors and Microsystems, 19-21 February 2008, Roma.

- R. Cunaccia, E. Morganti, L. Lorenzelli, L. Odorizzi, C. Collini, C. Lenardi, A. Gianfelice, E. Jacchetti, P. Milani. Study of cell and microparticle dielectrophoresis on a microelectrode array. National Bioengineering Congress 2008, 3-5 July 2008, Pisa.

- C. Ress, A. Tindiani, A. Adami, C. Collini, S. Pedrotti, L. Odorizzi, L. Lorenzelli. A multiparametric electrochemical microsensor for wine yeast quality assessment. Smart Systems Integration 2010, 23-24 March 2010, Como.

- C. Ress, A. Tindiani, A. Adami, C. Collini, S. Pedrotti, L. Odorizzi, L. Lorenzelli Wine yeast quality assessment with integrated multiparametric microsensors. Biosensors 2010, 26-28 May 2010, Glasgow, UK.

- C. Ress, A. Tindiani, A. Adami, L. Odorizzi, C. Collini, S. Pedrotti, L. Lorenzelli. A multiparametric microsensors platform for yeast growth monitoring. MEMS in Italy 2010, 28 June-1 July 2010, Otranto.